



TECHNISCHE
UNIVERSITÄT
WIEN
Vienna | Austria

Diploma Thesis

DEVELOPMENT OF NOVEL CHEMOENZYMATIC ONE-POT REACTIONS FOR THE SYNTHESIS OF FRAGRANCE ALDEHYDES

Conducted to obtain the academic degree: **Master of Science (MSc.)**

Under the supervision of:

Assoc. Prof. Dipl.-Ing. Dr.techn. Florian Rudroff

Institute of Applied Synthetic Chemistry

Submitted at:

TU WIEN

Faculty of Technical Chemistry

By:

Stefan Giparakis, BSc.

Schautagasse 48, 1100 Wien



Die approbierte gedruckte Originalversion dieser Diplomarbeit ist an der TU Wien Bibliothek verfügbar
The approved original version of this thesis is available in print at TU Wien Bibliothek.

Δεν ελπίζω τίποτα. Δε φοβούμαι τίποτα. Είμαι λέφτερος
- Nikos Kazantzakis



Die approbierte gedruckte Originalversion dieser Diplomarbeit ist an der TU Wien Bibliothek verfügbar
The approved original version of this thesis is available in print at TU Wien Bibliothek.

Acknowledgements

Thank you, Prof. Florian Rudroff, for giving me the opportunity to work on this challenging but very rewarding project in the BSC research group, for allowing me to explore my own ideas, and for the endless support I received throughout my thesis.

Thank you, Prof. Michael Schnürch, Prof. Marko Mihovilovic, and Dr. Christian Stanetty for the valuable input during the seminars.

Thank you to all the members of the BSC group in particular Clemens, Christoph, Lara, Verena, Lisa, Drasi, Kathi O., Hubert, Heci, Laszlo, Emmanuel Astrid, Nanditha, Rahele, Nina, Johanna, Freddy, Tom, Kathi S., Eleni, Viktor, Blanca, Farooq, Max, Dominik, Richi, Simon, Julia Lydia and Jakob for welcoming me with open arms, for the great working environment and many hours of entertainment in and out of the lab.

Thank you to all the people and especially Christoph Suster for measuring countless NMRs for me. You are the real heroes!

Thank you to my lab mates in the “Girl’s lab” for the great working environment! In particular, thank you Dominik Schnalzer for being the best bench neighbor a man can dream of (sorry for taking your second bench away), Viktor Savic for allowing me to sometimes play my music in the lab even though you oftentimes did not enjoy it, Eleni Papaplioura for helping me improve my Greek, Blanca Vega Alanis for always listening to my complaints, Katharina Schlögl for keeping the lab from collapsing, Maximilian Wutscher for continuing the project and the “Colorados” Richard Fried and Simon Leonhartsberger for the interesting discussions.

Thank you, Julia Jodlbauer and Thomas “Tom” Rohr, for introducing me to the wonders and sometimes the magic of biochemistry.

Thank you, Lydia Suchy, for the help and support throughout my thesis. Starting from the shaky SDS-PAGE gel introduction to our (almost) Heureka moments, it was always a great pleasure working with you.

Thank you, Katharina Obleser, for the countless interesting conversation in the lab and during bouldering. You are truly a remarkable person, and I am grateful for finding a friend like you.

Thank you, Sebastian Hecko, for the helpful advice in and out of the lab. You have been a great inspiration to me.

Thank you, Miriam Giparakis, for accompanying me on the path of life for so many years, even though it was not always easy.

I would especially like to thank my partner Thi Ngoc “Tini” Le. Thank you for always being there for me. Thank you for cheering me up after a hard day in the lab. Thank you for always believing in me, even though I often did not. The last 9 years with you have been a great joy and I look forward to the next 9 years.

Furthermore, I would like to thank my parents who, even though they are not around anymore to see me graduate, set me up on the right path and allowed me to follow my dreams and aspirations.

Lastly, I would also like to thank the Republic of Austria for providing me with this free and excellent education.

Table of content

Abstract	vi
Kurzfassung	viii
Abbreviations	x
Compound Library	xii

A. Introduction 15

A.1. Biocatalysis	16
A.1.1. Introduction to biocatalysis	16
A.1.2. Biocatalysis in organic synthesis	17
A.1.3. Recombinant protein production	17
A.1.4. Types of biocatalysts in organic synthesis	18
A.1.5. Enzymatic transformations	20
A.1.5.1. Alcohol Dehydrogenases	21
A.1.5.2. Esterase	24
A.1.5.3. Baeyer-Villiger-Monooxygenase (BVMOs)	26
A.1.5.4. Aromatic dioxygenase (ADO)	28
A.2. Cascade and one-pot reactions	29
A.2.1. Classification	29
A.2.2. Advantages of cascade reactions / one-pot reactions over traditional synthesis	30
A.2.3. Designing a chemoenzymatic one-pot reaction	31
A.3. Biocompatibility of chemical Synthesis	32
A.3.1. Introduction to Wacker oxidation	34
A.3.2. Pd catalyzed isomerization of 2-propenylbenzenes	38
A.4. Aldehydes as products of (chemo)enzymatic one-pot reactions	40
A.5. Aim of the thesis	43

B. Results and Discussion 44

B.1. Design of chemoenzymatic one-pot reactions for the synthesis of fragrance aldehydes	45
B.2. Screening for a biocompatible Wacker oxidation	47
B.3. Determining the substrate scope of PAMO, HAPMO, and TmCHMO	52
B.4. Determining the substrate scope of AlkJ	55
B.5. Comparison between the spontaneous hydrolysis and the hydrolysis facilitated by Pfl	57
B.6. Assembly of the enzymatic cascade	58
B.7. Assembly of the chemoenzymatic one-pot reaction	60
B.7.1. Chemoenzymatic one-pot reaction: PAMO	61
B.7.2. Chemoenzymatic one-pot reactions: TmCHMO	63

B.8. Increasing the scale of a chemoenzymatic one-pot reaction.....	65
B.9. Design and construction of a plasmid vector for the co-expression of TmCHMO and Pfel	68
B.9.1. Successful co-expression of TmCHMO and Pfel	70
B.9.2. Co-transformation with TmCHMO::Pfel and AlkJ	71
B.10. ADO: Route B	73
B.10.1. Isomerization	73
B.10.2. Assembly of the chemoenzymatic one-pot reaction with ADO75	
B.11. Conclusion and outlook	80
C. Materials and Methods	82
C.1. Stock Solutions.....	83
C.1.1. Antibiotics	83
C.1.2. Inducer	83
C.1.3. Compounds used for biotransformation	83
C.2. Standard media and buffers	83
C.2.1. Buffers	83
C.2.2. Standard media	84
C.2.3. Autoinduction media	84
C.2.4. SDS-PAGE	84
C.3. General procedures.....	85
C.3.1. Preparation of chemically competent cells	85
C.3.2. Transformation of chemically competent cells	86
C.3.3. General procedure for the preparation of cryostocks	86
C.3.4. Plasmid DNA isolation and quantification	86
C.3.5. DNA-Sequencing	87
C.3.6. Preparation of primers	87
C.3.7. Polymerase Chain Reaction (PCR)	87
C.3.8. Colony PCR	88
C.3.9. Agarose gel electrophoresis	89
C.3.10. Gel purification of PCR products	90
C.3.11. NEBuilder® Hifi DNA assembly	90
C.3.12. Sodium Dodecyl Sulfate Polyacrylamide Gel Electrophoresis (SDS-PAGE)	91
D. Experimental Part	93
D.1. General considerations	94
D.2. Construction of pETDuet1_TmCHMO::Pfel	94
D.2.1. Step 2	95
D.3. Sample preparation for GC analysis and quantification.....	96
D.4. General procedure for the cultivation of <i>E. coli</i> for enzyme expression by induction	96

D.5. General procedure for the cultivation of <i>E. coli</i> for enzyme expression by autoinduction.....	97
D.6. General procedure for whole-cell biotransformation.....	97
D.7. Procedure for the mixed culture whole-cell biotransformation (route A)	97
D.8. General Procedure for the whole-cell chemoenzymatic one-pot reaction (route A)	98
D.9. Large scale biotransformation (route A and B)	98
D.10. Preparation of lyophilized cells containing Pfl	98
D.11. Activity assay of Pfl⁵⁴	99
D.12. Protein expression conditions by induction	100
D.13. Synthetic procedures.....	100
D.13.1. General remarks	100
D.13.2. Screened Wacker oxidation procedures	101
D.13.2.1. PdCl ₂ catalyzed Wacker oxidation in DMA using molecular oxygen as terminal oxidant	101
D.13.2.2. PdCl ₂ catalyzed Wacker oxidation in ACN using MnO ₂ as terminal oxidant	101
D.13.2.3. Iron(II)chloride catalyzed Wacker oxidation using molecular oxygen	102
D.13.2.4. Hexadecafluorinated-iron-phthalocyanine catalyzed Wacker oxidation using molecular oxygen	102
D.13.3. Wacker oxidation of propenylbenzenes	103
D.13.3.1. General procedure A for the Wacker oxidation	103
D.13.3.2. Synthesis of phenylpropan-2-one 1b	104
D.13.3.3. Synthesis of 1-(3-methylphenyl)propan-2-one 2b	105
D.13.3.4. Synthesis of 1-(4-methylphenyl)propan-2-one 3b	106
D.13.3.5. Synthesis of 1-(4-methoxyphenyl)propan-2-one 4b	107
D.13.3.6. Synthesis of 1-(3,4-dimethoxyphenyl)propan-2-one 5b	108
D.13.3.7. Synthesis of 1-(2H-1,3-benzodioxol-5-yl)propan-2-one 6b	109
D.13.3.8. Synthesis of 1-(4-hydroxy-3-methoxyphenyl)propan-2-one 7b	110
D.13.3.9. Synthesis of 1-(4-acetoxy-3-methoxyphenyl)propan-2-one 8b	111
D.13.4. Isomerization of 2-propenylbenzenes	112
D.13.4.1. Isomerization of Eugenol 7a	112
D.13.4.2. General procedure A for the isomerization of 2-propenylbenzenes	112
D.13.4.3. Synthesis of 1-(prop-2-en-1-yl)benzene 1g	113
D.13.4.4. Synthesis of 1-methyl-3-prop-1-enylbenzene 2g	114
D.13.4.5. Synthesis of 1-methyl-4-prop-1-enylbenzene 3g	115
D.13.4.6. Synthesis of 1-methoxy-4-(prop-1-en-1-yl)benzene 4g	116
D.13.4.7. Synthesis of 1,2-dimethoxy-4-(prop-1-en-1-yl)benzene 5g	117
D.13.4.8. Synthesis of 5-(prop-1-en-1-yl)-2H-1,3-benzodioxole 6g	118
D.13.4.9. Synthesis of 2-methoxy-4-(prop-1-en-1-yl)phenol 7g	119
D.13.4.10. Synthesis of (E)- 2-methoxy-4-(prop-1-en-1-yl)phenol acetate 8g	120
D.13.5. General procedure for the demethylation of aromatic mono methyl ethers ¹³⁹	121
D.13.5.1. Synthesis of 4-(prop-2-en-1-yl)-1,2-benzodiol 11:	122

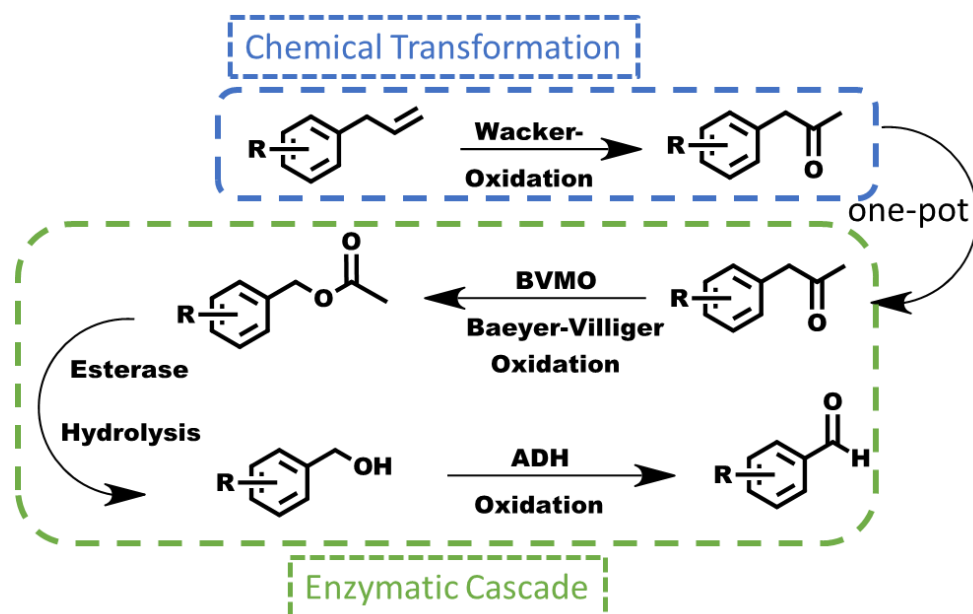
D.13.5.2. Synthesis of 4-(prop-2-en-1-yl)phenol 10.	123
D.13.5.3. Synthesis of 4-(prop-1-en-1-yl)phenol 9g	124
D.13.6. Synthesis of 5-(prop-2-en-1-yl)-2H-1,3-benzodioxole 6a ¹⁴¹	125
D.13.7. Synthesis of benzyl acetates	126
D.13.7.1. General procedure A for the synthesis of benzyl acetates ¹⁴²	126
D.13.7.2. General procedure B for the synthesis of benzyl acetates	127
D.13.7.3. Synthesis of 3-methylbenzyl acetate 2c	128
D.13.7.4. Synthesis of 4-methylbenzyl acetate 3c	129
D.13.7.5. Synthesis of 4-methoxybenzyl acetate 4c	130
D.13.7.6. Synthesis of 3,4-dimethoxybenzyl acetate 5c	131
D.13.7.7. Synthesis of (2H-1,3-Benzodioxol-5-yl)methyl acetate 6c	132
D.13.7.8. Synthesis of 4-(acetoxymethyl)-2-methoxyphenol acetate 8c and 4-(hydroxymethyl)-2-methoxyphenol acetate 8d	133
D.13.7.9. Synthesis of 4-acetoxymethyl-2-methoxyphenol 7c ¹⁴⁸	135

E. References 136

Cited Literature.....	137
-----------------------	-----

Abstract

Aromatic aldehydes are important flavour and fragrance compounds and are used extensively in the food and perfume industry. They are accessible through various means but are traditionally synthesized by stoichiometric step-by-step procedures. The main drawbacks of these methods are the dependence on high amounts of auxiliary substances, which leads to the formation of considerable amounts of waste, and they are also time-consuming. Chemoenzymatic one-pot reactions represent a variable strategy to circumvent these issues. Among other things, the coupling of several transformations into one reaction sequence eliminates the necessity for the isolation of intermediates which reduces the amount of waste produced. Herein a proof of concept for two novel chemoenzymatic one-pot reaction sequences for the synthesis of aromatic aldehydes from a renewable feedstock is demonstrated. Natural occurring propenylbenzene derivatives were chosen as the ideal starting point. Route A incorporates one chemical transformation coupled to a three-step enzymatic cascade (Scheme 1).

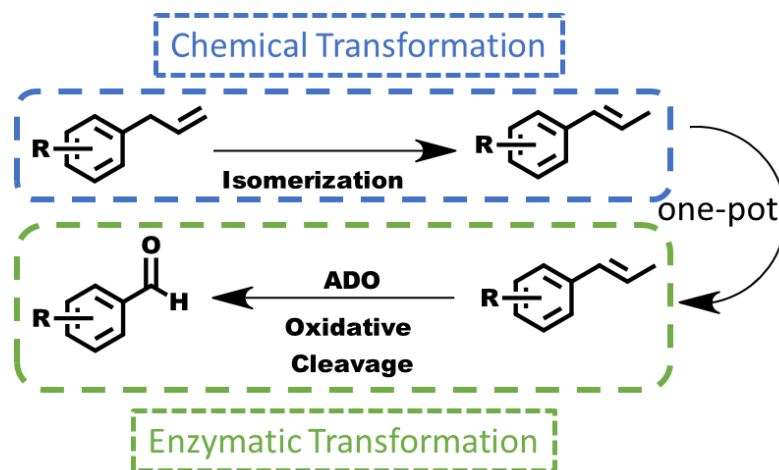


Scheme 1: Route A for the chemoenzymatic production of fragrance aldehydes.

In the first step, a Wacker oxidation transforms the propenylbenzene to the respective phenylpropan-2-ones. To enable the subsequent enzymatic reactions, biocompatible procedures from the literature were tested and optimized. The first enzymatic transformation in the form of a Baeyer-Villiger oxidation catalysed by a Baeyer-Villiger-monooxygenase (PAMO, TmCHMO) leads to the formation of the acetate ester. After subsequent hydrolysis by an esterase (PfeI) and oxidation of the formed primary alcohol by an alcohol dehydrogenase (AlkI) the desired aldehydes can be obtained. The enzymatic cascade was realized with a mixed culture approach

using whole-cell biocatalysis. The scope of the reaction sequence was demonstrated on eight natural and nonnatural 2-propenylbenzenes, and the respective aldehydes were obtained with varying yields.

Route **B** incorporates a chemical transformation which is coupled to an enzymatic step (scheme 2).

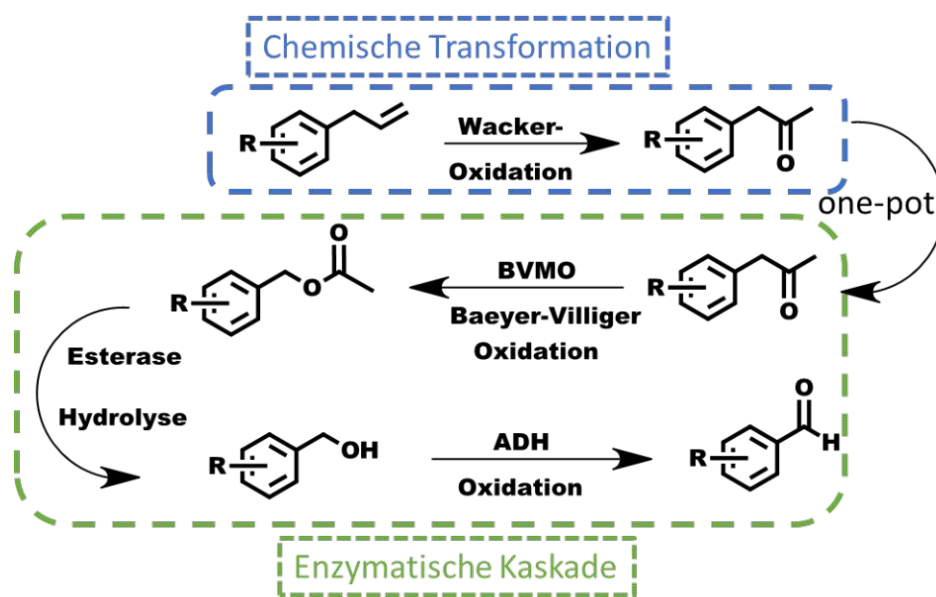


Scheme 2: Route B for the chemoenzymatic production of fragrance aldehydes.

The first step consists of a PdCl₂ catalysed isomerization of the terminal olefinic bond of a 2-propenylbenzene. For this, a convenient solvent-free method under mild conditions was utilized. The conjugated double bond is then enzymatically cleaved by an aromatic dioxygenase (ADO) to form the desired aldehyde. For the enzymatic step, whole-cell biocatalysis was used. Again, eight natural and nonnatural propenylbenzenes were tested. However, route B only allowed the conversion of isoeugenol to vanillin due to the limitation of the substrate acceptance of the enzyme.

Kurzfassung

Aromatische Aldehyde sind wichtige Aroma- und Duftstoffe und werden in großem Umfang in der Lebensmittel- und Parfümindustrie verwendet. Sie sind chemisch durch verschiedene Verfahren herstellbar, werden aber meist durch stöchiometrische Schritt-für-Schritt-Verfahren synthetisiert. Die Hauptnachteile dieser Methoden sind zum einen die Abhängigkeit von großen Mengen an Hilfsstoffen, wodurch es zur Bildung erheblicher Abfallmengen kommt, und zum anderen der hohe Zeitaufwand solcher Synthesen. Chemoenzymatische-Eintopfreaktionen stellen eine variable Strategie zur Umgehung dieser Probleme dar. Durch die Kopplung mehrerer Transformationen in einer Reaktionssequenz entfällt u.a. die Notwendigkeit der Isolierung von Zwischenprodukten, wodurch die Abfallmenge reduziert wird. In dieser Arbeit wird ein Konzeptnachweis für zwei neuartige chemoenzymatische Eintopfreaktionssequenzen zur Synthese aromatischer Aldehyde aus einem erneuerbaren Ausgangsstoff gezeigt. Als idealer Ausgangspunkt der Route wurden natürlich vorkommende Propenylbenzolderivate gewählt. Route A umfasst eine chemische Transformation, die mit einer dreistufigen enzymatischen Kaskade gekoppelt ist (Schema 1).

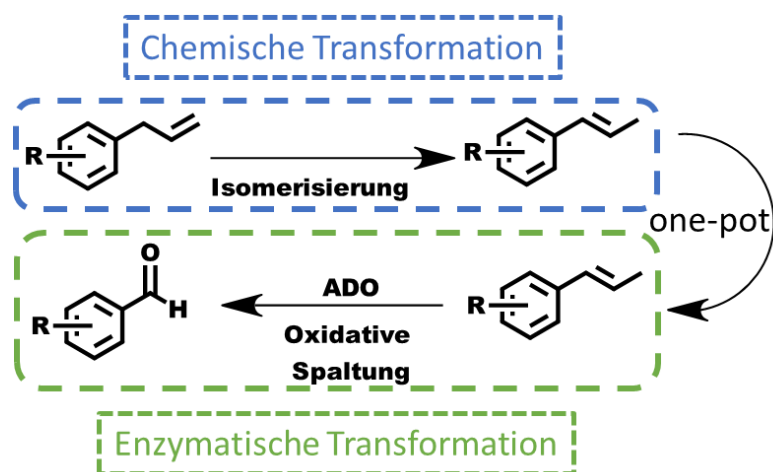


Schema 1: Route A für die chemoenzymatische Produktion von aromatische Aldehyden.

In der ersten Stufe werden die Propenylbenzole durch eine Wacker-Oxidation in die entsprechenden Phenylpropan-2-one umgewandelt. Um die nachfolgenden enzymatischen Reaktionen zu ermöglichen, wurden biokompatible Verfahren aus der Literatur getestet und optimiert. Die erste enzymatische Umsetzung in Form einer Baeyer-Villiger-Oxidation, katalysiert durch eine Baeyer-Villiger-Monooxygenase (PAMO, TmCHMO), führt zur Bildung des Acetatesters. Nach anschließender Hydrolyse durch eine Esterase (PfeI) und Oxidation des gebildeten primären Alkohols durch eine Alkoholdehydrogenase (AlkJ) können die gewünschten

Aldehyde gewonnen werden. Die enzymatische Kaskade wurde mit einem Mischkulturansatz unter Verwendung der Ganzzell-Biokatalyse realisiert. Die Anwendungsreichweite der Reaktionssequenz wurde an acht natürlichen und nicht-natürlichen Propenylbenzole demonstriert, und die entsprechenden Aldehyde konnten mit unterschiedlicher Ausbeute gewonnen werden.

Route B umfasst eine synthetische Umwandlung, die mit einem enzymatischen Schritt gekoppelt ist (Schema 2).



Schema 2: Route B für die chemoenzymatische Produktion von aromatische Aldehyden.

Der erste Schritt besteht aus einer PdCl₂-katalysierten Isomerisierung der endständigen olefinischen Bindung von Propenylbenzolen. Hierfür wurde eine einfache lösungsmittelfreie Methode unter milden Bedingungen verwendet. Die konjugierte Doppelbindung wird dann enzymatisch durch eine aromatische Dioxygenase (ADO) gespalten, um die gewünschten Aldehyde zu erhalten. Der enzymatische Schritt wurde unter Verwendung von Ganzzell-Biokatalyse durchgeführt. Auch hier wurden acht natürliche und nicht-natürliche Propenylbenzole getestet. Route B erlaubte jedoch nur die Umwandlung von Isoeugenol in Vanillin, aufgrund der niedrigen Substratakzeptanz des Enzyms.

Abbreviations

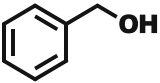
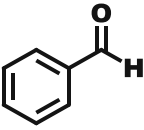
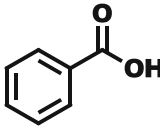
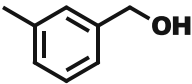
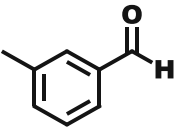
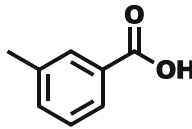
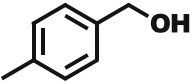
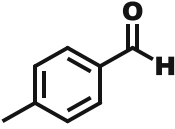
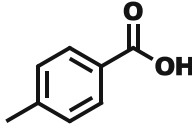
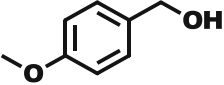
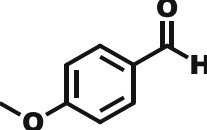
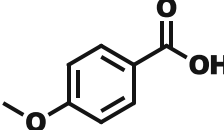
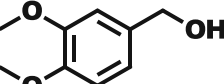
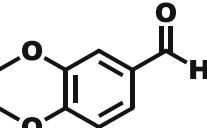
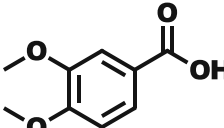
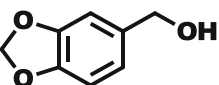
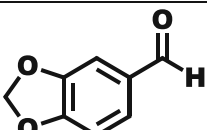
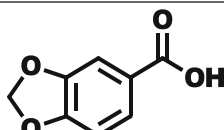
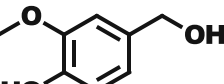
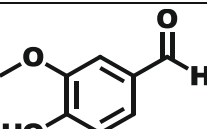
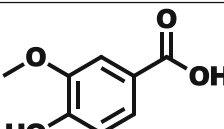
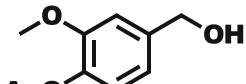
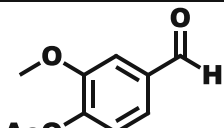
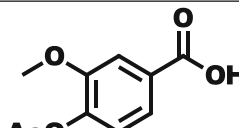
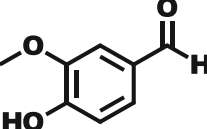
abs.	Absolute
ACN	Acetonitrile
ADH	Alcohol dehydrogenase
ADO	Aromatic dioxygenase
AlkJ	Alcohol dehydrogenase from <i>Pseudomonas putida</i>
Amp	Ampicillin
bp	Base pair
BVMO	Baeyer-Villiger monooxygenase
cam	Chloramphenicol
CAR	Carboxylic acid reductase
DMA	N,N-dimethylacetamide
DMF	N,N-dimethylformamide
DMSO	Dimethyl sulfoxide
DNA	Deoxyribonucleic acid
dNTP	Deoxyribonucleotide triphosphate mix
EC	Ethylene carbonate
ee.	Enantiomeric excess
EPR	Electron paramagnetic resonance
et al.	Et alii
EtOAc	Ethyl acetate
EtOH	Ethanol
<i>E. coli</i>	<i>Escherichia coli</i>
e.g.	<i>Exempli gratia</i>
FAD	Flavin adenine dinucleotide
FePcF ₁₆	Hexadecafluorophthalocyanine–Iron
GC	Gas chromatography
GMC	Glucose methanol choline oxidoreductases
HAPMO	4-hydroxyacetophenone monooxygenase from <i>Pseudomonas fluorescens</i>
H ₂ O	Water
IPTG	Isopropyl β-D-1-thiogalactopyranoside
iPrOH	Isopropanol
kDA	Kilodalton
Lac	Lactose
MeOH	Methanol
Mhz	Megahertz
ml	Millilitre
Mmol	Millimole
mM	Millimolar
mRNA	Messenger ribonucleic acid
NMR	Nuclear magnetic resonance
NAD(P)H	Nicotinamide adenine dinucleotide (phosphate)
NaOAc	Sodium acetate
NaTFA	Sodium trifluoroacetate
NOV1	Stilbene cleavage oxygenase from <i>Novophingobium aromaticorans</i>

NR	No reaction
OD ₅₉₀	Optical density at 590 nm
OYE1	Old yellow enzyme
PAGE	Polyacrylamide gel electrophoresis
PAMO	Phenylacetone monooxygenase from <i>Thermobifida fusca</i>
PBS-buffer	Phosphate buffered saline
Pd(dba) ₂	Bis-(dibenzylidenacetone)-palladium(0)
Pd(OAc) ₂	Palladium(II) acetate
Pd(TFA) ₂	Palladium(II) trifluoroacetate
PE	Petroleum ether
PfeI	Esterase from <i>Pseudomonas fluorescens</i>
PLE	Pig liver esterase
PMHS	Polymethylhydrosiloxane
ppm	Parts per million
PRC	Polymerase chain reaction
<i>p. putida</i>	<i>Pseudomonas putida</i>
RARE	reduced aromatic aldehyde reduction
rpm	Rotations per minute
rcf	Relative centrifugal force
rt	Room temperature
SDS	Sodium dodecyl sulphate
SOC medium	Super optimal broth medium with catabolite
TB medium	Terrific broth medium
T _a	Annealing temperature
tBuOH	tert-Butanol
tBuONO	tert-Butyl nitrite
T _m	Melting temperature
TmCHMO	Cyclohexanone monooxygenase from <i>Thermocrispum municipal</i>
UV	Ultraviolet
v	Volume
w	Weight
µg	microgram
µl	microliter

Compound Library

Substrates for the Wacker Oxidation (**1a - 8a**), substrates for the biocatalytic cascade (**1b - 8b**, **1g - 8g**), intermediates of the cascade (**1c - 8c**, **1d - 8d**) and products of the catalytic cascade (**1e - 9e**, **1f - 8f**)

	2-propenylbenzenes	Phenylpropanones	Benzyl acetates
1a		1b	1c
2a		2b	2c
3a		3b	3c
4a		4b	4c
5a		5b	5c
6a		6b	6c
7a		7b	7c
8a		8b	8c

	Benzyl alcohols	Benzaldehydes	Benzoic acids
1d		1e 	1f 
2d		2e 	2f 
3d		3e 	3f 
4d		4e 	4f 
5d		5e 	5f 
6d		6e 	6f 
7d		7e 	7f 
8d		8e 	8f 
		9e 	

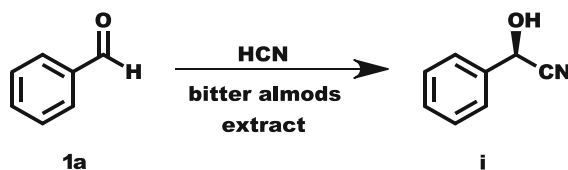
1-propenylbenzenes	
1g	
2g	
3g	
4g	
5g	
6g	
7g	
8g	
9g	

A. Introduction

A.1. Biocatalysis

A.1.1. Introduction to biocatalysis

Biocatalysis is the application of enzymes in traditional organic synthesis. ¹ The utilization of microorganisms in the form of fermentation for food production has played a significant role in the development of human civilization. ² It has been part of humanity's technological repertoire for thousands of years. One of the oldest examples can be found in ancient Egypt, where yeast was utilized to produce bread and beer almost 6000 years ago. ³ Although impressive, starting to unlock the full potential of enzymatic catalysis was only possible after advances in scientific research increased the knowledge of the components of living organisms. Eduard Bucher was the first to demonstrate that alcoholic fermentation is not directly performed by yeast itself but by soluble enzymes. ⁴ This is classified by some authors as the beginning of the "first wave of biocatalysis". Not soon after, Croft-Hill performed the first documented enzyme-catalyzed synthesis to obtain isomaltose using a yeast extract. ⁴ One other notable example is Rosenthaler's synthesis of (R)-mandelonitrile using bitter-almonds extract (scheme 3). ⁵



Scheme 3: Rosenthaler's synthesis of (R)-mandelonitrile.

The elucidation of biomolecular processes and their regulations on a genetic level opened the door to the second wave of biocatalysis around 1980 to 1990. ¹ Through mainly well-thought structure-based protein engineering but also through random mutagenesis, the substrate and product scope of enzymes applied in biocatalysis could be extended. ^{1, 6} This allowed the alteration microorganisms on a genetic level to obtain proteins that displayed different properties than their natural counterparts. Examples include applications in the manufacture of pharmaceuticals, such as in the cholesterol-lowering statin drugs, but also in the synthesis of various other precursors. ¹

In the late 1990s, the development of new directed evolution technologies for protein engineering marked the beginning of a new era for biocatalysis, also termed the third wave of biocatalysis. ¹ It allowed for the fast and rapid development of new enzyme variants with improved stability, substrate acceptance, and selectivity. With the increase in computational power in *silico* methods for protein design have also gained significant importance over the recent years. ⁷⁻⁸

A.1.2. Biocatalysis in organic synthesis

Similar to the evolution of living organisms, which frequently led them to the specialization for one specific ecological niche, enzymes followed a similar trajectory. Most metabolic enzymes are only able to catalyze one specific chemical conversion and often only for a limited number of substrates. The benefit of nature is apparent; increasing the selectivity means less undesired side reactions and allows the formation of highly complex metabolic routes with finely tuned mass balances.⁹⁻¹⁰ Their selectivity and specificity are oftentimes remarkable.¹¹ The high selectivity also proves to be a significant challenge for their application in synthetic chemistry. Traditionally, enzymes that catalyze a new type of chemical transformation or have the proper substrate scope were found in nature.¹²⁻¹³

Nowadays, development is also focused on protein engineering, and the adjustment of properties of a given enzyme is prevalent in biocatalytic research.¹ Despite all its limitations, biocatalysis has proven to be a valuable addition to traditional synthetic chemistry. Besides the obvious use cases like the deracemization of precursors and as toolboxes for asymmetric synthesis, industrial applications include the production of pharmaceuticals, flavors, fragrances, food, and much more.^{12, 14-16} Enzymes also allow the utilization of non-traditional carbon sources (e.g., ethanol, glucose, lignin) to synthesize more complex molecules or platform chemical.¹⁷⁻¹⁹

Combining multiple enzymes into reaction sequences can further expand the scope of biocatalytic transformations. Traditionally, enzymes had the drawbacks of low solvent tolerance and temperature stability.²⁰ Since modern developments in synthetic chemistry push toward using more sustainable procedures, these issues have become more and more irrelevant. Enzymes are inherently “green”; they are degradable and renewable, their optimal reaction solvent is water, and they work best in milder (thus less energy-intensive) reaction conditions.²⁰

Including the disconnections found in enzymatic catalysis into the retrosynthetic repertoire also enables the design of new synthetic routes and novel reaction sequences.²¹ They are generally shorter since protecting groups can often be avoided due to their high chemoselectivity.¹² In conclusion, a more consistent application of biocatalysis in organic synthesis would lead to greater atom efficiency, waste reduction, and the overall improvement of synthetic chemistry.

A.1.3. Recombinant protein production

For the production of heterologous proteins, new genetic material, mainly in the form of vectors, is introduced into a host *via* genetic engineering. Besides the gene of interest these vectors contain for example, modified versions of *lac*-operons (and the *lac*-repressor) which can be used to control the recombinant protein production through the addition of an inducer (IPTG)²². They are constructed with cloning techniques. Depending on the complexity of the vector, different

methods can be used. Traditional restriction enzyme based cloning is an old, time-consuming but reliable method. It is dependent on suitable restriction sites in the vector as well as in the insert.²³ Also, more advanced cloning techniques in the form of Gibson assembly or Golden Gate cloning can be applied for more complex vectors.²⁴⁻²⁵

For the design of the vectors, the formation of secondary structures of primers and fragments obtained by polymerase chain reaction (PCR) and the stability of mRNA transcripts have to be considered.²⁶ The host should be suitable for recombinant gene expression and protein production. That means the genetics of the organism need to be understood and display a low mutation rate. The two most used microorganisms are *Escherichia coli* (*E. coli*) and *Pichia pastoris*.²⁷⁻²⁸ They display rapid growth in a relatively cheap growth medium in undemanding growth conditions.

For the co-expression of more than one gene, the vector can be constructed in a polycistronic operon configuration (single promoter and terminator), pseudo-operon configuration (two promoters and one terminator), or a multiple monocistronic operon configuration with individual promoters and terminators for each gene (figure 1).²⁶

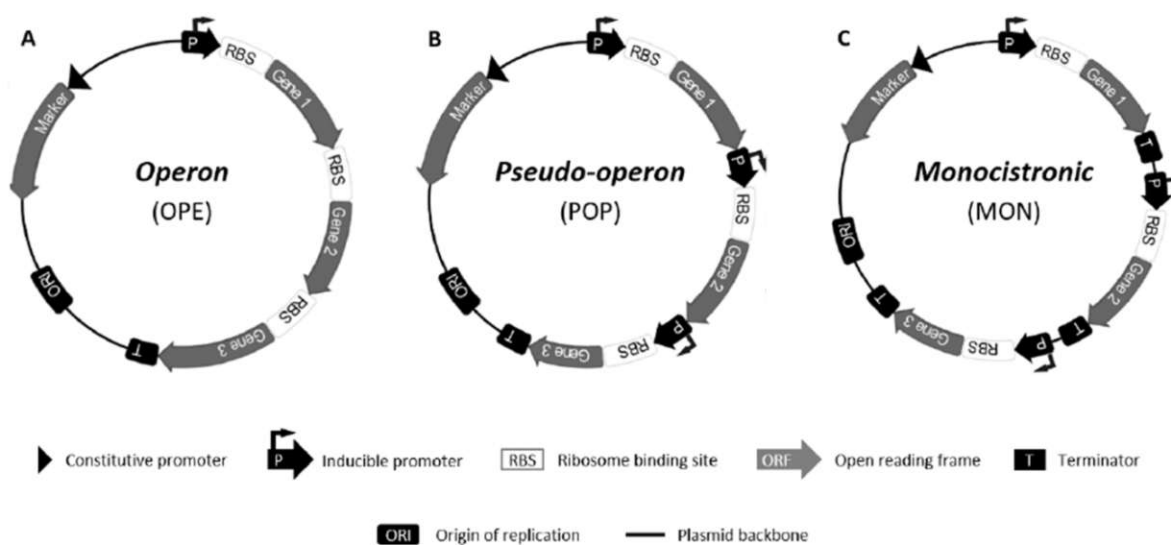


Figure 1: Plasmid configurations used in the construction of expression vectors. (A) Operon configuration harbors two target genes with only a single set of promoter and terminator. (B) In the pseudo-operon configuration, the expression of the target genes is controlled by two individual promoters and one terminator. (C) In the monocistronic configuration, each of the target genes has its own set of promoter and terminator. The figure was taken from Bayer et al.²⁹

A.1.4. Types of biocatalysts in organic synthesis

Depending on the scale of the biotransformation, type of the chemical transformations, and cost factors, biocatalysis can be performed *in vivo* (whole-cell biocatalysis) or *in vitro* (soluble enzymes, immobilized enzymes, or lyophilized enzymes).³⁰⁻³¹

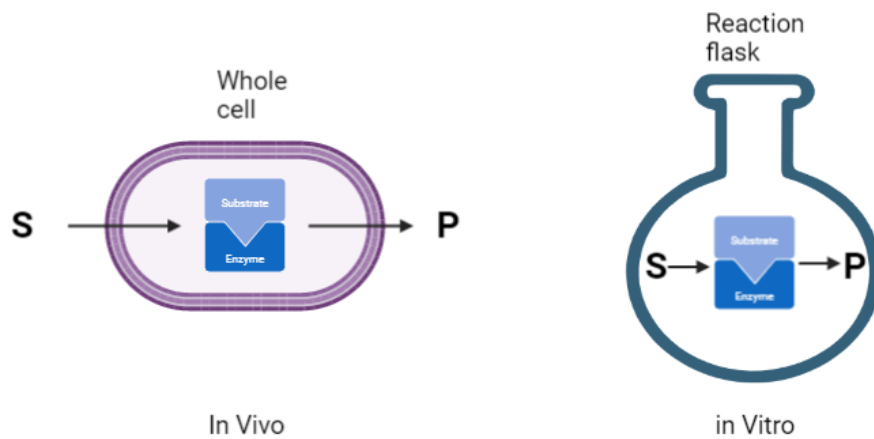


Figure 2: Types of Biocatalysts in organic synthesis. Whole-cell biocatalysis makes the membrane transport of the substrate in and out of the cell necessary. In Vitro biocatalysis uses a soluble enzyme for the transformation of the substrate in a reaction flask. Figure constructed with Biorender.com.

In *in vitro* techniques, the desired protein is separated from the organism used for protein production by cell lysis and centrifugation to generate cell-free extract containing the soluble enzyme. This crude cell extract can be used directly for catalysis, or the enzyme is further purified (e.g., affinity chromatography), separating the different soluble components of the cell extract.³¹ This soluble enzyme can also be immobilized to a solid support to increase stability and facilitate separation/recycling after the conversion. Immobilization is achieved *via* covalent bonding to a solid support, or the enzyme can be entrapped in a polymer matrix.³² The main advantage in the application of purified enzyme is the prevention of undesired side reactions during the biotransformation.³¹ However, purification and immobilization of the enzymes is a time-consuming process and whole cell biocatalysts are therefore generally less cost intensive to produce.³⁰

In *in vivo* techniques (whole-cell biocatalysis) directly employ the microorganism as a biocatalyst without further purification of enzyme. Whole-cell biocatalysis is performed with resting cells. These cells have been washed and resuspended in a suitable buffered medium, adjusting the pH and removing all unnecessary components of the growth medium. Resting cells are in a not replicating state but still offer an active metabolism that can be additionally stimulated with the addition of glucose to the resting-cell medium.³⁰ Since many enzymes require cofactors for a given transformation, whole-cell biocatalysis is an easy and cost-effective way to recycle the necessary reaction components *via* the host's metabolism.³⁰ In contrast, cofactor recycling is omitted entirely *via* stoichiometric amounts of cofactors, or recycling systems have to be employed in the case of *in vitro* catalysis.³³ Using stoichiometric amounts of cofactors is hardly ever feasible due to the high cost. Recycling systems can be implemented by, e.g., the coupled substrate method or by the coupled enzyme method using a sacrificial substrate as an electron donor/acceptor.³⁴ In the first case, the enzyme must be capable of also catalyzing the reverse

reaction (e.g., reductions of alcohols catalyzed by alcohol dehydrogenases with Isopropanol as the sacrificial substrate). In the latter case, a second enzyme is used to catalyze the reverse reaction using a sacrificial substrate and thus recycle the co-factor (e.g., glucose dehydrogenase with glucose as sacrificial substrate).

In the case of *in vitro* biotransformation, depending on the reaction parameters, stability issues may arise due to the exposed nature of the enzyme, whereas in whole-cell biocatalysis, the cell-membrane protects the enzymes from harsh external conditions.^{30, 35} The downside is that the reaction components like substrates and products also need to be transported through this barrier. This can lead to mass transport issues in and out of the cells and can also lead to the accumulation of reaction components, increasing the risk for further metabolization or cross-reactivity.³¹

Additionally, two-phase biocatalysis can be performed. A non-miscible organic phase is used to accumulate the formed product or act as a reservoir for the substrate preventing undesired side reactions.³⁶ The drawback comes in the form of an extra product separation step after the reaction.

A.1.5. Enzymatic transformations

Enzymes can catalyze a plethora of different transformations (figure 3).³⁷ They range from C-C bond formations catalyzed by aldolases (A) to the oxidation or reduction of functional groups performed by alcohol dehydrogenases (B), carboxylic acid reductases (C) or ene-reductases (D). The hydrolysis or formation of different carboxylic acid derivatives (e.g., esters, amines) is also an important enzymatic transformation with synthetic applications (E). Unusual reactions in the form of the Baeyer-Villiger-Oxidation (F), the oxidative cleavage of C-C bonds (G), or the incorporation of halogens into substrate molecules (H) are also part of the enzymatic repertoire.³⁷ In the following chapters, enzymes that were used in this scientific work are described in more detail.

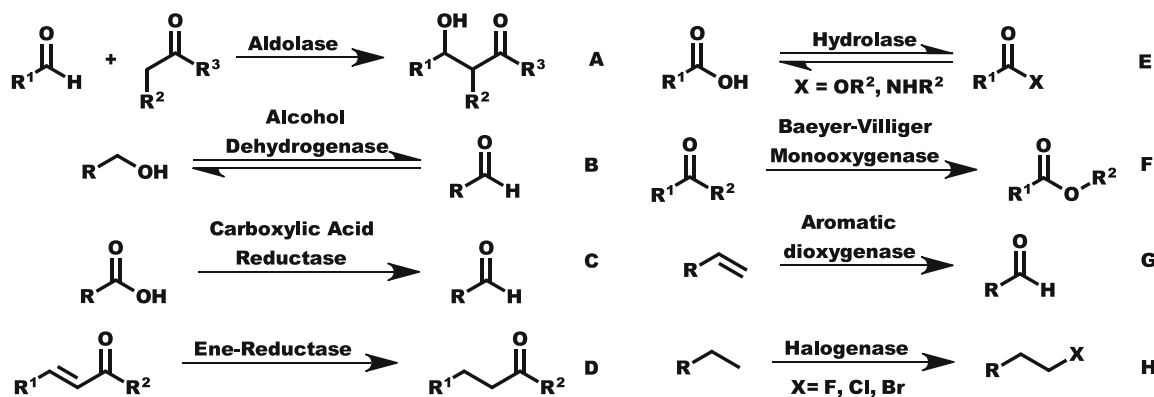
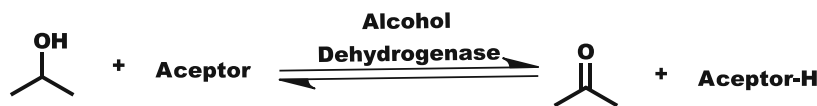


Figure 3: Brief overview of the possible chemical transformations that can be catalyzed by enzymes.

A.1.5.1. Alcohol Dehydrogenases

Alcohol dehydrogenases (ADHs) (E.C. 1.1.1.X) are enzymes that catalyze the oxidative transformation of alcohols to the respective carbonyls with the reduction of an electron acceptor (scheme 4).³⁸

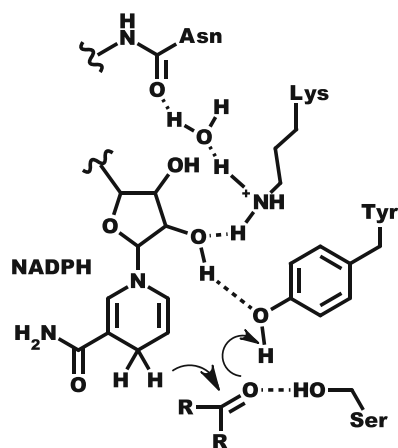


Scheme 4: Enzymatic transformation catalyzed by an ADH. The acceptor can be in the form of NAD(P)⁺.

Many of them are also able to catalyze the reverse reaction. ADHs are abundant in nature and can be found microorganisms such as fungi and bacteria but also in animals and plants.³⁹ This leads to great structural and mechanistic diversity.

Depending on the type of electron acceptor, ADHs can be classified into three groups: NAD(P)-dependent alcohol dehydrogenases, NAD(P)-independent alcohol dehydrogenases, and FAD-dependent alcohol dehydrogenases.³⁹ They belong to the enzyme family of oxidoreductases together with FAD-dependent alcohol oxidases, which use molecular oxygen for electron transfer yielding H₂O₂.⁴⁰ The first class of ADH can be further subdivided depending on the catalytic metal that is needed for the reaction (i.e., zinc-dependent, zinc-independent, and iron-activated).³⁹ The second class of ADH utilizes variations of pyrroloquinoline quinone (PQQ) or coenzyme F₄₂₀ as co-factors for the enzymatic conversion.⁴¹ FAD-dependent ADHs (as found in the glucose-methanol-choline (GMC) oxidoreductase superfamily, e.g., choline dehydrogenase from *E. coli*) employ a variety of quinones (e.g., ubiquinone), phenol radicals or metal ions for the electron transfer and have low reactivity towards molecular oxygen, which sets them apart from alcohol oxidases.^{42,43}

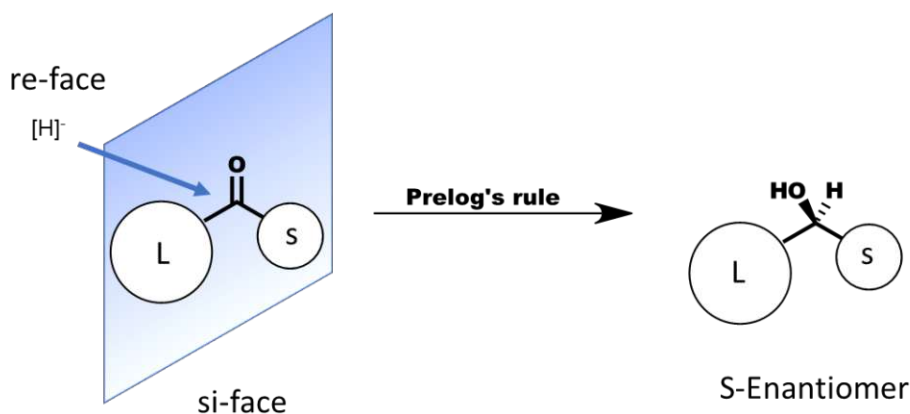
Due to the wide variety in ADHs, there is no general mechanism describing the catalytic mode of action. For example, for the reduction of ketones, NADPH-dependent short-chain ADHs rely on a delicate network of hydrogen bonds in their active site (scheme 5).³⁸



Scheme 5: Active site of a short-chain reductase/dehydrogenase catalyzing the hydride transfer from NADPH to a carbonyl compound. The scheme was taken from An et al.³⁸

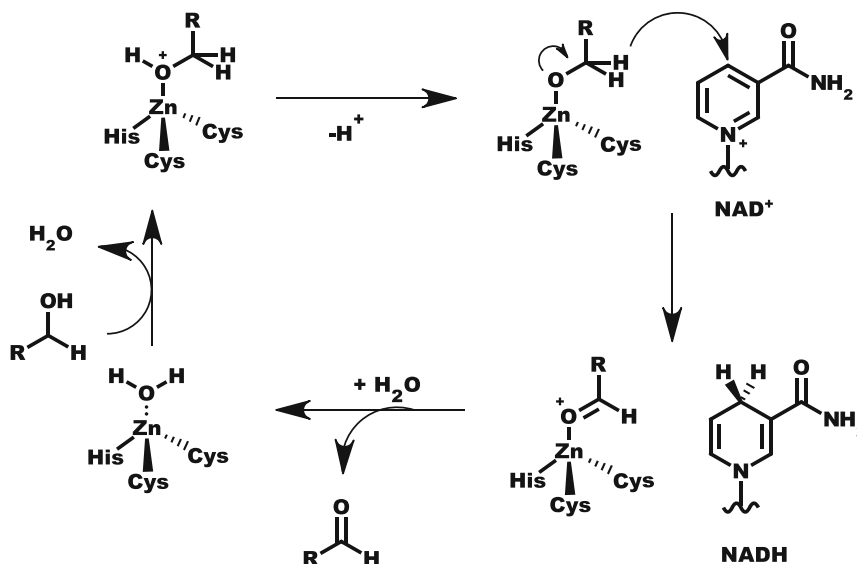
This hydrogen bonding from various amino acid residues, which form in this case a catalytic tetrad, accomplishes various objectives. For one, the serine residue binds the substrate in close proximity to the cofactor allowing the hydride transfer.³⁸ The highly conserved tyrosine residue acts in the form of an acid for protonation, stabilizing the alkoxide formed after hydride transfer.³⁸ This is facilitated by hydrogen bonding of the lysine residue, which leads to a decrease in the pKa of the hydroxyl group of tyrosine, increasing the acidity.³⁸ In the case of the reverse reaction, the alcohol is also activated in the same manner by these residues.

For the reduction of ketones, enantioselectivity is strongly dependent on the spatial arrangement of the substrate-binding pocket but also on the substituents of the substrate.³⁸ This allows for the selective transfer of either the pro-R or pro-S hydride of NADPH to one of the prochiral faces of the carbonyl functionality.³⁸ Depending on the enantiomeric outcome of the reaction, ADHs can be further classified into those that follow Prelog's rule and those that do not follow the rule (scheme 6).⁴⁴



Scheme 6: To follow Prelog's rule, the hydride must be transferred from the re-face of the prochiral ketone leading to the S-enantiomer.⁴⁴

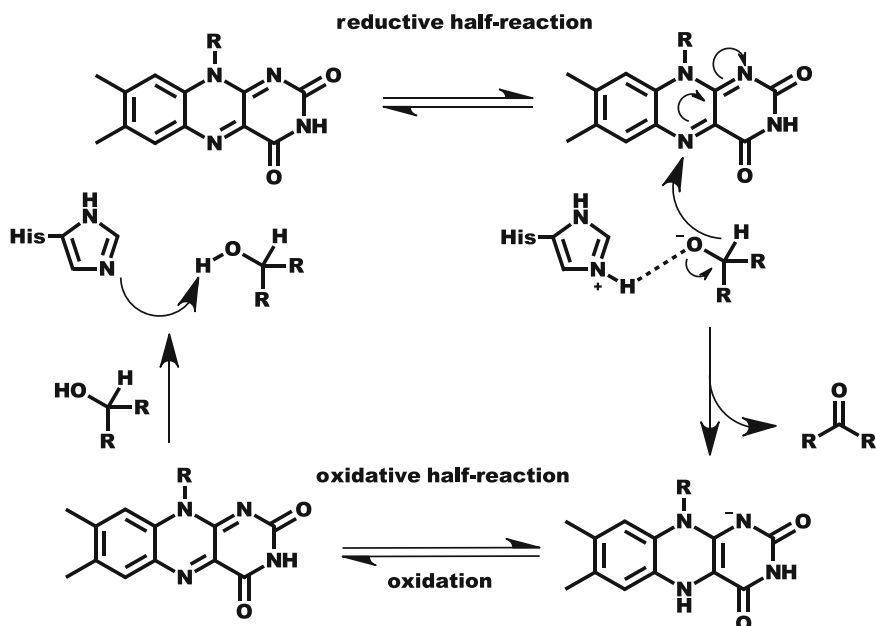
Zinc-dependent alcohol dehydrogenases (e.g., liver alcohol dehydrogenases) act similarly. In this case, the Zinc metal (coordinated to cysteine and histidine residues in the active site) activates the alcohol as a Lewis acid allowing the subsequent hydride transfer to NAD^+ and generating the carbonyl functionality (scheme 7).⁴⁵



Scheme 7: Oxidation of alcohols by liver alcohol dehydrogenase. The scheme was adapted from Parkin.⁴⁵

In contrast, FAD-dependent alcohol dehydrogenases consist of a conserved FAD-binding domain in the form of, e.g., a Rossman fold coupled to a variable substrate-binding domain.⁴² The active site is additionally decorated with an oftentimes conserved histidine amino acid residue pair that takes the role of the proton shuttle.⁴² Their mechanistic pathway is similar to FAD-dependent oxidoreductases.

Generally, the catalytic cycle can be separated into a reductive and an oxidative half-reaction (scheme 8).⁴³ In the reductive half-reaction, the alcohol is activated by hydrogen bonding with the histidine residue, followed by a hydride transfer to the FAD cofactor, which is reduced as a result. After the expulsion of the formed carbonyl compound, the reduced FADH is oxidized back to its active catalytic form in the oxidative half-reaction.⁴³ In the case of alcohol oxidases molecular oxygen is employed as oxidizing agent, ultimately forming H_2O_2 .⁴² In the case of ADHs alternative electron acceptors are employed as mentioned above. For example, the proposed electron acceptor for AlkJ from *pseudomonas putida*, a FAD dependent alcohol dehydrogenase, is ubiquinone coupled further to the respiratory chain of the bacterium.⁴⁶

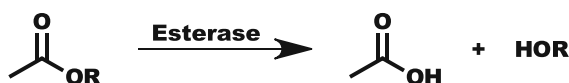


Scheme 8: Mechanism of FAD-dependent ADHs. The scheme was adapted from Wongnate et al. ⁴³

ADHs are used industrially for fermentation processes to produce alcohol and vinegar. ⁴⁷ Synthetically they are employed in the enantioselective reduction of various ketones to produce chiral alcohols. ⁴⁴ Additionally, since many ADHs display a different enantiomeric reaction rate, they are also used in the kinetic resolution of various ketones.

A.1.5.2. Esterase

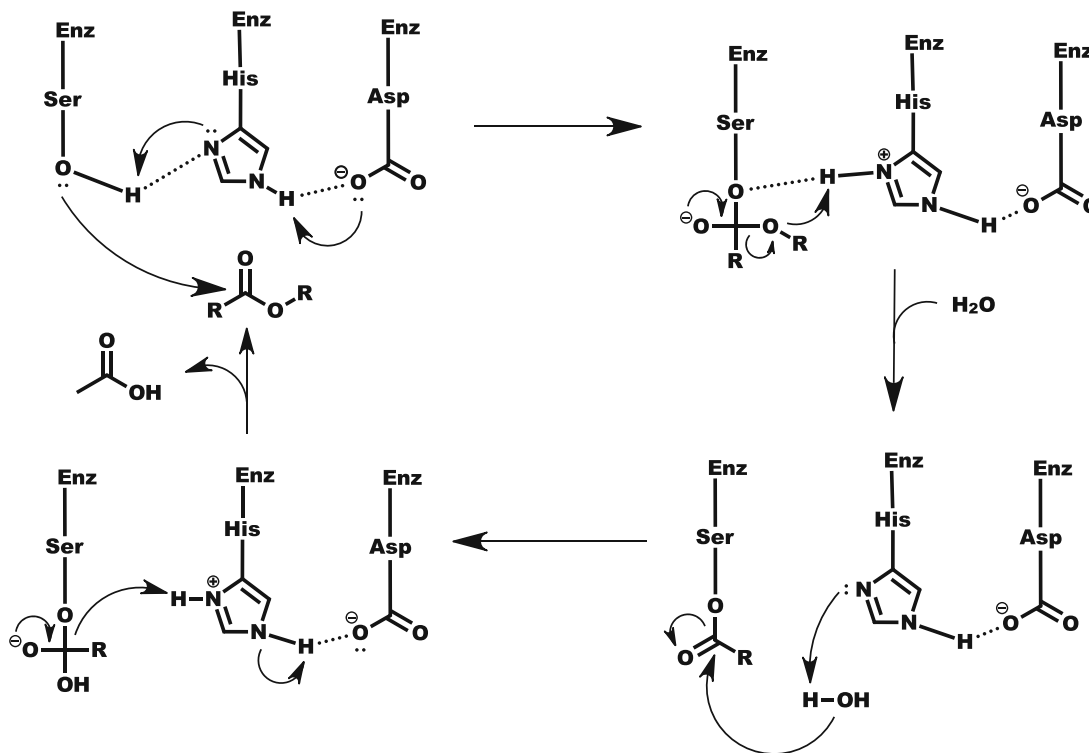
Esterase (EC 3.1.1.3) are part of the enzyme-class family of hydrolases and can widely be found in microorganisms (bacteria, fungi), plants, and animals. ⁴⁸ They are responsible for the hydrolysis of a diverse group of esters, allowing the utilization of different carbon energy sources for the organism (scheme 9). ⁴⁸



Scheme 9: Hydrolysis of an ester catalyzed by an esterase.

In organic synthesis, they are a valuable enzyme class and are used extensively for the hydrolysis of different esters. Since many of them also display high degrees of stereospecificity, one of their primary applications also includes the kinetic resolution of racemic acetates and alcohols and play an essential role in the synthesis of enantiopure compounds. ⁴⁹⁻⁵⁰ For some esterases, the enantioselective behavior can be predicted by Kazlauskas rule. ⁵¹ Their catalytic activity is a result of a highly ordered active site consisting of amino acid residues, which are arranged in specific manner, called the catalytic triad. ⁵² These residues, which are oftentimes a combination of the

amino acids *Ser-Asp-His*, are arranged in a way that allows for efficient intramolecular H-bond transfer. This enables the stabilization of the transition states but also the activation of the nucleophile, accelerating the reaction.⁵³ The proposed mechanism for this reaction is depicted in reaction scheme 10 and is described in more detail in the following section.⁵²



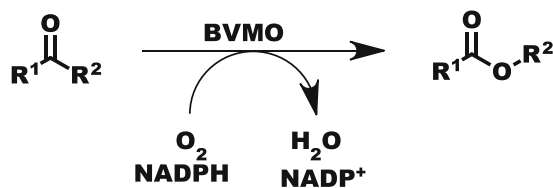
Scheme 10: Mechanism for the hydrolysis of an ester facilitated by the catalytic triad in the active site of the enzyme.⁵²

Firstly, the substrate, located in the active site, is bound to the activated hydroxy group of the serine residue following a S_N2 reaction mechanism. This enzyme substrate complex is stabilized by hydrogen bonding from the histidine and aspartate residues. Additionally, the oxyanion, which is formed during the nucleophilic addition step, is further stabilized by the oxyanion hole in the active site of the enzyme (not depicted in scheme 10).⁵² The sp^3 -tetrahedral intermediate then collapses, releasing the alcohol and forming an acyl-enzyme complex. Subsequently, a nucleophile – water in the case of hydrolysis or alcohol in the case of transesterification – activated by hydrogen bonding attacks the carbonyl carbon atom by a nucleophilic attack, again forming a tetrahedral intermediate. After the release of the product, the catalytic cycle can begin anew.⁵²

The traditional Michaelis-Menten theory can best describe their catalytic activity, which sets them apart from other hydrolases like lipases in aqueous medium.⁴⁸ Examples of prominent enzymes would be the pig liver esterase and the esterase from *Pseudomonas fluorescens*.⁵⁴

A.1.5.3. Baeyer-Villiger-Monooxygenase (BVMOs)

Baeyer-Villiger-Monooxygenases (EC 1.14.13.xx) belong to the family of flavoprotein monooxygenases.⁵⁵⁻⁵⁶ Depending on the class of BVMO, most of them are FAD and NADPH dependent and catalyze the enzymatic insertion of molecular oxygen into a substrate molecule. For example, they catalyze the Bayer-Villiger-Oxidation of ketones to the respective esters but also the oxidation of heteroatoms in sulfides or amines (scheme 11).⁵⁵

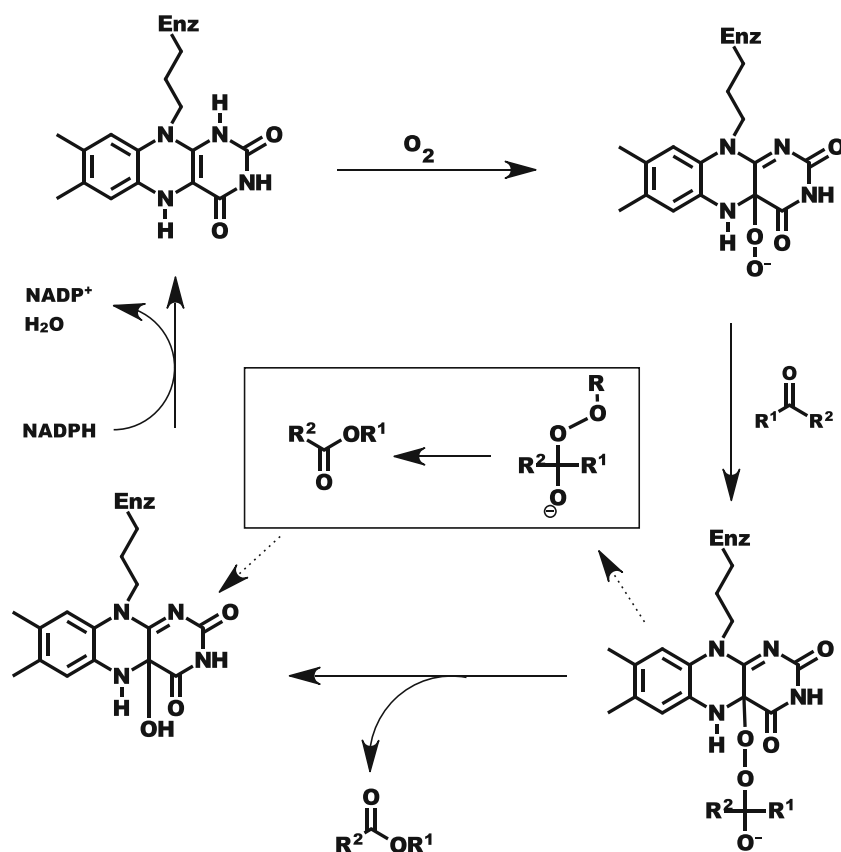


R¹,R²= aliphatic, aromatic

Scheme 11: Baeyer-Villiger oxidation of a ketone catalyzed by a BVMO.

Over the last couple of years, BVMOs have attracted much attention due to the desire to replace wasteful synthetic methods with more environmentally benign alternatives.⁵⁵ In contrast to BVMOs, which use molecular oxygen as the oxidizing agent, the synthetic variant of this transformation relies on the application of heat and shock-sensitive hydroperoxides or peroxy acids.⁵⁵ Besides their tendency to decompose violently, they also lead to the formation of hazardous waste oftentimes in stoichiometric amounts.^{55, 57} Practically, hydroperoxides oftentimes also suffer from difficult separability from the final product, making the reaction procedure more elaborate.

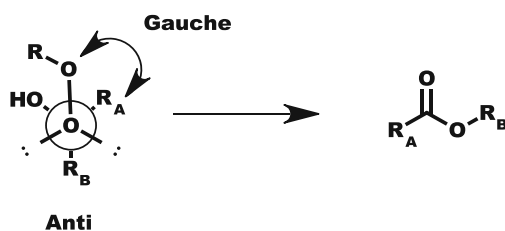
BVMO consists of a multidomain protein structure composed of a FAD-binding domain, an NADP-binding domain, and a helical domain.⁵⁵ The proposed mechanism for their mode of action can be found in scheme 12 and is described in more detail in the following section.⁵⁵



Scheme 12: Mechanistic pathway of a BVMO oxidizing a ketone. Scheme adapted from Fürst et al. ⁵⁵

The catalytic cycle is initiated by the radical reaction of molecular oxygen with the reduced FAD on the C4-position of flavin. A nucleophilic attack from the deprotonated peroxy group to a suitable carbonyl compound leads to the formation of a tetrahedral intermediate. Subsequently, through a concerted migration step, the intermediate collapses, leading to the formation of the product and the cleavage of the O-O bond. The catalytic cycle is closed by the reduction of flavin by NADPH. ⁵⁵

The migration tendency of the substituents generally follows the rules from synthetic Baeyer-Villiger-Oxidation. As a rule of thumb, the carbon atom that is able to stabilize cationic charge best has the highest migratory potential. ⁵⁸ The reaction outcome can also be explained by stereoelectronic and steric effects. The C-C bond, which stands antiperiplanar to the peroxy C-O bond in the intermediate of the reaction, display the greatest migration tendency. ⁵⁹ Due to steric interactions between the substituent in the gauche position with one of the oxygen atoms of the peroxy group, the bulkier substituents generally adapt the antiperiplanar position in non-cyclic substrates (scheme 13). ⁵⁸ Additionally, this orientation allows for the strongest orbital interactions between the two atoms involved in the migration process. ⁵⁸



Scheme 13: Gauche interaction leads to a conformation in which the bulkiest group (which is oftentimes the most substituted carbon atom) adopts the anti position. Scheme adapted from Snowden et al. ⁵⁹

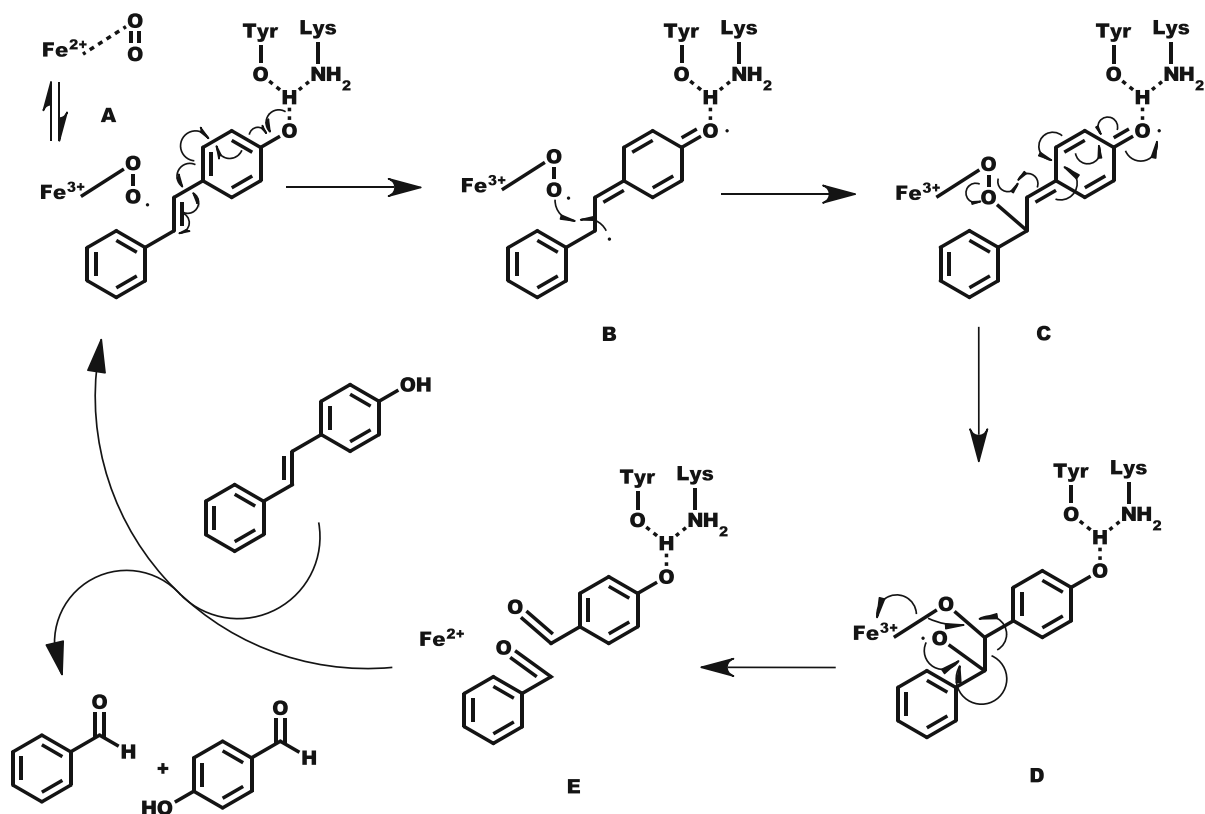
In enzymes, this arrangement can additionally be influenced by steric restraints imposed by the enzyme on the substrate during the nucleophilic attack or afterward on the formed FAD-substrate intermediate. These intermolecular steric restraints allow in the enzymatic Baeyer-Villiger-oxidation for the formation of products that are chemically not accessible. ⁶⁰

A.1.5.4. Aromatic dioxygenase (ADO)

ADO or aromatic dioxygenase is an enzyme discovered by Ni et al. in the thermophilic fungus *Thermothelomyces thermophila*. ⁶¹ It supposedly belongs to the family of carotenoid oxygenases (44 % amino acid identity with CsO2 from *Caulobacter segnis*). ⁶¹ Among other things, dioxygenases catalyze the enzymatic cleavage of olefinic bonds to form the respective carbonyl compounds and are utilized by, e.g., mammals for the enzymatic cleavage of β -carotene to form retinal and retinol. ⁶²⁻⁶³ In contrast to heme-dependent dioxygenases, they utilize a non-heme iron group (or a different metal) for the activation and insertion of molecular oxygen. ⁶⁴

Mechanistic insight into the enzymatic oxidative cleavage performed by these dioxygenases was gained by a study by McAndrew *et al.* (scheme 14) which is described in more detail in the following section. ⁶⁵ They were successfully able to obtain X-ray structures of NOV1 (stilbene cleavage oxygenase from *Novophingobium aromaticicorans*) in complex with its substrate (resveratrol) and product. From this and additional EPR analysis (electron paramagnetic resonance), they elucidated that the active site consists of a Fe^{2+} cofactor bound to four histidine amino acid residues. Molecular oxygen is activated by the iron and bound in a side-on fashion (A). This formed Fe^{3+} -oxygen radical then reacts with the conjugated double bond of the substrate *via* a radical reaction. The olefinic bond can additionally be activated by hydrogen bonding of the 4-hydroxy group with a tyrosine and lysine residue located in the active site. This leads to delocalization of electron density towards the olefinic carbon atom reacting with the Fe^{3+} -oxygen electrophile (B). After subsequent electron rearrangements (C), the C-C bond is cleaved, which leads to the formation of the carbonyl functionality (F).

However, the authors state that, although this mechanistic mode of action is supported by crystallographic (spatial arrangement of the active site) and spectroscopic data (formation of intermediate A), a different reaction mechanism could also be feasible. ⁶⁵



Scheme 14: Catalytic cycle for the oxidation of resveratrol catalyzed by NOV1. The scheme was adapted from McAndrew et al.⁶⁵

In contrast to traditional chemical oxidative cleavage (e.g., Ozonolysis), enzymatic oxygenases are able to differentiate between different olefinic bonds in the same substrate. This allows for the synthesis of products that are difficult to obtain by chemical means.⁶⁶

So far, oxygenases have been used industrially for the production of e.g., various precursors for the pharmaceutical industry, like hydroxylated steroids.⁶⁷ However, their application often faces hurdles due to their limited stability, elaborate purification procedures, and low substrate promiscuity⁶⁷. Nevertheless, recently carotenoid oxygenases have been employed for the valorization of lignin-derived compounds. For example, ADO is able to catalyze the co-factor-free oxidative cleavage of isoeugenol to vanillin.⁶¹

A.2. Cascade and one-pot reactions

A.2.1. Classification

Cascade reactions are multistep conversions in which a product is formed through the stepwise consecutive transformation of chemical functionality without the need for separation or isolation of the reaction intermediates. Each chemical conversion is dependent on the previous one and occurs spontaneously after the preceding transformations have taken place. In other words: the

reactions become “entangled.” If each step is conducted under the same reaction conditions and no new reagents are added after the starting point, then the cascade is performed in concurrent mode. Cascade reactions performed in sequential mode (or one-pot reactions) are similar in the fact that two or more chemical transformations are coupled together to form a product without the isolation of the reaction intermediates. However, they allow the addition of new reagents after the initial step and also the change of the reaction conditions. ⁶⁸⁻⁷⁰

Depending on the type of reactions a cascade reaction is composed of, a distinction is mainly made between multi-enzymatic (or just enzymatic), chemoenzymatic, and purely chemical cascades (or one-pot reactions). The first example consists of only enzymatic transformations, while the latter incorporate “synthetic” transformation into the reaction sequence. ⁶⁹

A.2.2. Advantages of cascade reactions / one-pot reactions over traditional synthesis

The following section is mostly based on the review of Bruggink et al. ⁷¹

Traditional organic synthetic chemistry i.e., chemistry that is performed by humans, follows the basic step-by-step principle (figure 4). This means that in a multistep synthetic route, a starting material A is converted into an intermediate B which has then to be isolated and purified for the following steps. This, of course, needs to be repeated for each step of the synthetic route. The reactions characteristics are oftentimes moderately high concentrations of the reaction components, and the prevalent stoichiometric steps are often combined with catalytic steps. Selectivity in these types of reactions is oftentimes an issue due to competing side reactions. The consequences are that high amounts of auxiliary substances (i.e., solvents, reagents) are necessary for each gram of synthesized product. This, of course, leads to the generation of waste and is also highly energy intensive.

In contrast, most natural compounds are synthesized by nature in a multistep-cascade reaction, mainly in the cells of living organisms. This allows to convert a starting material A into the final product C without the necessary isolation and purification of respective intermediate B. The selectivity of those biosynthetic pathways is oftentimes remarkable. Nature achieves this by keeping the concentration of each reaction component and product low to prevent the formation of side products, and also conversions are catalyzed by highly evolved and selective enzymes. The formed product is removed by specialized transport systems allowing for high throughputs and helping to drive thermodynamic equilibria in a certain direction. In summary, entangling reactions steps into a cascade decreases reaction time, the quantity of auxiliary substances, and waste produced.

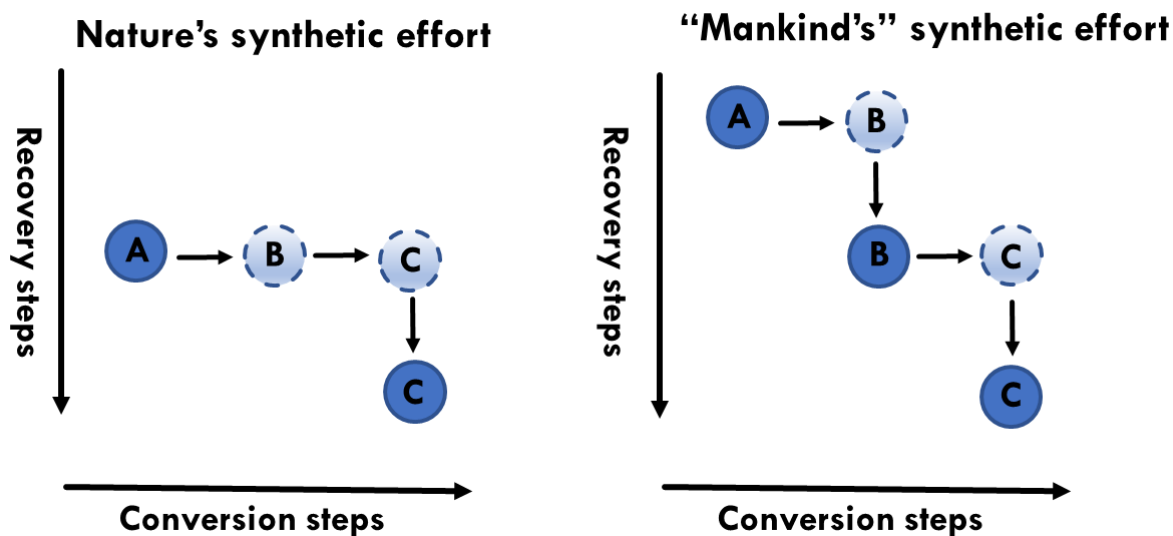


Figure 4: Comparison between nature's synthetic to mankind's synthetic effort. Figure adapted from Bruggink et al. ⁷¹

Over the last couple of years, there has been a growing consciousness in the chemical industry but also in academics about the environmental impact of chemistry. ⁷² Of course, increasing the sustainability of a whole industry is a difficult task to achieve, and new strategies and ideas need to be found. One solution is to replace wasteful synthetic procedures with environmentally benign alternatives. This includes the replacement of stoichiometric with catalytic procedures but also the consequent implementation of cascade reactions into synthetic routes. ⁷² Especially attractive is the combination of several enzymatic transformations since enzymes are seen as intrinsically environmentally benign. ⁶⁹ Also, due to the fact that life is only possible in a limited parameter range, their transformation conditions are mostly compatible with each other. ⁶⁹ Even though there is an immense variety in enzymatic transformations found in nature, not all chemical transformations can be replaced by enzymatic reactions. Therefore, compromises need to be found. These compromises can be in the form of nature-inspired organic chemical synthesis – the combination of chemical and enzymatic conversions in a one-pot or cascade fashion. Since most chemical reactions are inherently, bio-incompatible alternative conversion procedures need to be developed.

A.2.3. Designing a chemoenzymatic one-pot reaction

Many factors need to be considered for the successful design and implementation of a chemoenzymatic one-pot reaction. ^{70, 73} For example, the design of the reaction sequence itself, the mode of the chemoenzymatic transformation, and how the biocatalytic system is implemented. After selecting the desired target compound, the cascade is designed by retrosynthetic analysis, but for simpler molecules, forward synthetic planning (from a specific

starting point) can also be performed. Each intermediate and every step in the reaction sequence needs to be carefully selected based on the availability of enzymes capable of catalyzing the transformation and the stability and cross-reactivity of each intermediate. Lastly, thermodynamic factors in the form of chemical equilibria, pH, and the solubility of the substrate, intermediates, and product in the reaction media need to be considered for the enzymatic steps.⁷⁴

The chemoenzymatic reaction sequence can be conducted in a one-pot fashion or in the form of a true cascade.⁷⁰ In the first case, the chemical reaction and the enzymatic transformation occur sequentially and can be conducted under different reaction conditions such as pH, temperature, and new reagents can be added after the initial step. In the latter case, the chemical transformation and the enzymatic transformation occur concurrently, as described above.⁷⁰

Due to the limited parameter tolerance of most enzymes, the chemical reaction must be performed under bio-compatible reaction conditions. This means a low amount of organic solvent and the reaction components either need to be separated after the chemical transformation or display low reactivity towards the biocatalyst.⁷³ The enzymatic transformation can be performed *in vivo* or *in vitro* (see chapter A.1.5).³¹

If the reaction sequence consists of more than one enzymatic step, then co-expression to produce more than one enzyme in a single host cell is necessary for whole-cell biocatalysis.²⁶ Additionally, it is also possible to express the enzymes individually in distinct strains of host cells and combine them after growth and protein production to obtain the desired enzymatic cascade. This method is known as the “mixed culture approach”.⁷⁵ It is used if the combined production of the proteins in a single cell is not possible due to the high metabolic burden on the organism.⁷⁶ Also, since no additional cloning is needed, it is a fast method to test the enzymatic cascade in a first shot experiment. Since the cells can also be combined in any ratio, it can also help to obtain the proper enzymatic stoichiometry for the optimal reaction kinetics.

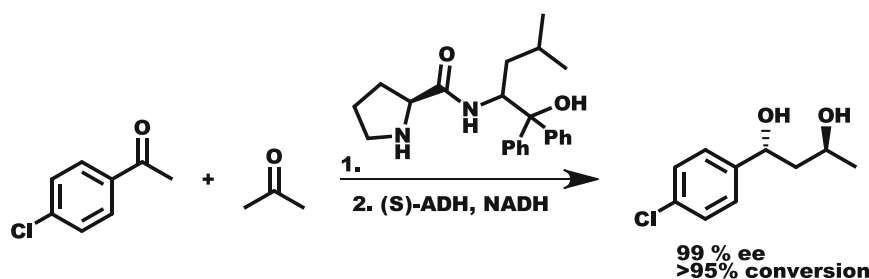
A.3. Biocompatibility of chemical Synthesis

Many organic synthetic reactions are intrinsically not compatible with biological systems and *vice versa*. This can have many reasons: (1) moisture sensitivity of the reaction components, (2) incompatible reaction conditions (temperature, pressure, solvent system), (3) inhibition of enzymes through reagents and products.

Although not all of these hurdles can be overcome, there are some strategies to increase biocompatibility and allow the combination of organic reactions with enzymes in a reaction sequence.⁷³ Also, through the means of genetic engineering, it is also possible to increase the chemocompatibility of enzymes in the form of a higher solvent and temperature tolerance.⁷⁷

In general, if the reaction allows it, one of the simplest methods is the screening for biocompatible reaction conditions. For example, if an enzymatic reaction is prevented due to the organic solvent used in the chemical transformation, increasing the water content of the solvent system might already be enough, as demonstrated with numerous metal catalyzed reactions (e.g., Suzuki coupling, Wacker oxidation, Heck reaction).⁷³

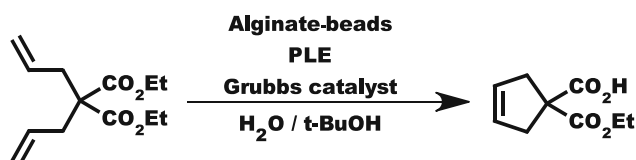
It is also possible to omit the use of solvent entirely in a chemical transformation and perform a solvent-free reaction which can then be coupled to an enzymatic transformation in a sequential one-pot fashion. Baer et al. demonstrated this principle for the synthesis of chiral 1,3-diols through a “solvent-free” (acetone was used in 4 equiv.) asymmetric organocatalyzed aldol condensation followed by an asymmetric enzymatic reduction in a sequential one-pot fashion (scheme 15).⁷⁸



Scheme 15: Chemoenzymatic one-pot procedure for the synthesis of chiral 1,3-diols. System developed by Baer et al.⁷⁸

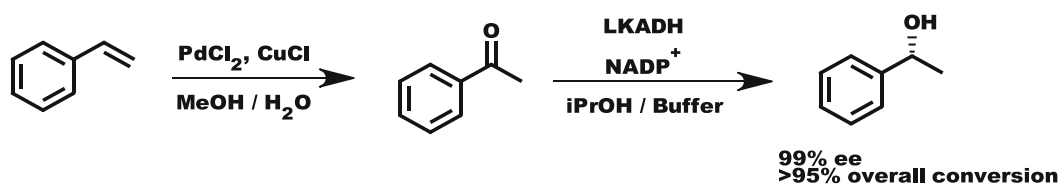
One of the more elegant strategies for the combination of chemical with enzymatic catalysis lies in the form of compartmentalization. The catalyst and the reaction components of the chemical transformation get spatially separated through the use of, e.g., membranes or porous beads. This leads to increased selectivity but also prevents the deactivation of the enzyme by the reagents.

For example, a Grubbs second-generation catalyst could be combined in a one-pot fashion with a pig liver esterase (PLE) to produce cyclic malonic acid monoester out of diethyl malonate. The authors achieved this through the combined entrapment of the metal catalyst and enzyme in a porous modified alginate core-shell bead. This spatial separation between the enzyme and the metal catalyst led to an increase in selectivity for product formation from 1 % without to 75 % with the beads (scheme 16).⁷⁹



Scheme 16: Chemoenzymatic one-pot procedure for the synthesis of cyclic malonic acid monoester developed by Gröger et al.⁷⁹

Compartmentalization was also used by Sato *et al.* for the oxidation of styrene derivatives to the respective aromatic alcohol. The system consists of a two-step chemoenzymatic one-pot reaction. The styrene is oxidized *via* a Wacker oxidation to the respective ketone in the first step. The reaction is performed in aqueous medium, which allows biocompatibility. However, components of the catalytic system (in the form of CuCl/PdCl₂) led to an inhibition of the ADH in the subsequent reduction step. To solve this issue, the chemical reaction was separated from the enzymatic transformation through the use of a PDMS (polydimethylsiloxane) membrane. This membrane allows the diffusion of the product of the Wacker oxidation while it holds back the inhibiting Cu-salts. Through this, they synthesized various chiral 1-phenylethanols with high conversion and ee. (scheme 17).⁸⁰



Scheme 17: Chemoenzymatic one-pot procedure for the synthesis of chiral benzylic alcohols developed by Sato *et al.*⁸⁰

In summary, depending on the procedure, a few different strategies can be applied to develop biocompatible synthetic transformations. In the following chapters, some synthetic reactions that were optimized for biocompatibility in the present scientific work are described in more detail.

A.3.1. Introduction to Wacker oxidation

The Wacker oxidation describes the palladium-catalyzed oxidative nucleophilic addition of water to an olefin.⁸¹ In 1894, Phillips discovered that in the presence of stoichiometric amounts of palladium(II) salts, ethylene could be oxidized to acetaldehyde.⁸¹ A chemist used this principle at the Wacker-Chemie group to develop the first transition metal-catalyzed industrial process to convert ethylene to acetaldehyde. They achieved this with catalytic amounts of Pd(II)Cl₂ in the presence of Cu(II)Cl₂ under aerobic conditions in acidic aqueous medium, which made the reaction catalytic in regards to PdCl₂.⁸² In 1976 Tsuji demonstrated that the substrate scope of the traditional Wacker oxidation, which suffered from the poor solubility of most organic substrates in the aqueous medium, can be significantly expanded *via* the use of DMF as a cosolvent.⁸³ This marked the starting point for the utilization of the Wacker oxidation in organic synthesis.

The generally accepted mechanism for the palladium-catalyzed Wacker Oxidation can be seen in figure 5 and is described in more detail in the following section.^{82,84}

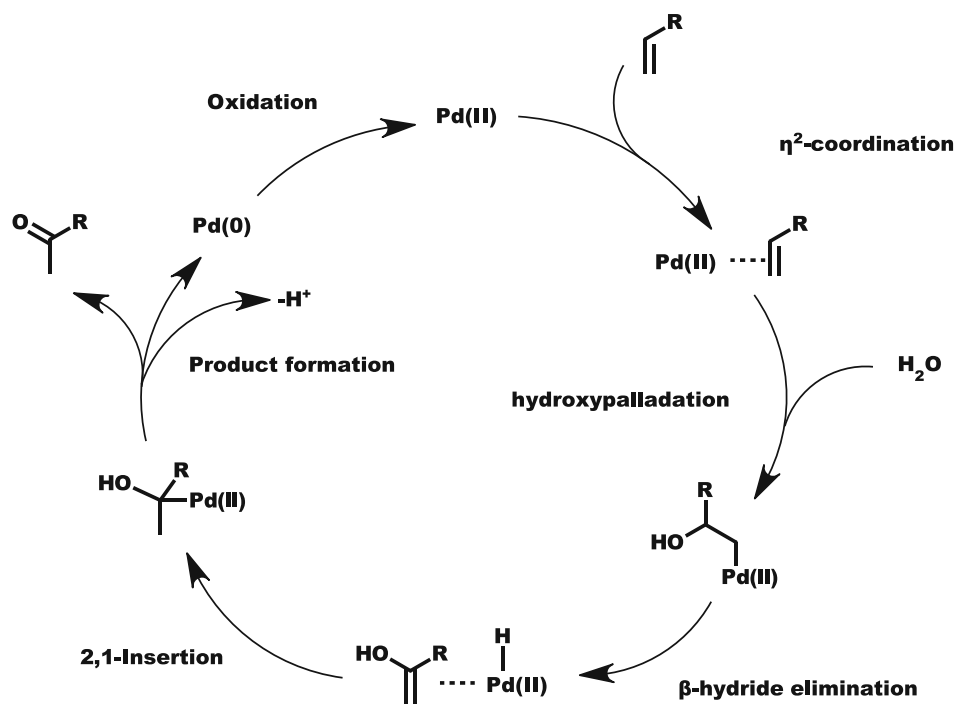


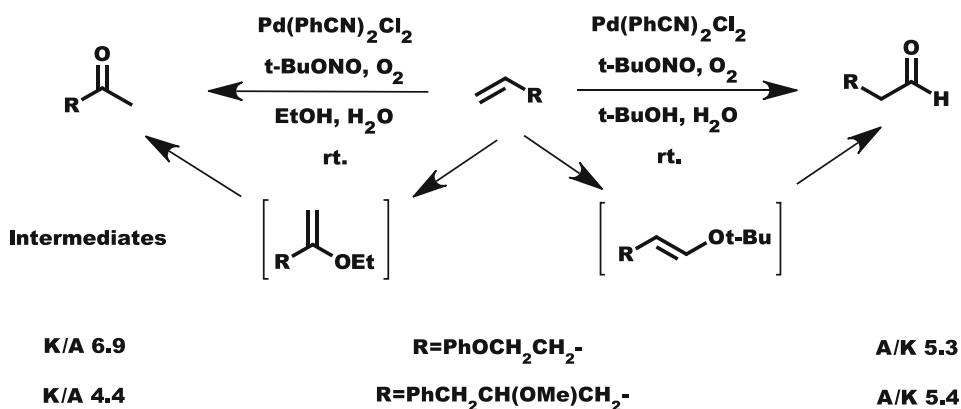
Figure 5: Catalytic cycle of the Wacker oxidation

The first step of the catalytic cycle consists of a coordination of the olefin to the metal catalyst to form a η^2 -complex. This is followed by a hydroxy palladation of the olefin through a nucleophilic attack from a water molecule. After subsequent β -hydride elimination, the enol can dissociate from the complex, and after tautomerization, the product is formed. Depending on the reaction conditions and the stability of the enol-palladium complex, a 1,2 insertion can occur instead, followed by reductive elimination leading to the formation of the product. The resulting Pd(0) is re-oxidized to complete the catalytic cycle. Traditionally this is achieved *via* the use of cupric chloride under aerobic conditions, which acts as an electron transfer mediator with oxygen as the terminal oxidant of the system.

Even though much scientific effort has been made to elucidate the reaction mechanism, some mechanistic uncertainties still exist. Especially the step of the hydroxy palladation is the center of scientific debate. Depending on the reaction conditions, the nucleophile can attack the olefin either *exo* (from the solution) or *endo* (from the metal complex).⁸⁴ Also, depending on the carbon atom which is attacked during the reaction, two different isomers can be formed. If the nucleophile attacks the more substituted carbon atom, the Markovnikov product is formed, whereas if the nucleophile attacks the less substituted carbon, the anti-Markovnikov product is formed instead.⁸² The ratio between the two isomers is highly substrate-dependent, but also steric consideration of the attacking nucleophile also plays an important role.⁸²

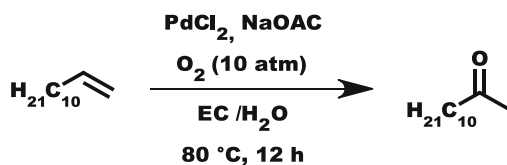
For example, Hu *et al.* developed a system for the Wacker oxidation that either affords the Markovnikov or the anti-Markovnikov product.⁸⁵ This solely depends on the type of solvent

(which also acts as the nucleophile of the reaction) that is used in the transformation (scheme 18). If the sterically less hindered EtOH is used, then Markovnikov addition is followed, and the ketone is obtained as the main product of the transformation. On the other hand, when tBuOH is used, the anti-Markovnikov product in the form of the aldehyde is obtained instead.⁸⁵

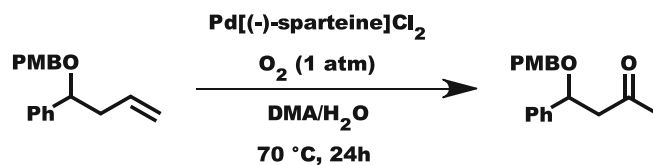


Scheme 18: Regioselective Wacker oxidation depending on the solvent. The ratio between ketone and aldehyde (K/A) or aldehyde and ketone (A/K) is specified for some substrates tested. System developed by Hu et al.⁸⁵

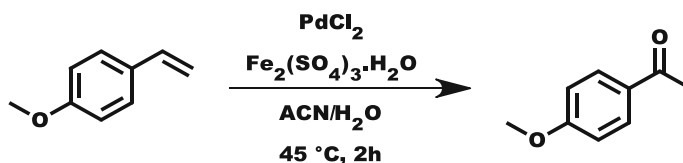
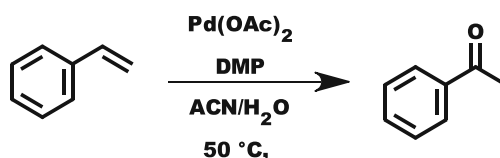
The traditional reaction conditions greatly suffer from the formation of by-products such as chlorinated organic compounds or isomers but also from the low catalytic activity of the catalyst for many types of substrates.⁸⁶⁻⁸⁷ This is partly a result of the use of copper(II)chloride as a terminal oxidizing agent and can be somewhat diminished by switching to stoichiometric amounts of copper(I)chloride.⁸⁸ Additionally, the use of copper salts leads to toxic and hazardous waste products. Over the years, many different strategies have been developed to solve these issues. One possible classification for these methods can be based on the way by which the reoxidation of the Pd(0) intermediated species is achieved. If the reoxidation is directly coupled to the reduction of the terminal oxidant (e.g., oxygen), then the Pd(0) intermediate has to be stabilized in solution. For the oxidation with molecular oxygen this is achieved either by polar coordinating solvents such as DMA and ethylene carbonate (EC) or *via* a defined inner coordination sphere (scheme 19, 20).⁸⁹⁻⁹¹



Scheme 19: Wacker oxidation in ethylene carbonate developed by Wang et al.⁸⁹

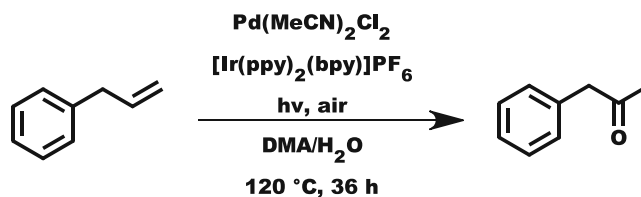
Scheme 20: Ligand assisted Wacker oxidation developed by Cornell et al.⁹¹.

Alternatively, inorganic and organic oxidants such as metal salts, hypervalent iodine, or peroxides can be used instead (scheme 21,22).⁹²⁻⁹⁴

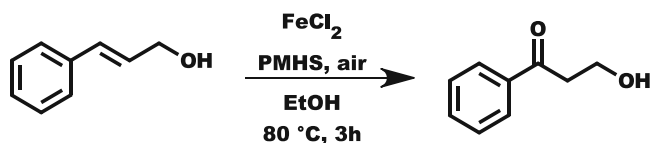
Scheme 21: Wacker oxidation using iron(II)sulfate as the terminal oxidant. The system was developed by Fernandes et al.⁹⁵Scheme 22: Wacker oxidation using DMP (Dess-Martin periodinane) as the terminal oxidant. The system was developed by Chaudhari et al.⁹²

The Pd(0) species can also be oxidized *via* an electron transfer mediator. They mediate the electron transfer in the redox reaction and transfer them along a low-energy pathway.⁹⁶

Examples are the traditional CuCl₂ co-catalyzed Wacker oxidation but also quinone-based systems and photoredox-catalysis (scheme 23) using oxygen as terminal oxidant.^{84, 97-98}

Scheme 23: Wacker oxidation coupled to a photoredox-catalyst in visible light. The system was developed by Ho et al.⁹⁷

Additionally, newer developments also allow for an iron(II) salts catalyzed Wacker oxidation (scheme 24).⁹⁹⁻¹⁰⁰

Scheme 24: Iron catalyzed Wacker oxidation. System developed by Liu et al. ¹⁰¹

Since the Wacker oxidation is performed in aqueous medium, it makes the reaction an ideal candidate for the coupling to an enzymatic system.

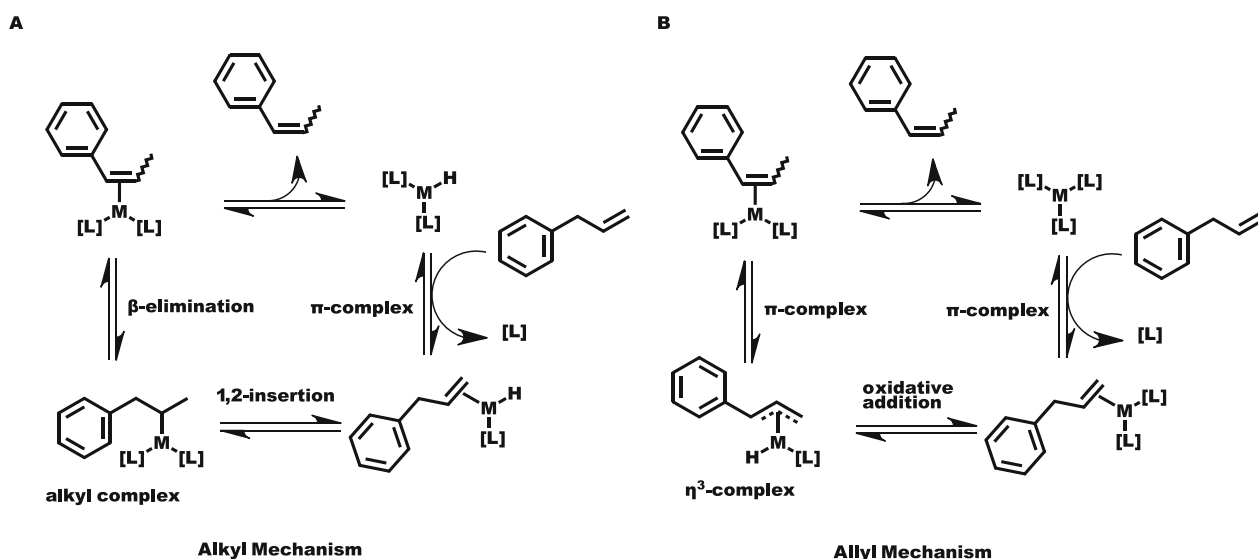
A.3.2. Pd catalyzed isomerization of 2-propenylbenzenes

The following section is mostly based on the review of Hassam et al. ¹⁰²

The preparation of 1-propenylbenzenes (**1g-8g**) from 2-propenylbenzenes (**1a-8a**) is an important procedure in industrial chemistry. 1-Propenylbenzenes have various applications ranging from the food industry as flavor or fragrance compounds to synthetical applications as intermediates or starting materials for the preparation of complex molecules. ¹⁰³⁻¹⁰⁴

The isomerization of 2-propenylbenzenes to 1-propenylbenzenes can occur through various means. The two most prominent methods for isomerization include base-mediated and transition metal-mediated isomerization procedures. ¹⁰² The product of the isomerization is thermodynamically more favored since the olefinic bond is additionally stabilized through hyperconjugation by the methyl group.

Metal-mediated isomerization can proceed through two distinct but generally accepted mechanisms (scheme 25) which are described in more detail in the following section. ¹⁰⁵

Scheme 25: General reaction pathways for the metal-catalyzed isomerization of propenylbenzenes. Scheme adapted from Hassam et al. ¹⁰²

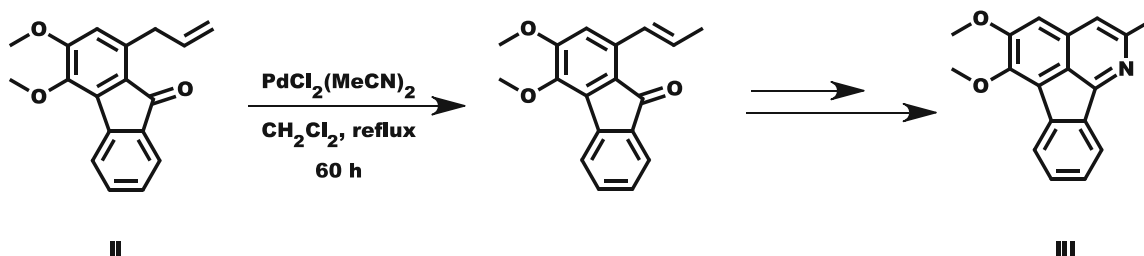
The alkyl mechanism (A) relies on a metal catalyst that has an empty two electron coordination site and also bonds a hydride ligand (typically generated *in situ*). In the first step of the reaction,

the metal-catalyst forms a η^2 - complex with the olefin, which then undergoes 1,2-insertion forming a discrete metal-carbon bond intermediate. Through β -elimination, the olefinic bond is regenerated, generating the thermodynamically more stable olefin. Dissociation of the metal catalyst releases the isomer starting the catalytic cycle anew. Depending on the conformation of the carbon chain during the β -elimination, either the cis or the trans isomer can be obtained. Under thermodynamic control of the reaction, the formation of the trans isomer is generally favored.

The allyl mechanism (B), on the other hand, proceeds *via* an oxidative addition of the metal catalyst in the allylic C-H bond, forming an η^3 - allyl hydride metal complex. After the subsequent collapse of this intermediate, the thermodynamically more stable olefin is formed. Again, dissociation of the metal catalyst releases the product, starting the catalytic cycle anew. As before, both isomers of the olefin are formed, but under thermodynamic control, the formation of the trans isomer is favored. Of course, the actual reaction pathway of a given isomerization is strongly influenced by the reaction conditions, type of metal catalyst, and coordinated ligands. A hybrid form between the two general mechanisms is also possible.^{102, 105}

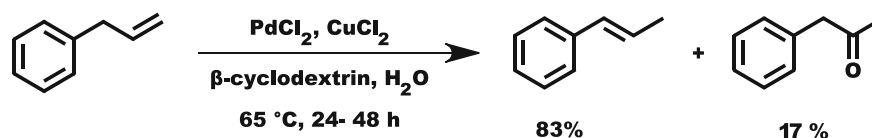
Palladium-catalyzed isomerization procedures are widely used in organic synthesis for the isomerization of 2-propenylbenzenes. Different types of catalyst (e.g. PdCl_2 , $\text{PdCl}_2(\text{MeCN})_2$, $\text{Pd}(\text{dba})_2$ and $\text{Pd}(\text{OAc})_2$) with various different solvents (e.g., CH_2Cl_2 , MeOH, EtOH, toluene) under different reaction conditions have been successfully employed.¹⁰² They allow for the isomerization of a wide range of propenylbenzene derivatives with generally low catalyst loadings and oftentimes good selectivity.¹⁰²

For example, Silveira and *et al.* used a $\text{PdCl}_2(\text{MeCN})_2$ catalyzed isomerization of the propenylbenzene **II** derivative (obtained after intramolecular cross-coupling) in CH_2Cl_2 for the total synthesis of 2-methyltricycline **III** (scheme 26).¹⁰⁶



Scheme 26: Isomerization step in the total synthesis of 2-methyltricycline. The scheme was adapted from Hassam *et al.*¹⁰²

Oftentimes, the isomerized products are also obtained in other palladium-catalyzed reactions as undesired side products. For example, Zahalka and *et al.* discovered that under traditional Wacker oxidation conditions (PdCl_2 , CuCl_2), utilizing β -cyclodextrin as phase-transfer catalyst, mostly the isomerized starting material in the form of 1-propenylbenzene (83 %) is obtained

(Scheme 27).⁸⁷

Scheme 27: Wacker oxidation of allylbenzene yielding the respective isomer as the main product.

A.4. Aldehydes as products of (chemo)enzymatic one-pot reactions

Aldehydes are an important group of chemical compounds. Many aldehydes are important fragrance and flavor compounds and are used extensively in the food and perfume industry.¹⁰³ More important is their application in chemical research and the pharmaceutical industry as precursors.¹⁰⁷⁻¹⁰⁸

Therefore, finding a suitable way to make them accessible is crucial for the chemical industry. Luckily there are a plethora of different options for their synthesis (figure 6). Traditional synthetic methods most obviously include the oxidation of primary alcohols but also the reduction of carboxylic acids derivatives such as esters, acyl chlorides and nitriles.¹⁰⁹ Electrophilic aromatic substitution (e.g., Vilsmeier-Haak reaction) is also a reliable method for the production of aromatic aldehydes.¹¹⁰ Lastly, also more peculiar methods like e.g., the oxidative cleavage of alkenes by ozonolysis and also the hydroboration of alkynes can be used.¹⁰⁹

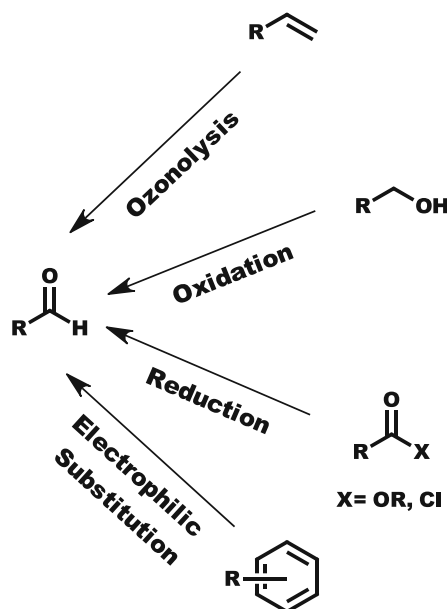


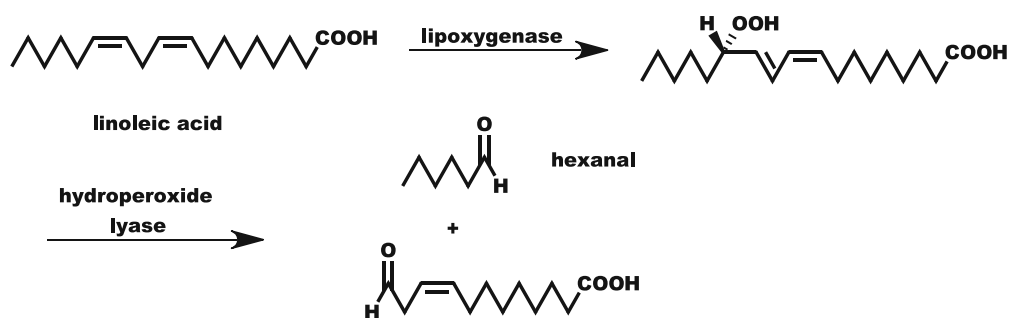
Figure 6: Methods for the preparation of aldehydes

Recently also, enzymatic procedures gained relevance in producing fragrance aldehydes.¹¹¹⁻¹¹² They can be obtained from the same functional groups as in traditional organic synthesis (e.g.,

oxidation of Alcohols by ADHs, or reduction of carboxylic acids by CAR).¹¹¹ The main advantage of using microbial means for their production are the mild and green reaction conditions, i.e., no toxic or hazardous chemicals are necessary. However, due to the inherently toxic nature of aldehydes for most microorganisms, *in vivo* enzymatic methods suffer from diminished yields. The main reason is their rapid conversion by endogenous proteins to the corresponding alcohols or carboxylic acids.¹¹² Strategies to circumvent these problems include the use of so-called knock-out strains that display reduced aromatic aldehyde reduction (RARE).¹¹³ Another strategy, as already mentioned in chapter A.1.4, is the use of biphasic catalysis. The organic solvent accumulates the formed aldehydes and prevents side reactions. Also, recycling systems can be used. Bayer et al. demonstrated that the formation of carboxylic acid could be diminished during the oxidation of primary alcohols *via* the use of an additional enzyme (Carboxylic acid reductase CAR_{NI}) which catalyzes the reverse reaction.²⁹

However, most of the time, synthetic procedures consist of more than a one-step conversion. This is, of course, strongly influenced by the availability of the starting material and other cost factors. Therefore, more lengthy synthetic procedures need to be used to convert a starting material to an intermediate that contains the desired functionality that can then be transformed into the aldehyde. (Chemo)enzymatic cascades or sequential one-pot reactions can be valuable tools for their production.

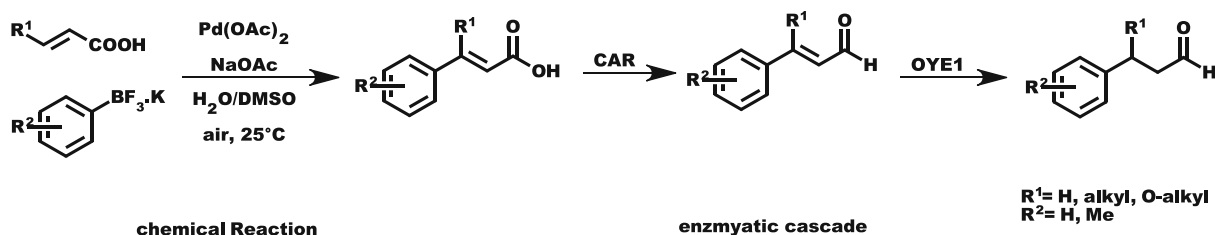
For example, Noordermeer et al. were able to develop a method to produce volatile C6-aldehydes on a large scale through a sequential one-pot reaction sequence. Vegetable oils were converted by soybean lipoxygenase in the first step to the corresponding hydroperoxy fatty acids, which were then subsequently cleaved by hydroperoxide lyase into hexanal. They were able to achieve this with high molar conversion (50 % for hexanal), and no side products were formed (scheme 28).¹¹⁴



Scheme 28: Cleavage of linoleic acid into hexanal and dodecenoic acid in two steps.¹¹⁴

Schwendenwein et al. developed a system to produce chiral fragrance aldehydes through a sequential chemoenzymatic one-pot reaction. The chemical transformation in the form of an oxidative Heck coupling was used to produce α or β substituted cinnamic acid derivatives out of α,β -unsaturated carboxylic acids, and organo-trifluoroborates. They optimized the reaction conditions focusing on increasing biocompatibility. Subsequently, this intermediate was subjected to an enzymatic cascade. In the first step, a carboxylic acid reductase was used to produce the respective α,β -unsaturated aromatic aldehydes. This was followed by the conjugate reduction catalyzed by an ene-reductase to yield the desired fragrance aldehydes (scheme 29).

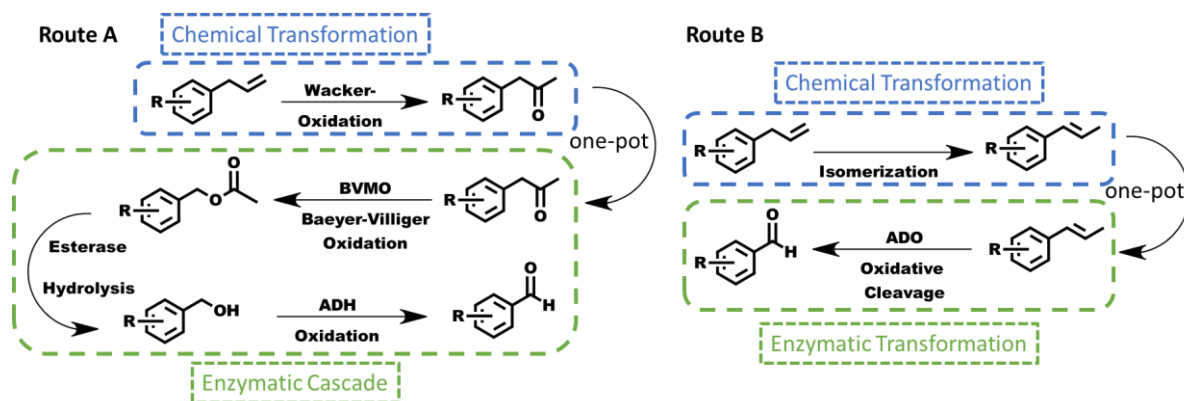
115



Scheme 29: Production of aromatic aldehydes in three steps. The first step consists of a chemical Heck coupling followed by an enzymatic cascade: a CAR (carboxylic acid reductase) yields the unsaturated aldehyde, which is then converted after a conjugate reduction catalyzed by OYE1 (Old-Yellow-Enzyme) to the desired fragrance aldehyde.¹¹⁵

A.5. Aim of the thesis

The purpose of this thesis is the development of novel chemoenzymatic one-pot reactions for the synthesis of aromatic aldehydes from propenylbenzenes. The starting point was the general idea that a Wacker oxidation, a BVMO, and an ADH should be utilized for this transformation (scheme 30, route A). Additionally, a second route that utilizes ADO was also considered (scheme 30, route B). To achieve this, a screening for a biocompatible chemical transformation needs to be conducted as well as finding suitable enzymes for the enzymatic cascade. The procedure for the Wacker oxidation should also omit the use of copper(II) salts and, if possible, utilize oxygen as a terminal oxidant. The best method for the implementation of the enzymatic cascade also needs to be determined. If feasible, then a *de novo* enzymatic pathway should be implemented to express all enzymes in a single host. After the scope of the transformation has been elucidated, the scalability of the one-pot-reaction should also be demonstrated.



Scheme 30: Route A: 1) Wacker oxidation of propenylbenzenes to obtain the respective ketone. 2) Enzymatic Baeyer-Villiger oxidation of the ketone to obtain the ester. 3) Hydrolysis and oxidation of the ester yields the desired aldehyde. Route B: 1) Isomerization of 2-propenylbenzenes to respective 1-propenylbenzene. 2) Enzymatic oxidative cleavage of the conjugated olefinic bond leads to the desired aldehyde.

B. Results and Discussion

B.1. Design of chemoenzymatic one-pot reactions for the synthesis of fragrance aldehydes

As mentioned in the previous chapter, aldehydes can be synthesized by a variety of different procedures. In general, the chemistry behind their synthesis is well established, and this holds true for bio-enzymatic methods as well as in organic synthesis. The meaning behind this is that many different functional groups can be successfully converted into the desired aldehydes, and it is therefore logical that many different methods and different synthetic routes will lead to satisfying results. Since the chemistry is not the limiting factor of their synthesis, other parameters can be explored, which are oftentimes overlooked when planning a *de novo* synthesis of a complex molecule. Such parameters include, for example, selecting the most suitable starting point but also deciding on the means which are necessary for the desired synthesis. The long-term goal of synthetic chemistry and technical chemistry, as laid out by the twelve principles of green chemistry, is to decrease their environmental impact.⁷² Therefore, it is not sensible in this case to use toxic or hazardous reagents or generate unproportionate amounts of waste. One different strategy to increase the sustainability of a synthetic route and to save resources which are based on fossil fuels is the use of a renewable starting materials. Considering these points, the natural compound class of propenylbenzenes stood out as an ideal starting point for the chemoenzymatic one-pot reaction. Examples of naturally occurring propenylbenzene are estragole **4a** (A), safrole **6a** (B), and eugenol **7a** (C) (figure 7).

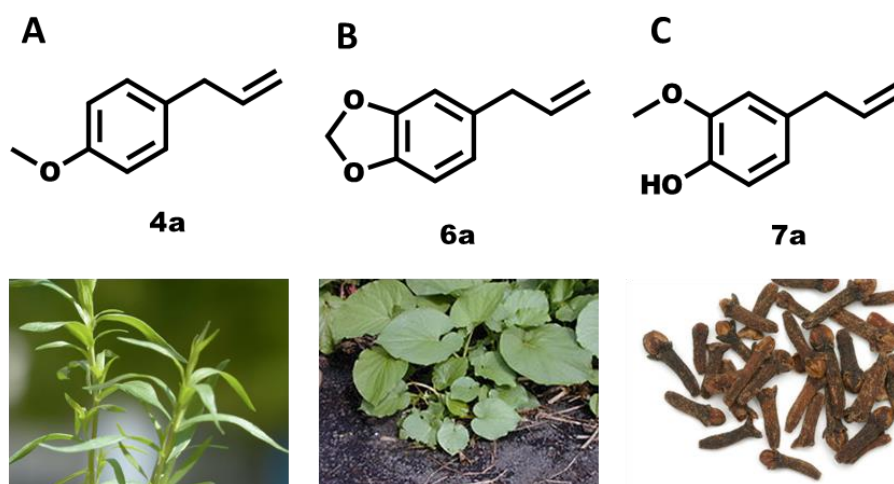


Figure 7: (A) Estragole **4a** can be isolated from Estragon¹¹⁶. (B) Safrole **6a** can be isolated from Makulan¹¹⁷. Picture: Forest & Kim Starr (CC BY 3.0). (C) Eugenol **7a** can be isolated from Clove¹¹⁸. Picture adapted from Brian Arthur (CC BY-SA 4.0)

They have a supposedly similar biosynthetic pathway to naturally occurring aromatic aldehydes **4e-8e** (derived from phenylalanine, although data is limited) and share the same structural motif in the aromatic moiety.¹¹⁹⁻¹²⁰ They can be isolated from plants and are, therefore, arguably a

renewable material source. Their main application is mainly in the food industry as fragrance and flavoring compounds.^{103, 121} Additionally, they are arguable synthetically less valuable than the corresponding aromatic aldehydes. Finding a suitable way for their interconversion would correspond to the recycling principle of converting a material from “waste to value”.

With these considerations in mind, mainly the choice of the starting material, the prevention of waste, and increasing the time efficiency, two synthetic routes (route **A** and **B**) were designed utilizing forward synthetic planning. The consequence of these goals was the incorporation of as many enzymatic steps as possible into the synthetic route as well as the desire to perform the entire reaction in a one-pot fashion. The reaction scheme for both routes can be seen in figure 8.

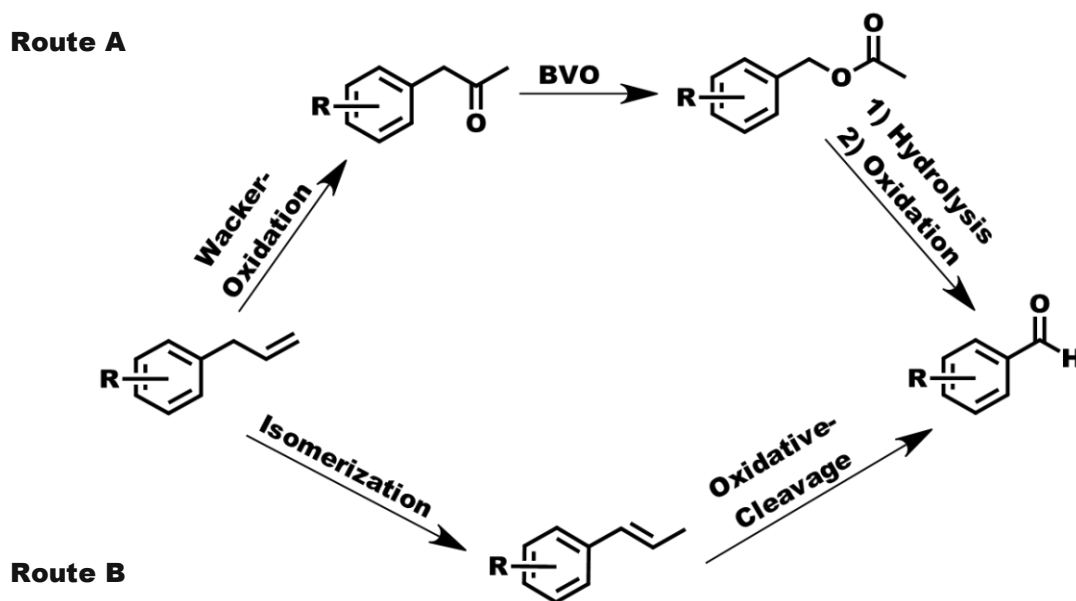


Figure 8: The two designed routes for the synthesis of aromatic aldehydes. Route A: 1) Wacker oxidation of propenylbenzenes to obtain the respective ketones. 2) Enzymatic Baeyer-Villiger oxidation of the ketone to obtain the ester. 3) Hydrolysis and oxidation of the ester yields the desired aldehyde. Route B: 1) Isomerization of 2-propenylbenzenes to respective 1-propenylbenzenes. 2) Enzymatic oxidative cleavage of the conjugated olefinic bond leads to the desired aldehyde.

Route **A** consist of 4 steps: first a Wacker oxidation that converts the propenylbenzene into the respective phenylpropanone. This synthetic transformation is coupled to three enzymatic steps arranged in an enzymatic cascade. The first enzymatic step is a Baeyer-Villiger oxidation which converts the ketone to the respective ester, and after subsequent hydrolysis, the benzylic alcohol is formed. Lastly, an enzymatic oxidation leads to the desired product of the route, the aromatic aldehyde. Since traditional Wacker oxidation is dependent on copper(II)chloride as the oxidizing agent with DMF as a cosolvent (see Introduction), a different reaction procedure has to be selected. Mainly, the use of Cu-salts is problematic since it generates hazardous waste. Also, to make this reaction biocompatible, a solvent system with a high water ratio and a non-toxic co-solvent needs to be found. The screening for the Wacker oxidation is described in detail in the following chapter. For the first enzymatic step, the Baeyer-Villiger oxidation, three literature

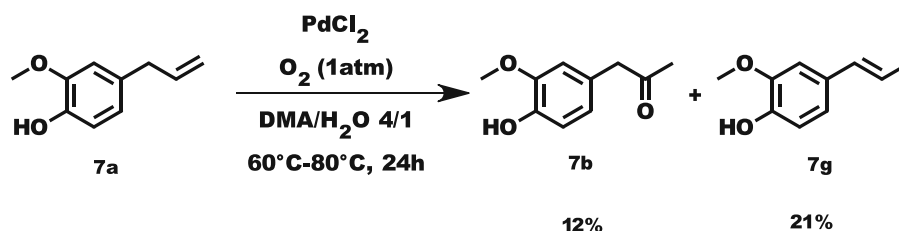
known Baeyer-Villiger monooxygenases were selected, namely, PAMO (phenylacetone monooxygenase) from *Thermobifida fusca*¹²², TmCHMO (cyclohexanone monooxygenase) from *Thermocrisum municipal*¹²³, and HAPMO (4-hydroxyacetophenone monooxygenase) from *Pseudomonas fluorescens*¹²⁴ which seemed the most promising candidates for the substrate class of propenylbenzenes. The hydrolysis should either proceed “spontaneously”, facilitated by naturally expressed hydrolases from the host, or through the addition of an external esterase in the form of PflE from *Pseudomonas fluorescens*.⁵⁴ For the last enzymatic step, the oxidation of the benzylic alcohol, the literature known alcohol dehydrogenase AlkJ from *Pseudomonas putida*⁴⁶ was selected for this purpose.

Route **B** consists of 2 steps: An isomerization of the terminal olefinic bond of 2-propenylbenzenes leads to the formation of 1-propenylbenzene derivatives. The oxidative cleavage of this conjugated double bond forms the desired aromatic aldehyde. For the route to proceed in a one pot manner, biorthogonal reaction conditions must be found for the isomerization of propenylbenzenes. The oxidative cleavage in the last steps is catalyzed by the literature known ADO (aromatic dioxygenase).⁶¹ To optimize the reaction conditions and to determine the scope of the transformations eight different substrates were selected.

B.2. Screening for a biocompatible Wacker oxidation

As mentioned in the introduction, there are many different methods and procedures to perform a Wacker oxidation. Since we decided to combine the chemical transformation with the following enzymatic cascade, a procedure had to be selected that operates within the limited parameter range of an enzymatic transformation (solvent system with a high water ratio and low toxicity for the cells). This also includes the ease of separability of the reagents after a successful transformation. Additionally, only procedures were selected that omit the use of toxic and hazardous reaction components and preferentially utilize a green terminal oxidant (e.g., oxygen). The screening was performed with the two model substrates **1a** and **7a**.

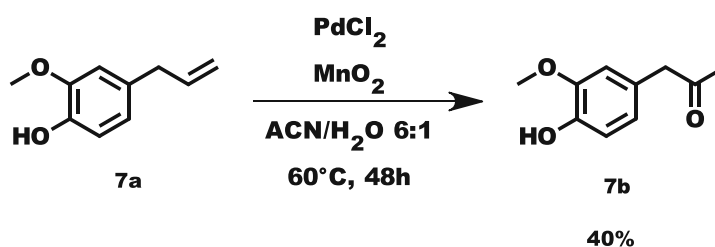
The starting point for the screening of reaction conditions was the procedure developed by Mitsudome *et al.* (scheme 31).^{90,125} It employs PdCl₂ as the catalyst in a mixture of DMA/H₂O with oxygen as the terminal oxidant.



Scheme 31: Wacker oxidation with PdCl₂ in DMA/H₂O under oxygen atmosphere. System developed by Mitsudome *et al.*¹²⁶

Testing this procedure with Eugenol led to the formation of a mixture of the desired ketone (12 %) in small amounts and also the main product in the form of isoeugenol (21 %). Additionally, during the addition of the substrate almost immediate decomposition of the catalyst was observed in the form of Palladium black. Parreira *et al.* showed that high oxygen pressure is necessary to circumvent catalyst decomposition.¹²⁷ Allylbenzene **1a** proved to be a better substrate for this reaction under the same conditions with little to no observed decomposition of catalyst and a yield of the desired ketone **1b** of 70 %. DMA also proved to be a problematic solvent due to its high boiling point and toxicity issues.

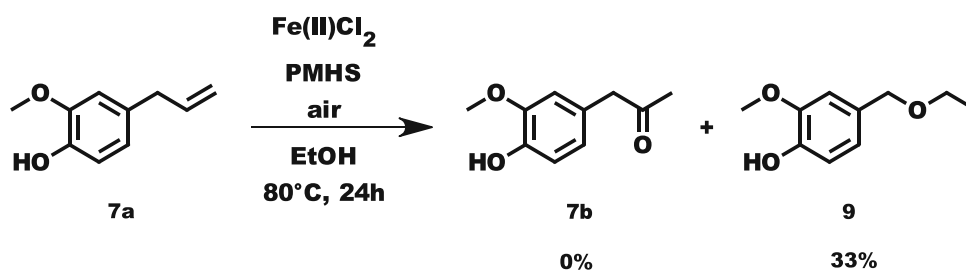
The next procedure that was tested was developed by Fernandes *et al.* PdCl₂ is again employed as catalyst with MnO₂ as terminal oxidizing agent in a mixture of ACN and water (scheme 32).⁹³



Scheme 32: Wacker oxidation with PdCl₂ in ACN/H₂O and MnO₂ as terminal oxidant. System developed by Fernandes *et al.*⁹³

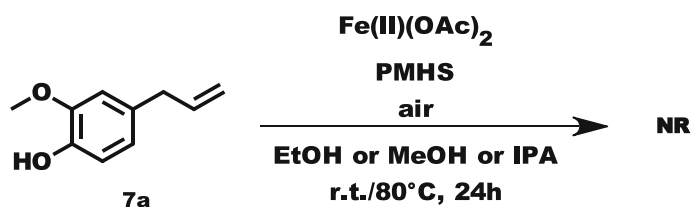
Due to the heterogenous nature of this system the separation of oxidizing agent from the solution is facilitated after the reaction. Eugenol was used as the test substrate. Initial results were promising as the desired ketone was successfully isolated. Unfortunately, the reaction progress halted after a conversion of around 40 %. Increasing the temperature and varying MnO₂ mesh sizes and increasing the share of reactive surface bond hydroxyl groups led to no observable difference in the outcome. Interestingly, the addition of more catalyst made the reaction proceed only slightly further, indicating a limiting factor in the reoxidation process.

Procedures of iron-catalyzed Wacker oxidations were also tested as possible candidates for the chemoenzymatic one-pot reaction. Iron is a green alternative to traditional palladium catalysis, which is a depleting resource. Liu *et al.* discovered the iron (II) salts catalyzed variant that uses as PMHS poly(methylhydrosiloxane) as reducing agent to complete the catalytic circle (schemes 33 and 34).¹⁰⁰⁻¹⁰¹ The reaction proceeds under air or oxygen atmosphere in ethanol as the solvent.



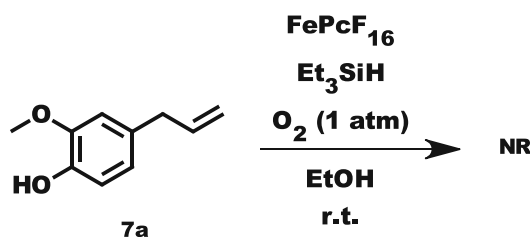
Scheme 33: Iron catalyzed Wacker oxidation with Fe(II)Cl_2 , PMHS in EtOH under air atmosphere. System developed by Liu et al.¹⁰⁰

The iron(II)chloride catalyzed variant was able to convert the starting material but only led to the formation of the ethyl ether instead. This is a remarkable result since this intermediate can be used for the direct production of vanillin. However, the yield of this reaction was not ideal, with only 33 % isolated product.



Scheme 34: Iron catalyzed Wacker oxidation with Fe(II)OAc_2 , PMHS in EtOH under air atmosphere. System developed by Liu et al.¹⁰⁰

In contrast, no conversion was observed in the iron(II)acetate catalyzed variant of this procedure. Different solvents (MeOH, IPA) and temperatures (80°C) were tested with no observable difference. The same results were obtained while testing a procedure developed by Puls *et al.* that uses FePcF_{16} (hexadecafluorinated iron-phthalocyanine) as a catalyst and triethyl silane as a reducing agent. This reaction proceeds in ethanol under an oxygen atmosphere (scheme 35).⁹⁹

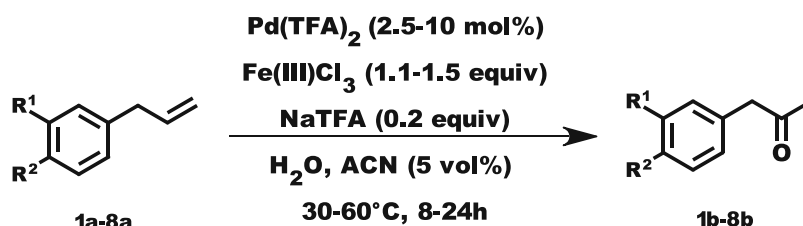


Scheme 35: Iron catalyzed Wacker oxidation with FePcF_{16} , Et_3SiH in EtOH under oxygen atmosphere. System developed by Puls et al.⁹⁹

In conclusion, neither the solvent assisted, nor the iron-catalyzed Wacker oxidation yielded satisfying results. Eugenol proved to be a problematic substrate, and in the case of the palladium-catalyzed reactions, catalyst decomposition was observed. This is a result of the slow reoxidation step in the catalytic cycle due to the low concentration of terminal oxidant in solution (low

solubility of oxygen in solution and heterogenous nature of MnO_2). To circumvent these issues, an oxidant in high concentrations proved to be necessary.

The most promising system for this was developed by González-Martínez et al., which they used for the chemoenzymatic production of amines from phenylpropenes. The system uses $\text{Pd}(\text{TFA})_2$ (palladium(II)-trifluoroacetat) as a catalyst, NaTFA (sodium trifluoroacetate) as an additive for the catalyst, and iron(III)salts as terminal oxidizing agents (scheme 36).¹²⁸



Scheme 36: $\text{Pd}(\text{TFA})_2$ catalyzed Wacker oxidation with NaTFA and FeCl_3 in $\text{H}_2\text{O}/\text{ACN}$. System developed by González-Martínez et al.⁹⁴

Table 1: Substrates for the $\text{Pd}(\text{TFA})_2$ catalyzed Wacker oxidation.

Substrate	Substituents	Product
1a	$\text{R}^1 = \text{H}$ $\text{R}^2 = \text{H}$	1b
2a	$\text{R}^1 = \text{Me}$ $\text{R}^2 = \text{H}$	2b
3a	$\text{R}^1 = \text{H}$ $\text{R}^2 = \text{Me}$	3b
4a	$\text{R}^1 = \text{H}$ $\text{R}^2 = \text{OMe}$	4b
5a	$\text{R}^1 = \text{OMe}$ $\text{R}^2 = \text{OMe}$	5b
6a	$\text{R}^1 = \text{R}^2 = \text{OCH}_2\text{O}$	6b
7a	$\text{R}^1 = \text{OMe}$ $\text{R}^2 = \text{OH}$	7b
8a	$\text{R}^1 = \text{OMe}$ $\text{R}^2 = \text{OAc}$	8b

The reaction is performed in water with 5 vol% ACN as cosolvent. González-Martínez also demonstrated the wide substrate scope of this procedure which almost entirely matched with the substrates selected for the designed chemoenzymatic one-pot reaction. It also turned out to be advantageous that the solubility of iron species in solution is strongly dependent on the pH.¹²⁹

This allows for the removal of most of the oxidizing agent after the reaction by precipitation, thus preventing interference in the enzymatic cascade. The first results with allylbenzene seemed promising, with an obtained isolated yield of 60%.

In contrast, eugenol only afforded a low isolated product yield of 17 %. Therefore, additional optimization of the reaction conditions had to be conducted as the reported yields were not obtainable with the stated conditions. For the screening of the reaction conditions, eugenol and allylbenzene were selected as the model substrates, and a single variation of parameters method was utilized. Some of the results of this screening can be found in table 2.

Table 2: Optimization of the Wacker oxidation for the substrates **1a**, **7a**.

Substrate	Entry	Cat.	Additive	Oxidant	Co-Solvent	pH	Temp.	Yield
7a	1	2.5 mol%	0.2 equiv.	1.5 equiv.	5 vol%	2	45 °C	17 %
7a	2	2.5 mol%	0.2 equiv.	1.5 equiv.	5 vol%	2	60 °C	15 %
7a	3	10 mol%	0.2 equiv.	1.5 equiv.	5 vol%	2	45 °C	46 %
7a	4	2.5 mol%	0.2 equiv.	1.5 equiv.	5 vol%	1.2	45 °C	44 %
7a	5	10 mol%	0.2 equiv.	1.5 equiv.	5 vol%	1.2	45 °C	52 %
7a	6	10 mol%	0.2 equiv.	1.5 equiv.	5 vol%	1.0	45 °C	54 %
1a	1	2.5 mol%	0.2 equiv	1.5 equiv	5 vol%	2	45 °C	60 %
1a	2	5 mol%	0.2 equiv.	1.2 equiv.	5 vol%	2	45 °C	77 %

For eugenol, the equivalents of catalyst and oxidizing agent, as well as the pH of the solution, seemed to have the most significant impact on the yield of the reaction. The literature shows that eugenol can undergo radical dimerization (polymerization) under typical Wacker oxidation conditions *via* a benzoquinone type intermediate¹³⁰. Decreasing the pH of the solution to around 1 (entry 6) seemed to reduce the tendency for its formation, thus increasing the yield. Since the remaining substrates lacked the structural feature of eugenol in the form of the 4-hydroxy group in the aromatic moiety, which is necessary for the dimerization to occur, the pH of the solution had a diminished impact on the reaction outcome.

It was determined that for allylbenzene the most important parameters were the reaction temperature, the amount of oxidizing agent and the equivalents of catalyst. After optimization of the reaction conditions (entry 8) the yield of the reaction could be increased to 77 %.

Lastly, the reaction was also performed on the remaining substrates (**1a-6a**, **8a**). Again, some

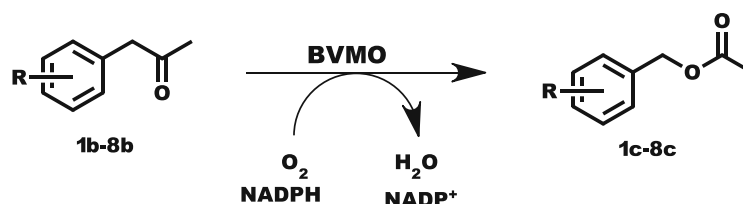
optimization of the reaction conditions was performed. The amount of catalyst and equivalents of oxidant had the most significant effect on the reaction outcome. The optimal reaction temperatures for the transformation were taken from the work of Gonz ales-Mart nez.⁹⁴ The results can be found in table 3.

Table 3: Optimization of the Wacker oxidation for **2a-8a**.

Substrate	Entry	Cat.	Additive	Oxidant	Co-Solvent	pH	Temp.	Yield
2a	1	5 mol%	0.2 equiv.	1.5 equiv.	5 vol%	2	30 �C	73 %
3a	2	5 mol%	0.2 equiv.	1.5 equiv.	5 vol%	2	30 �C	71 %
4a	3	5 mol%	0.2 equiv.	1.2 equiv.	5 vol%	2	45 �C	75 %
5a	4	5 mol%	0.2 equiv.	1.5 equiv.	5 vol%	2	60 �C	65 %
6a	5	5 mol%	0.2 equiv.	1.2 equiv.	5 vol%	2	60 �C	73 %
8a	6	10 mol%	0.2 equiv.	1.5 equiv.	5 vol%	2	45 �C	57 %

For substrates **3a** and **4a** $\text{Fe}_2(\text{SO}_4)_3$ instead of FeCl_3 proved to be the most optimal oxidizing agent as demonstrated by Gonz ales-Mart nez.⁹⁴ The desired ketones could be obtained with satisfying yields. Even though stoichiometric amounts of oxidizing agent are necessary for this, the use of high amounts of water in the solvent mixture coupled to the ease of removal of the reaction components makes this procedure an ideal candidate to test for biocompatibility.

B.3. Determining the substrate scope of PAMO, HAPMO, and TmCHMO



Scheme 37: Enzymatic Baeyer-Villiger-Oxidation of the substrates **1b-8b**.

To find a suitable enzyme for first step of the enzymatic cascade, the Baeyer-Villiger oxidation, PAMO, HAPMO, and TmCHMO were tested for their substrate scope. For this, whole-cell biocatalysis under standard conditions (OD_{590} 20, 50 mM PBS-puffer pH 7.4, 5 mM substrate concentration, 37  C for PAMO, 30  C for TmCHMO and HAMPO) was performed as described in

the experimental chapter. Substrates **1b-8b** were subjected to the enzymes. The results for the biotransformation with PAMO for the substrates **1b-4b** can be found in figure 9.

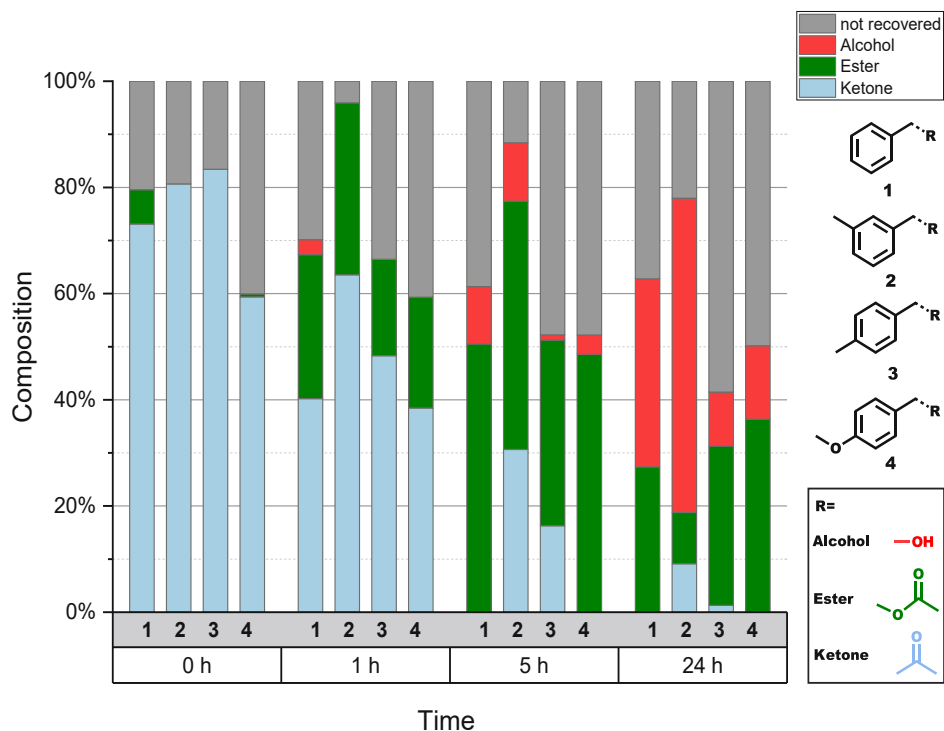


Figure 9: Results of the biotransformation with PAMO for the substrates **1b-4b**.

The results of the biotransformation with PAMO for the substrates **5b-8b** can be found in figure 10.

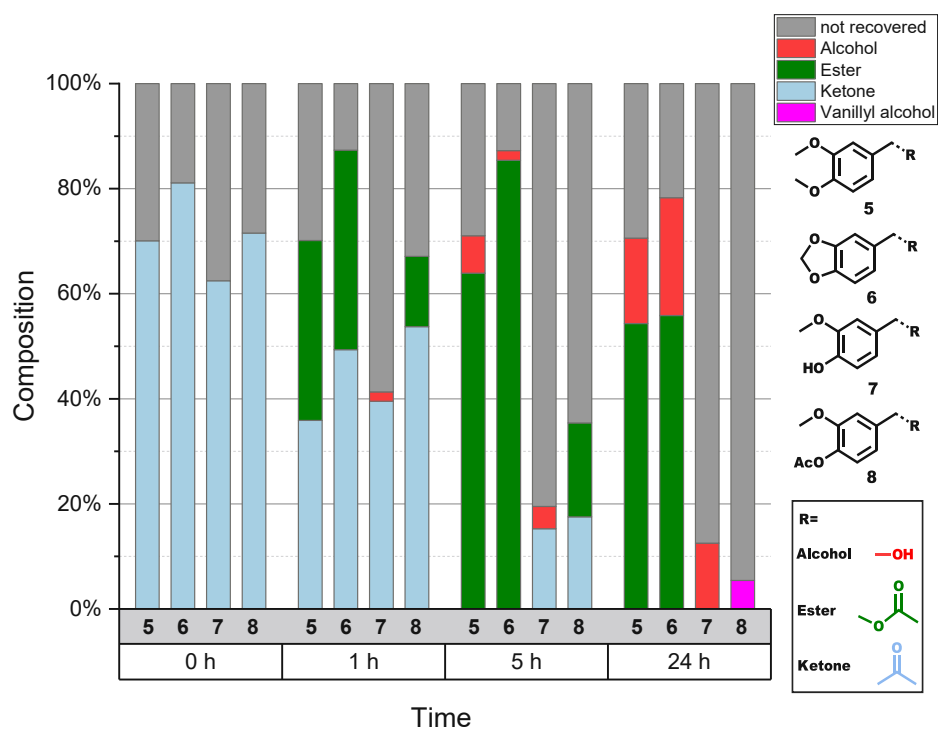


Figure 10: Results of the biotransformation with PAMO for the substrates **5b-8b**.

The results of the biotransformation with TmCHMO for the substrates **1b-4b** can be found in figure 11.

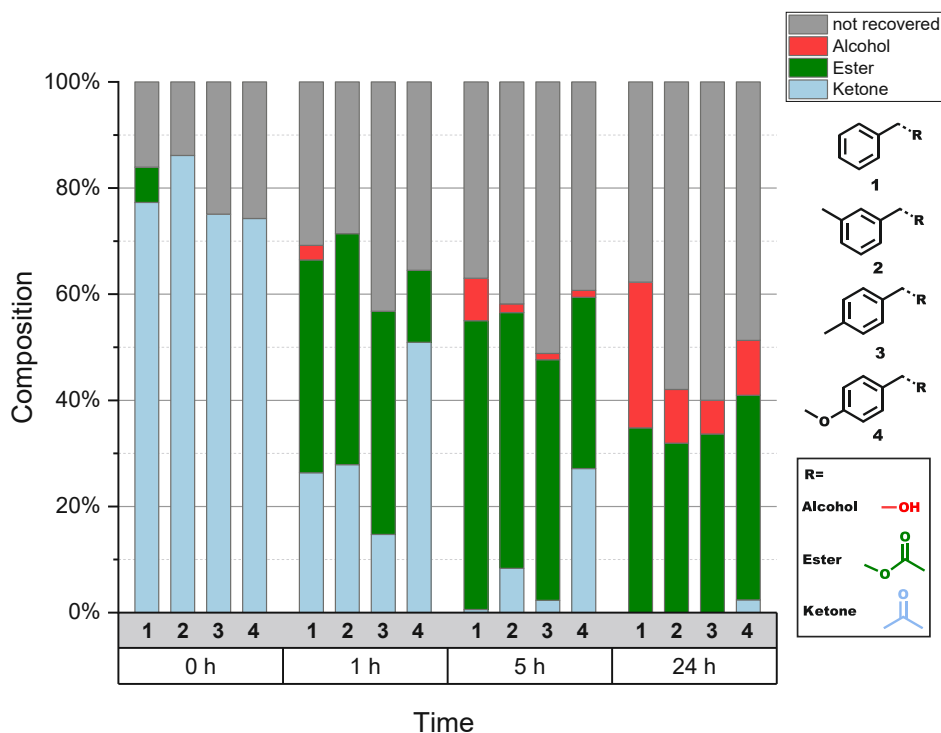


Figure 11: Results of the biotransformation with TmCHMO for the substrates **1b-4b**.

The results of the biotransformation with TmCHMO for the substrates **5b-8b** can be found in figure 12.

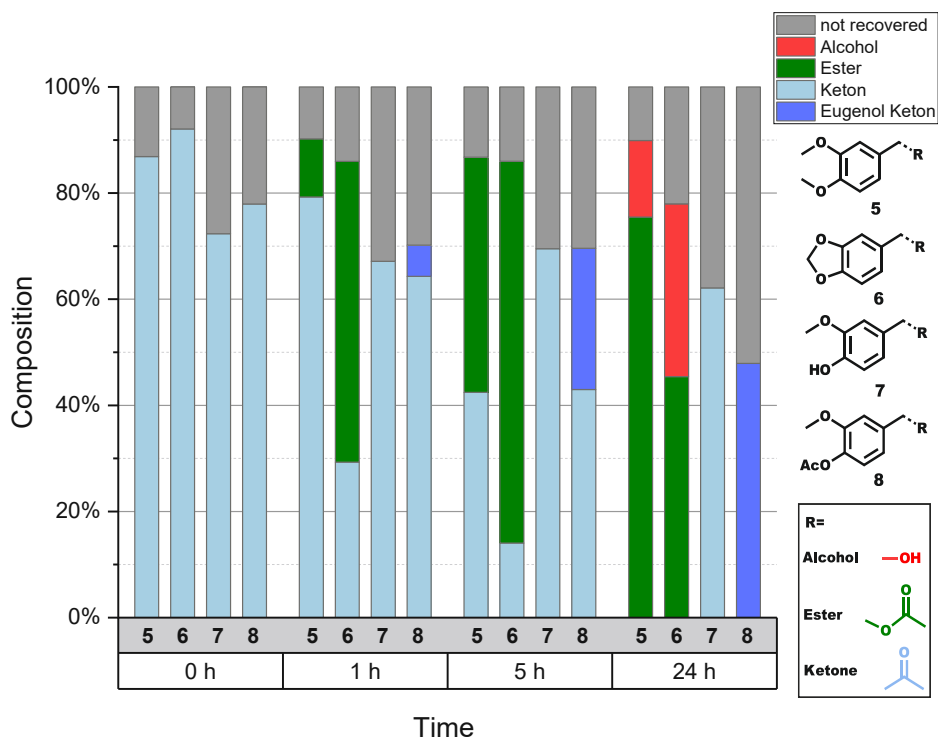
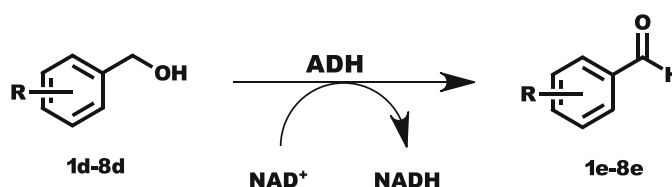


Figure 12: Results of the biotransformation with TmCHMO for the substrates **5b-8b**.

PAMO and TmCHMO showed activity towards most of the subjected substrates since they were successfully able to oxidize them into the respective acetates. HAPMO displayed no substance acceptance for the two substrates (**1b** and **7b**) tested in a preliminary screening and was therefore omitted from further considerations. TmCHMO showed good substrate acceptance for most substrates (**1b - 6b**) except for **7b** and **8b**. PAMO transformed all substrates **1b - 8b** into the respective acetates. To perform a successful subsequent oxidation and to obtain the desired product of the enzymatic cascade, the formed ester needs to be hydrolyzed into the free alcohol. In the case of whole-cell biocatalysis, hydrolases, which are naturally expressed by *E. coli*, facilitate this process. This effect can be seen at the 24-hour point, where some alcohol could be detected. Nevertheless, most of the initially formed ester is still present for most substrates. This is especially true for substrates that contain heteroatoms on the aromatic moiety. Additionally, there is no significant difference between the two enzymes in terms of the product distribution after 24 hours. The losses in recovery can be explained by the incomplete extraction of the organic compounds from the aqueous solution, especially at the 0 h time point, but also by further metabolism or side reactions of the very reactive acetate esters and aromatic alcohols by the whole-cell biocatalyst. This is especially prevalent in the case of **7b** and **8b**. Nevertheless, TmCHMO, as well as PAMO, proved to be suitable candidates for the enzymatic cascade.

B.4. Determining the substrate scope of AlkJ



Scheme 38: Enzymatic oxidation of the aromatic alcohols **1d-8d**.

To determine if AlkJ is a suitable enzyme for the enzymatic cascade, its substrate scope was determined. For this AlkJ was expressed in *E. coli*, as described in the experimental section, and whole-cell biocatalysis (OD₅₉₀ 20, 50 mM PBS-puffer pH 7.4, 5 mM substrate concentration, 30 °C) with the aromatic alcohols **1d-8d** was performed. The results of this biotransformation can be found in figure 13 and figure 14.

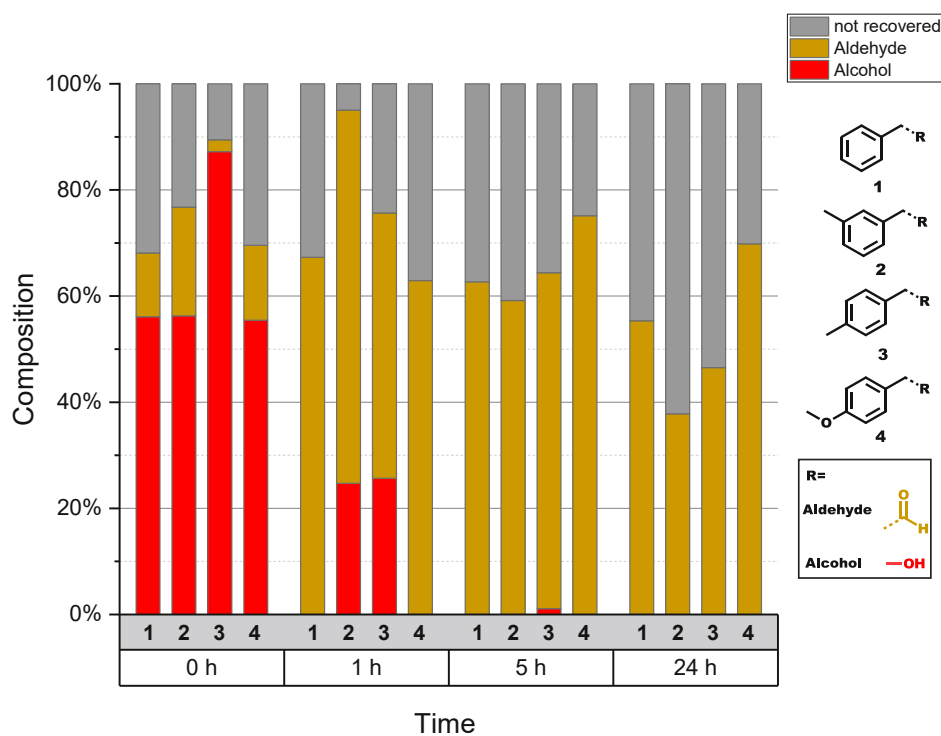


Figure 13: Results of the biotransformation with Alkj for the substrates 1d-4d.

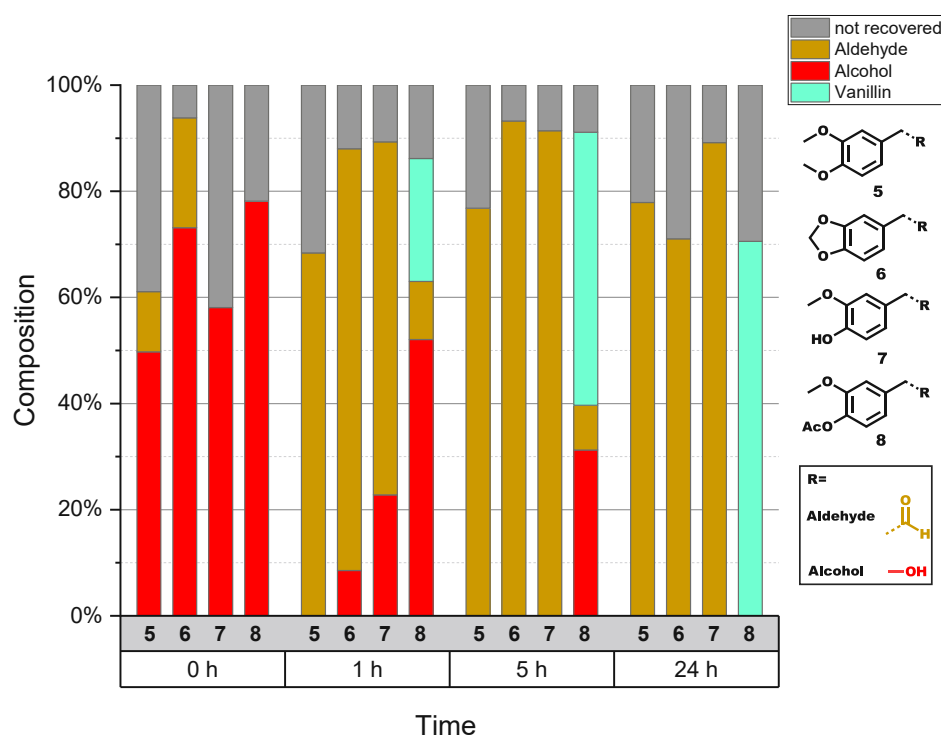


Figure 14: Results of the biotransformation with Alkj for the substrates 5d-8d.

The enzyme was able to selectively oxidize all desired alcohols into the respective aldehydes. Complete conversion was achieved after 24 hours. Depending on the substrate, the conversion rate varied considerably. Additionally, the acetate of **8c** was hydrolyzed during the

transformation, resulting in **7e** instead of **8e**. The incomplete mass recovery is a result of the incomplete extraction during the preparation of the GC-sample, further metabolization of the formed aldehyde and losses due to the volatility of the products. Nevertheless, AlkJ proved to be a suitable enzyme for the enzymatic cascade.

B.5. Comparison between the spontaneous hydrolysis and the hydrolysis facilitated by Pfl

As mentioned before, the acetate ester – the product of the enzymatic Bayer-Villiger-Oxidation – needs to be hydrolyzed into the respective alcohol so that AlkJ can oxidize them into the aldehyde. This hydrolysis should preferentially occur spontaneously in the aqueous solution catalyzed by hydrolases which are naturally expressed by *E. coli*. This hydrolysis occurs, as shown in figures 9-12 but at a rate that is not sufficient for the enzymatic cascade. To solve this problem, an external esterase was used in the form of Pfl, which is known in the literature to hydrolyze aromatic acetates.⁵⁴ Pfl was added in the form of lyophilized cells with a specific activity of U= 100 $\mu\text{Mol/mg}$. In figure 15, a comparison between the “spontaneous hydrolysis” and the hydrolysis facilitated by Pfl after an enzymatic Bayer-Villiger oxidation of **2a** can be found.

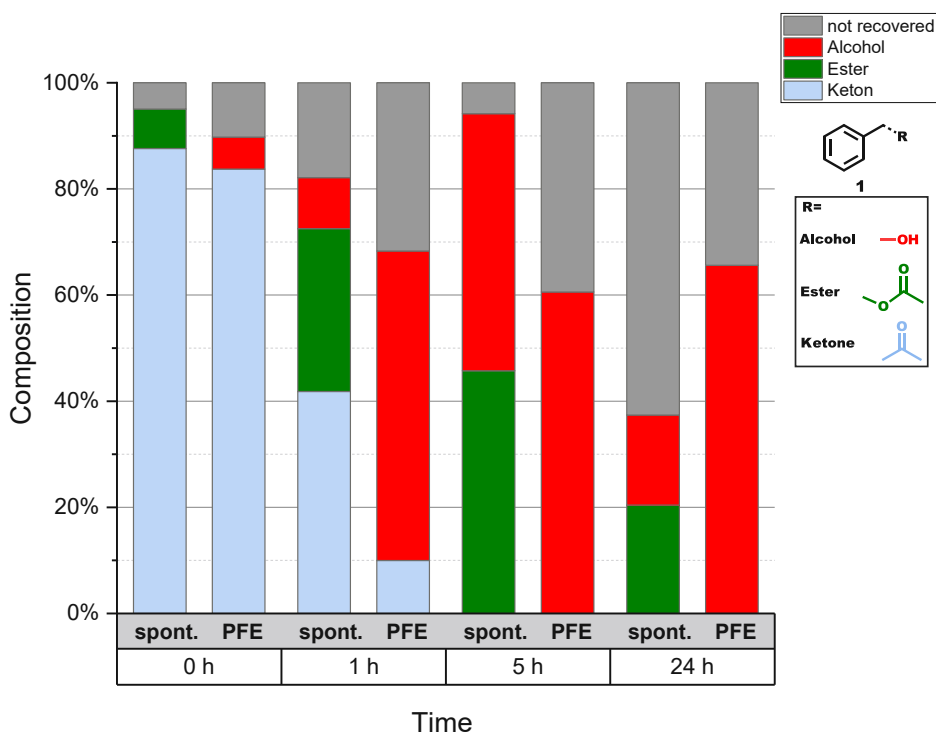


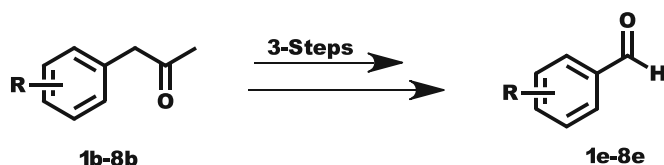
Figure 15: Comparison between the spontaneous hydrolysis and the hydrolysis facilitated by Pfl.

As seen in the former case, acetate is still present in the reaction mixture even after 24 hours. In the latter case, the ester is hydrolyzed so rapidly that it was not detectable by GC analysis. Thus, adding an external esterase makes the hydrolysis more reliable, improving the overall speed and

efficiency of the enzymatic cascade.

B.6. Assembly of the enzymatic cascade

The enzymatic cascade could be assembled after successfully testing all enzymes and determining their substrate scope (scheme 39).



Scheme 39: Three-step enzymatic cascade: 1) Bayer-Villiger-Oxidation of the ketone 2) Hydrolysis of the acetate 3) Oxidation of the primary alcohol to the desired aldehyde. Substrates: **1b-8b**.

For this, the form of a mixed culture approach was chosen. The enzymes (BVMO, ADH, and Esterase) were expressed individually in host cells and then added together as resting cells to obtain the enzymatic cascade as described in detail in materials and methods. For preliminary testing, PAMO was used as the enzyme for the enzymatic Baeyer-Villiger-Oxidation. The results of the biotransformation can be found in figure 16 and figure 17.

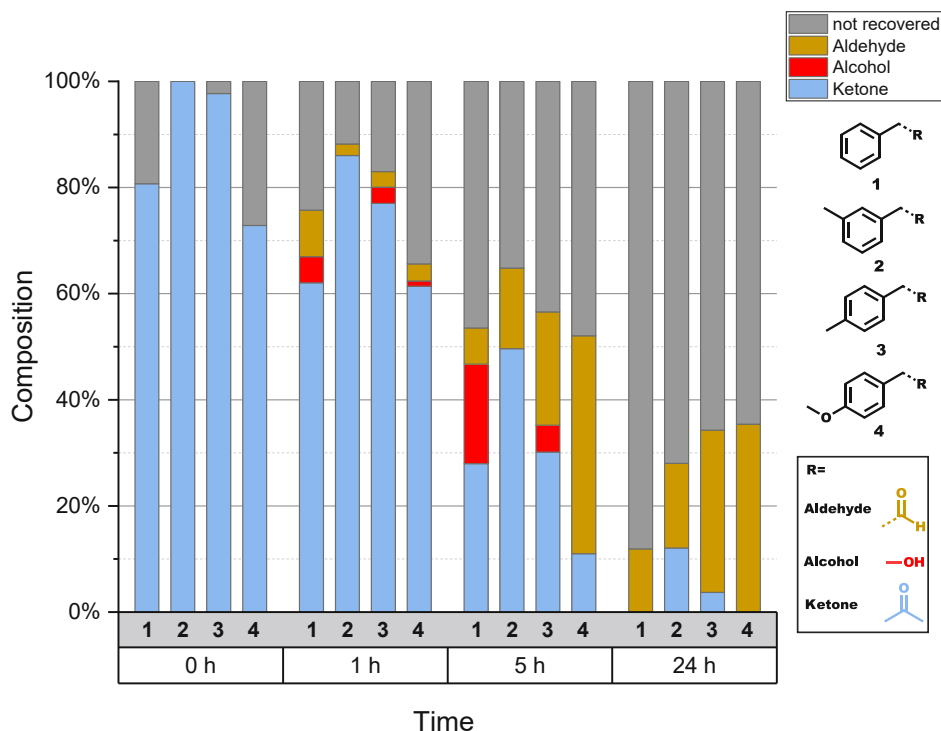


Figure 16: Results of enzymatic cascade with PAMO for the substrates **1b-4b**.

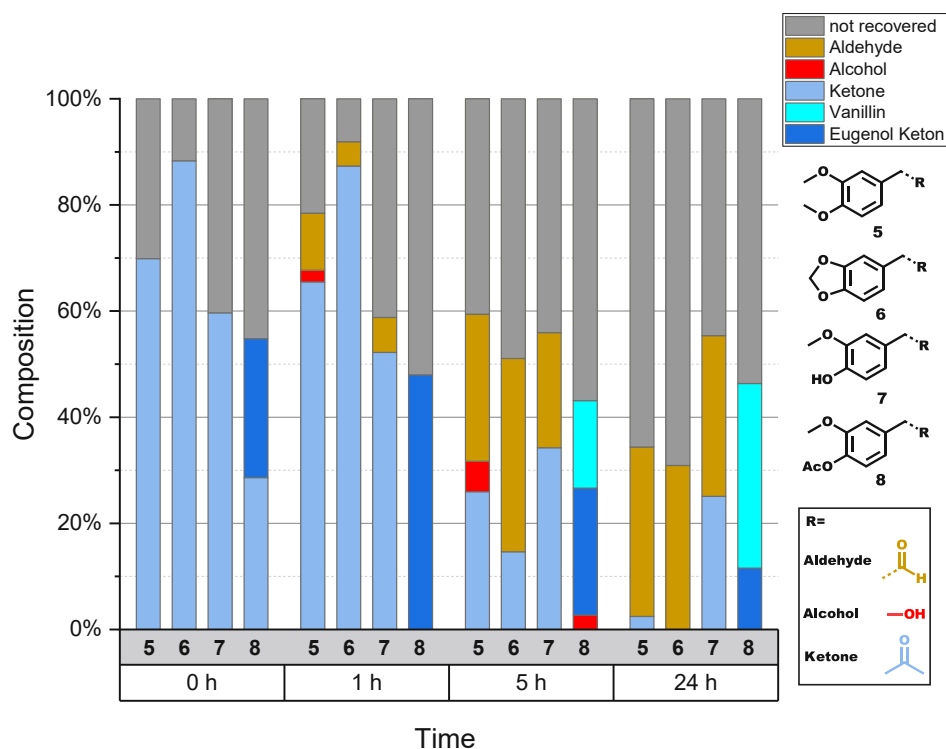


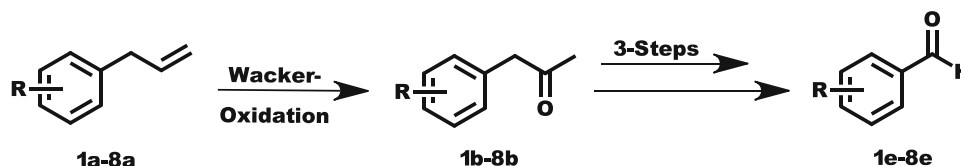
Figure 17: Results of enzymatic cascade with PAMO for the substrates **4b-8b**.

The mixed culture approach successfully produced the desired aldehydes from the respective phenyl propanones in three steps. The rate-determining step for this enzymatic cascade is the oxidation of the ketone to the ester. This is also shown by the fact that almost no intermediate could be detected besides the starting material and the final product. Hydrolysis of the phenolic acetate group in **8b** led to the formation of **7b** over the course of 1 hour. This species then underwent the enzymatic cascade, yielding **7e** as the product. The loss in recovery can again be attributed to incomplete extraction of the polar organic molecules from the aqueous solution and further metabolization of the product. For example, the formed aldehyde is subjected to further oxidation over the course of the reaction. The formation of the respective carboxylic acid could be detected in the chromatogram, but quantification was not feasible due to a nonlinear response. As a consequence of the mixed culture approach, high working cell densities are necessary to obtain the required concentration of each enzyme. However, a higher cell density also increases the probability of such side reactions. Simple aromatic aldehydes with no electron-donating moiety on the aromatic system were especially prone to overoxidation (**1e-3e**), whereas natural aldehydes (**4e-8e**) showed slower oxidation. Therefore, the yield of the enzymatic cascade is strongly dependent on the type of substrate and the reaction time.

For most of the substrates, complete conversion was achieved after 5 hours. After that, only overoxidation of the aldehyde is observed. Therefore, optimization of the reaction time is a simple strategy for increasing the yield.

B.7. Assembly of the chemoenzymatic one-pot reaction

The reaction mixture obtained after the Wacker oxidation and the enzymatic cascade were combined as described in the experimental section to perform a sequential chemoenzymatic one-pot reaction (scheme 40).



Scheme 40: Chemoenzymatic one-pot reaction: 1) Wacker oxidation 2) Bayer-Villiger-Oxidation of the ketone 3) Hydrolysis of the acetate 4) Oxidation of the primary alcohol to the desired aldehyde. Substrates: **1a-8a**.

The transformation consists of 4 steps. The first step is the chemical transformation in the form of the Wacker oxidation coupled to the enzymatic cascade. For the Wacker oxidation Fe(III)Cl_3 is employed as an oxidizing agent and gets converted to Fe(II)Cl_2 after the reaction is finished. In solution, Fe(II) and Fe(III) ions are only soluble in acidic conditions (~4).

By adjusting the pH of the reaction mixture with the addition of the resting cells suspended in 100 mM PBS buffer with a pH of 7.4 results in the precipitation of the iron ions as iron oxides are formed. Additionally, the Pd catalyst also precipitates, and Pd(0) is formed. So simply by adjusting the pH of the reaction mixture, most of the reagents remaining from the chemical transformation precipitate and can be removed by filtration or centrifugation as can be seen in figure 18.



Figure 18: Removal of the reaction components after the Wacker oxidation by centrifugation.

This diminishes the adverse influence of these reagents on the biocatalytic system negating the degradation of the catalyst or the promotion of possible side reactions. Since these precipitates are hardly soluble in water, it is also feasible to leave them in the mixture as they are relatively inert. After the formation of the product, the precipitates remain in the aqueous phase during the extraction. All substrates were subjected to this one-pot reaction. TmCHMO, as well as PAMO, were tested as the BVMO. The reaction mixture of the Wacker oxidation was stored at $-30\text{ }^\circ\text{C}$ and thawed just before the enzymatic cascade. Again, a mixed culture approach was applied to

assemble the enzymatic cascade.

B.7.1. Chemoenzymatic one-pot reaction: PAMO

The results of the chemoenzymatic one-pot reaction using PAMO as the BVMO, for the substrates **1b-4b** can be found in figure 19.

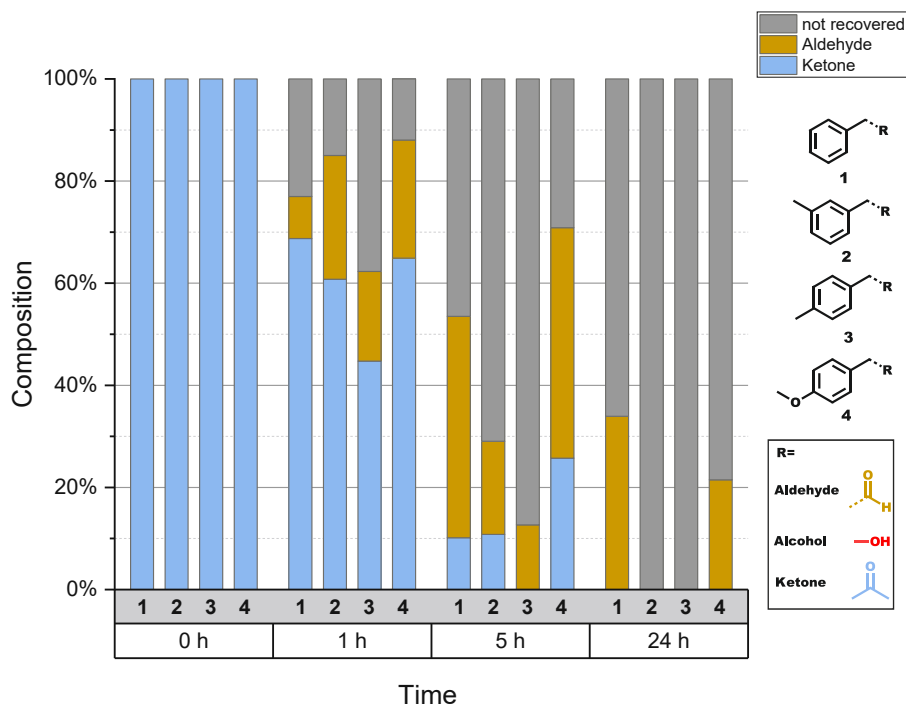


Figure 19: Results of the chemoenzymatic one-pot reaction with PAMO for the substrates **1b-4b**.

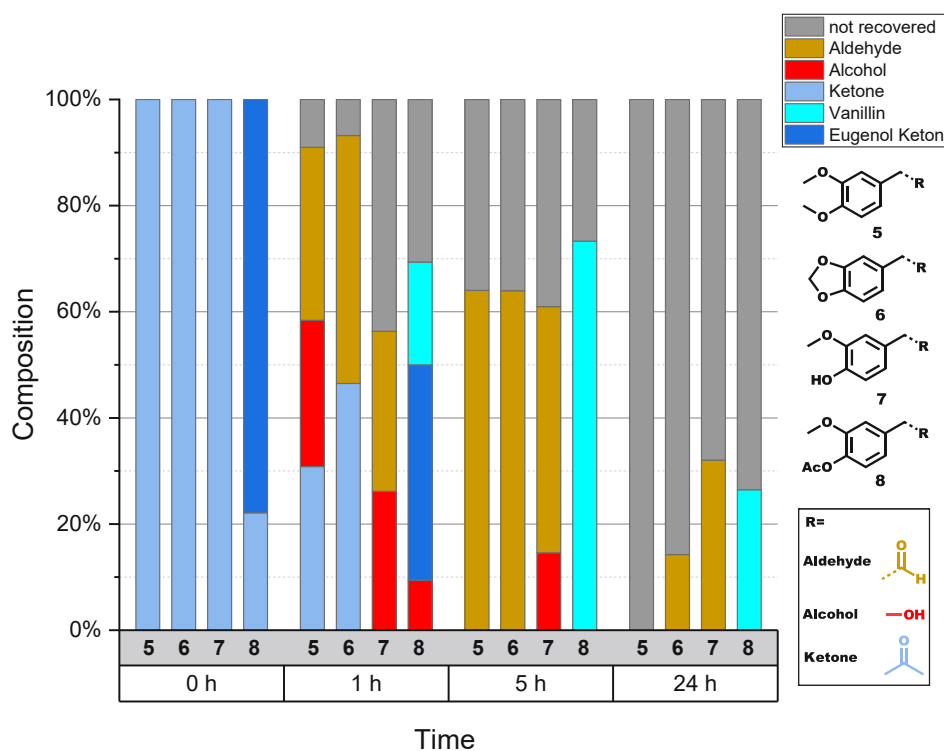
For the substrates **1b-4b**, it was possible to couple the enzymatic cascade to the chemical transformation in a sequential one-pot fashion to obtain the desired aldehydes. Almost complete conversion was achieved after 5 hours. As mentioned in the previous chapter over the course of the reaction, the recovery of the analyte decreases due to the formation of further metabolites or the oxidation of the aldehydes to the respective carboxylic acids.

After 24 hours, almost all of the formed aldehyde except for **1b** and **4b** had been further converted. Remarkably, neither the ester (step 2) nor the alcohol (step 3) was detectable during the conversion. This again suggests that the rate-determining step is the Baeyer-Villiger-Oxidation of the ketone (step 1). The yields of the Wacker oxidation, the enzymatic cascade, and the combined yield of the whole chemoenzymatic one-pot reaction can be found in table 4.

Table 4: Yields of the chemoenzymatic one-pot reaction with PAMO and substrates 1b-4b. *Yield determined at t = 0h.

Substrate	Yield Wacker [%]*	Yield enzymatic cascade [%]	Yield combined (step) [%]
1b	63 %	43 % (5 h)	27 % (72 %)
2b	64 %	18 % (5 h)	12 % (58 %)
3b	69 %	17 % (5 h)	20 % (59 %)
4b	45 %	51 % (5 h)	23 % (70 %)

The detected concentration of the substrate at t = 0h was used to determine the yield of the chemical transformation. Due to the incomplete extraction, the actual yield of the Wacker oxidation may be higher than determined. The yield of the enzymatic cascade was determined by the ratio of the concentration of the formed aldehyde at t = 5 h to the concentration of the substrate at t = 0 h. The combined and the step yield was determined by multiplication of the yield of the Wacker oxidation with the yield of the enzymatic cascade. For **1b**, the desired aldehyde could be detected with a yield of 27 % at 5 hours after four steps with a remarkable step yield of 72 %. In comparison, the yield of the enzymatic cascade leading to naturally occurring p-anisaldehyde **4e** (51 %) is higher than for the substrates that form only carbon-containing aldehydes **1b-3b**. This is either a result of the ease of oxidation or the enzymatic conversion rate. The results for the chemoenzymatic one-pot reaction using PAMO as the BVMO, for the substrates **4b-8b**, can be found in figure 20.

Figure 20: Results of the chemoenzymatic one-pot reaction with PAMO for the substrates **5b-8b**.

As before, full conversion of the starting material was achieved after 5 hours. In comparison to

1b-4b, some alcohol could be detected after 1 h and 5 h. For **8b**, hydrolysis of the phenolic acetate leads to the formation of vanillin **7e** as the product of the transformation. The yields of the Wacker oxidation, the enzymatic cascade, and the combined yield of the whole chemoenzymatic one-pot reaction can be found in table 5.

Table 5: Yields of the chemoenzymatic one-pot reaction with PAMO and substrates 5b-8b. *Yield determined at t = 0h.

Substrate	Yield Wacker [%]*	Yield enzymatic cascade [%]	Yield combined (step) [%]
5	57 %	64 % (5h)	36 % (78 %)
6	36 %	83 % (5h)	30 % (74 %)
7	24 %	46 % (5h)	11 % (57 %)
8	53 %	73 % (5h)	39 % (79 %)

In general, the yield for the enzymatic cascade for naturally occurring aldehydes (**5b-8b**) is generally higher than for the simpler aldehydes (**1b-3b**). Piperonal, for example, could be obtained with a yield of 30 % after 5 hours and a remarkable step yield of 74 %. The transformation of eugenol **7a** was only moderately successful due to a poor Wacker oxidation. Nevertheless, vanillin **7e** could be obtained with a yield of 11 % and a step yield of 57 %.

B.7.2. Chemoenzymatic one-pot reactions: TmCHMO

The results for the chemoenzymatic one-pot reaction using TmCHMO as the BVMO for the substrates **1b-4b** can be found in figure 21.

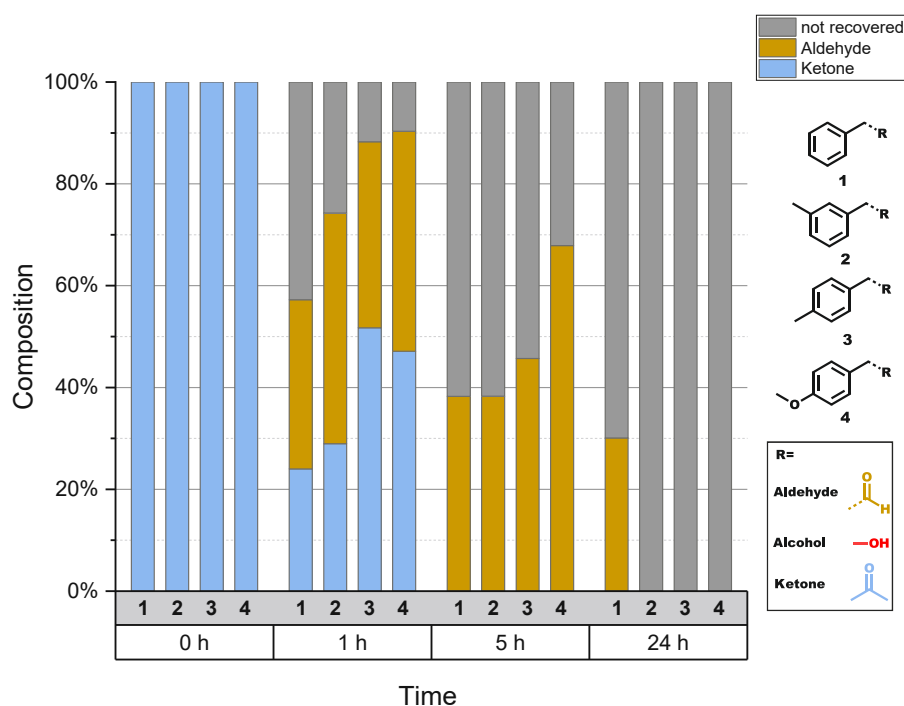


Figure 21: Results of the chemoenzymatic one-pot reaction with TmCHMO for the substrates **1b-4b**.

Full conversion of the starting material was achieved after 5 hours. After 24 hours, most of the obtained product was further converted into the corresponding carboxylic acid or metabolized otherwise by the whole-cell biocatalyst. The yields of the Wacker oxidation, the enzymatic cascade, and the combined yield of the whole chemoenzymatic one-pot reaction can be found in table 6.

Table 6: Yields of the chemoenzymatic one-pot reaction with TmCHMO and substrates 1b-4b. *Yield determined at t=0h.

Substrate	Yield Wacker [%]*	Yield enzymatic cascade [%]	Yield combined (step) [%]
1	51 %	38 % (5h)	20 % (66 %)
2	53 %	38 % (5h)	20 % (67 %)
3	57 %	45 % (5h)	25 % (71 %)
4	40 %	67 % (5h)	27 % (72 %)

Notable is the enzymatic cascade of **4b** yielding 67 % in three steps. In total p-anisaldehyde **4e** could be obtained with a yield of 27 % and a step yield of 72 %. The yields of the enzymatic cascade of the substrates **1b-3b** are also satisfying, ranging from 38- 45 %.

The results for the chemoenzymatic one-pot reaction using TmCHMO as the BVMO for the substrates **5b-8b** can be found in figure 22.

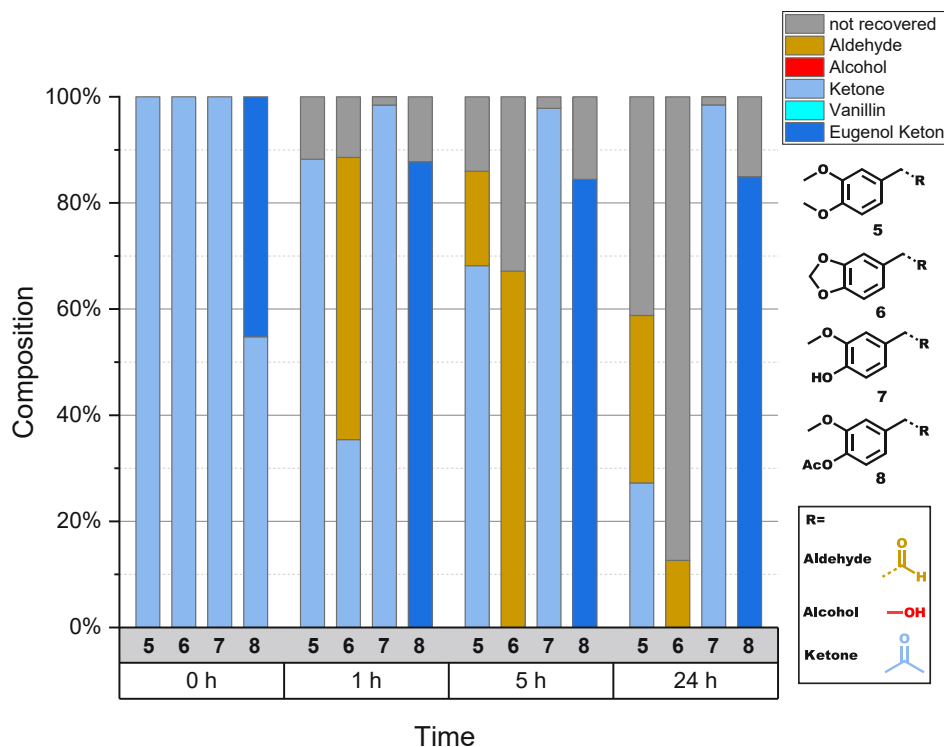


Figure 22: Results of the chemoenzymatic one-pot reaction with TmCHMO for the substrates 4b-8b.

As expected, TmCHMO was not able to convert **7b** and **8b** into the respective aldehydes. Additionally, complete conversion of **5b** was not achieved even after 24 hours. The yields of the

Wacker oxidation, the enzymatic cascade, and the combined yield of the whole chemoenzymatic one-pot reaction can be found in table 7.

Table 7: Yields of the chemoenzymatic one-pot reaction with TmCHMO and substrates 4b-8b. *Yield determined at t = 0h.

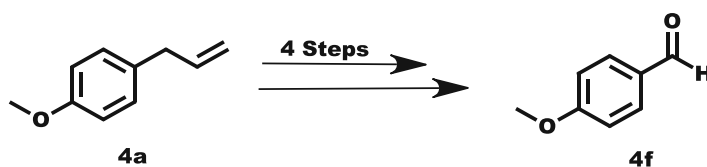
Substrate	Yield Wacker [%]*	Yield enzymatic cascade [%]	Yield combined (step) [%]
5	43 %	31 % (24 h)	14 % (60 %)
6	51 %	67 %	34 % (76%)
7	/	/	/
8	/	/	/

Piperonal **6e** was obtained with a yield of 34 % with an impressive step yield of 76 %. In the big picture, the results of the TmCHMO catalyzed enzymatic cascade are comparable to the PAMO catalyzed one. For simpler substrates (**1b-4b**), TmCHMO generally affords slightly better results in the enzymatic transformation than PAMO. On the other hand, PAMO is able to transform the substrates **7b** and **8b** to yield vanillin, which is unobtainable with TmCHMO.

Nevertheless, it was indeed possible to couple the chemical transformation in the form of a Wacker oxidation to the enzymatic transformation. As expected, overoxidation of the aldehydes to the corresponding carboxylic acids could be observed. The amount of acid is again strongly dependent on the reaction time and the substrate. The best results were obtained after 5 hours. Simpler aldehydes (**1b-4b**) are generally more prone to overoxidation.

B.8. Increasing the scale of a chemoenzymatic one-pot reaction

To demonstrate the scalability of the chemoenzymatic sequential one-pot reaction and to verify the results from GC-analysis, a larger scale experiment was conducted (37 mg). 4-Allylanisole **4a** was used as the model substrate for this transformation and TmCHMO for enzymatic Baeyer-Villiger-Oxidation (Scheme 41).



Scheme 41: Chemoenzymatic one-pot reaction of 4-allylanisole to p-anisaldehyde.

Biotransformation was performed under standard conditions except for the volume of the whole-cell biocatalyst, which was increased from 1 ml (OD₅₉₀ 20) to 50 ml (OD₅₉₀ 12). The reaction mixture resulting from the Wacker oxidation was used after the removal of the reaction components after pH adjustment and centrifugation. The yield of the Wacker oxidation was

determined at the $t = 0$ h point of the enzymatic transformation. The conversion of the substrate in the enzymatic cascade was regularly checked with GC analysis. The results can be found in figure 23.

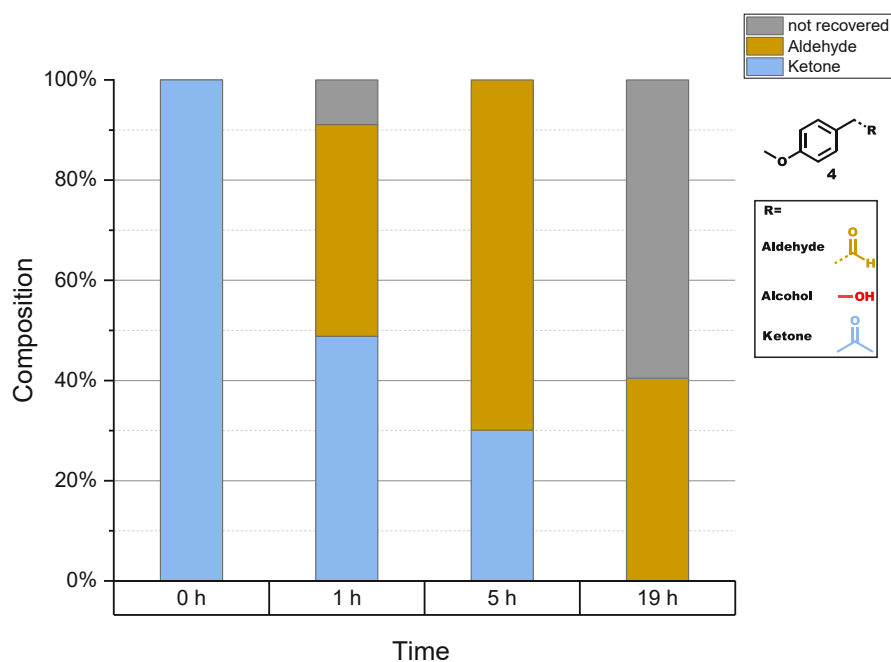


Figure 23: Results of the biotransformation for **4b**.

The reaction was stopped at 19 hours point, and the mixture was acidified and extracted with EtOAc. After removal of the solvent under reduced pressure, $^1\text{H-NMR}$ -analysis of the residue was performed (figure 24).

Vega5GI-193-001.1.fid

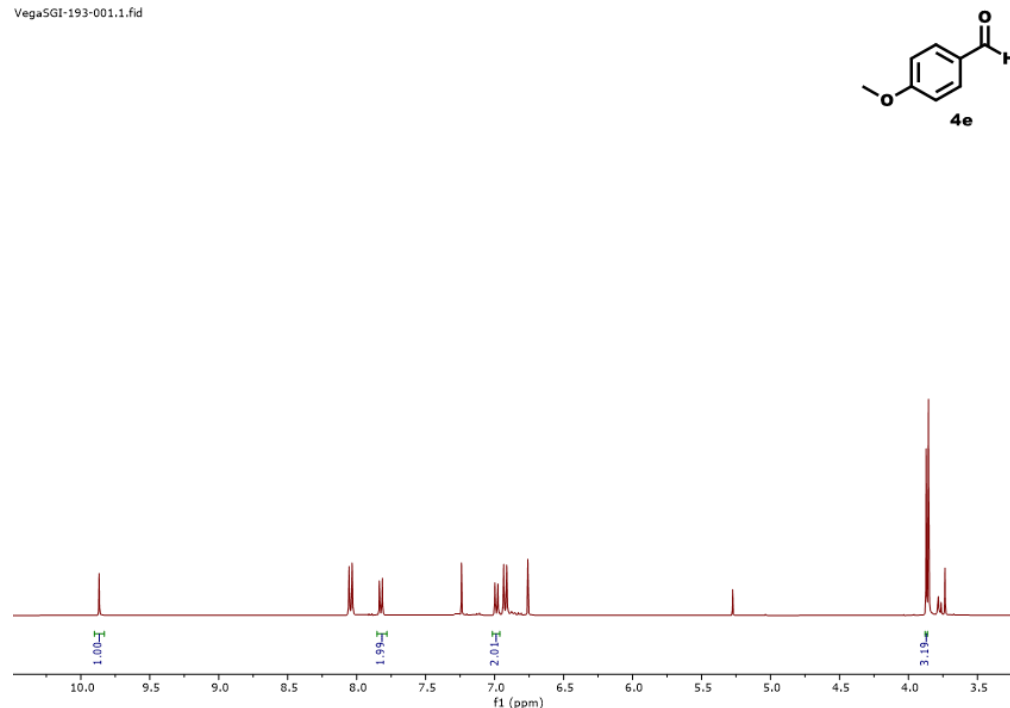


Figure 24: $^1\text{H-NMR}$ of residue resulting from the chemoenzymatic one-pot reaction. A mixture of p-anisaldehyde and 4-methoxy benzoic acid could be detected.

As expected, a mixture of acid and aldehyde was obtained. The characteristic aldehydic proton signal is clearly visible at around 9.8 ppm. To deduce the yield of the transformation, the molar ratio between the two species in the NMR spectrum was calculated (1:0.65 Acid: Aldehyde). The yield of the reaction can be found in table 8.

Table 8: Yields of the large-scale chemoenzymatic one-pot reaction. *Yield determined at t = 0h.

Substrate	Yield Wacker [%]*	Yield enzymatic cascade [%]	Yield combined [%]
4b	71 %	40 %	30 % (GC-Analysis) 34 % (Gravimetric)

The yield determined by GC-analysis (30 %) corresponds well to the yield determined by quantification of the ¹H-NMR spectrum (34 %). Additionally, this experiment confirms that it is indeed possible to increase the scale of the enzymatic cascade. This is an important first step for the enzymatic cascade to be used on a synthetic scale. Additionally, if necessary, the acid could theoretically be removed by simple acid-base extraction during the work-up.

B.9. Design and construction of a plasmid vector for the co-expression of TmCHMO and Pfl

To solve the issues arising from the high combined cell density since all three enzymes are expressed individually, a vector for the co-expression of TmCHMO and Pfl was designed. TmCHMO was selected for the enzymatic Baeyer-Villiger-Oxidation due to the generally higher yields in the enzymatic cascade, as can be seen in the previous chapter. The genes for TmCHMO and for Pfl were already available and were subcloned into the desired plasmid system. A pETDuet-1 vector system in a pseudo-operon configuration (Figure 25) was selected for this.

The plasmid contains two IPTG inducible LacI/P_{T7lac} promoter regions, which allow for high levels of expressions in *E. coli*. Transcription can additionally be controlled by autoinduction. For this, a growth medium is used, which contains a limited amount of glucose for the initial cell growth, in addition to α -lactose, which acts as the inducing agent. The plasmid contains a pBR32 high copy origin which is, more importantly, also compatible for the co-transformation with the pKA1 plasmid system entailing AlkJ.



Figure 25: Design of the vector pETDuet1_TmCHMO::Pfl.

The vector was constructed with the help of NEBuilder® HiFi DNA Assembly, which is based on the Gibson assembly. Gibson assembly or Gibson isothermal assembly allows for the ligation of multiple DNA fragments in a single step, and additionally, this method is sequence-independent. This sequence independence omits the reliance on specific cloning restriction sites, making this method a highly convenient technique. It solely depends on homologous DNA regions in each of the fragments, which can be added by appropriate primers.²⁴ The overhang regions need careful design to increase the probability of successful cloning. Typically, 20 – 30 base pairs are necessary, but also G and C rich regions at the start or the end of the homologous region are beneficial to prevent the formation of interfering secondary structures.

The kit consists of three enzymes: a T5 exonuclease, a high-fidelity DNA polymerase, and a DNA ligase. The general procedure for Gibson assembly can be found in figure 26.

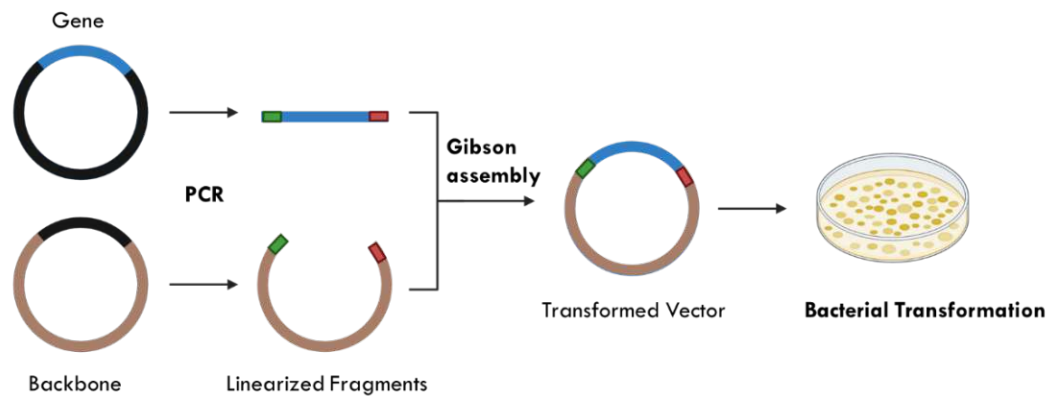


Figure 26: Workflow for Gibson Assembly: T5-exonuclease creates complementary 5' overhangs in the backbone and insert. After annealing, the strands are joined by DNA polymerase and then DNA ligase. Figure constructed with Biorender.com.

The construct was assembled in two steps: First, the gene of PflI was inserted into the backbone on the first multiple cloning site upstream of the terminator. Lastly, the gene of TmCHMO was inserted into the remaining multiple cloning site. Successful insertion was validated *via* Sanger sequencing (figure 27) and colony PCR (see chapter D.2.).

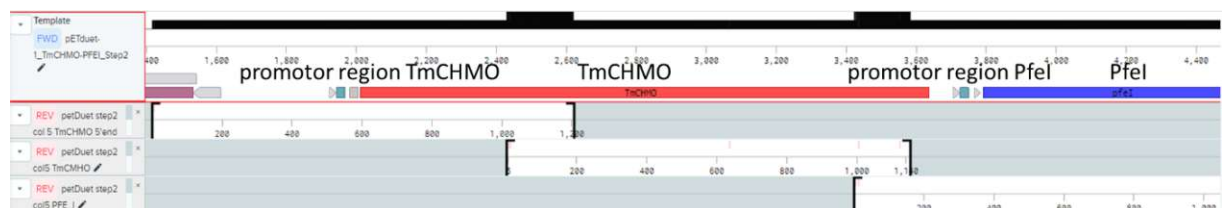


Figure 27 Result of the sequence alignment between the constructed vector and three ~1 kb long Sanger sequencing fragments. Both promoter regions, as well as the sequences for both genes, were successfully validated.

Since the limitation of Sanger sequencing lies around ~ 1 kb pairs, three sequencing rounds were necessary to validate the entire genetic region of the inserts. Nevertheless, both inserts as well as both promoter regions of the construct in pseudo-operon configuration, showed no mutations, except for two silent deviations in the sequence of TmCHMO. The codon GAA (translating to glutamic acid) in the literature known sequence of TmCHMO was exchanged in two cases to GAG (also translating to glutamic acid) at the positions 3064 and 3435.

B.9.1. Successful co-expression of TmCHMO and Pfel

The plasmid was transformed into *E. coli* BL21 (DE3) cells. Autoinduction was used to test ten clones for protein production (figure 28). SDS-PAGE analysis of the whole-cell biocatalyst showed strong overexpression of Pfel but only weak for TmCHMO.

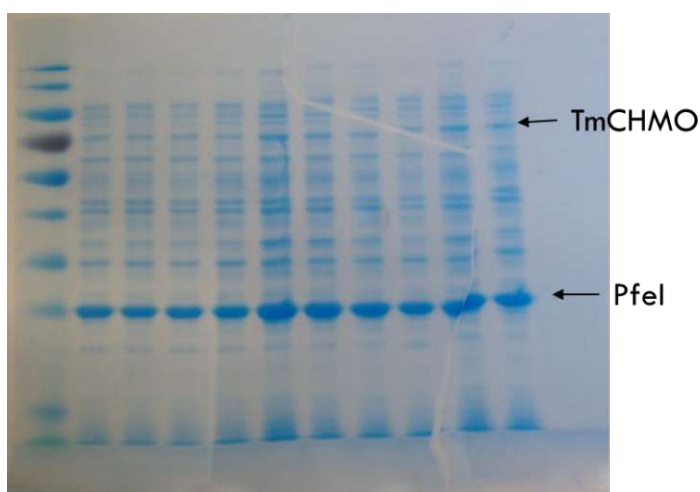
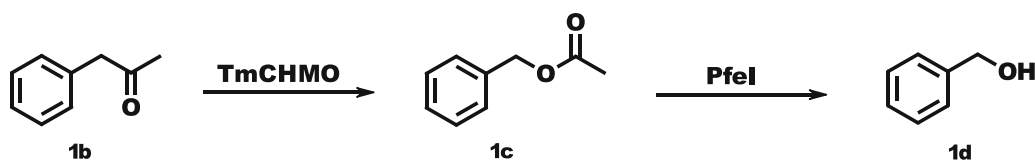


Figure 28: SDS-PAGE analysis of the co-expression of TmCHMO and Pfel.

Biotransformation under standard conditions (OD_{590} 20, 50 mM PBS-buffer pH 7.4, 30 °C) (see chapter D.6.) was performed to determine the activity of the enzymes. Phenylacetone **1b** was used as the model substrate (scheme 42) with a concentration of 1 mM (standard concentration is 5 mM).



Scheme 42: Two-Step enzymatic cascade for the conversion of phenylacetone **1b** to benzyl alcohol **1d** performed by a whole-cell biocatalyst co-expressing TmCHMO and Pfel.

The results can be seen in figure 29. The transformation was monitored with GC-analysis after 0, 3, and 24 hours. Full consumption of the starting material was obtained after 24 hours. The intermediate product in the form of benzyl acetate, which is formed after the first step of the

enzymatic cascade, was hardly detectable, suggesting high activity levels of the esterase.

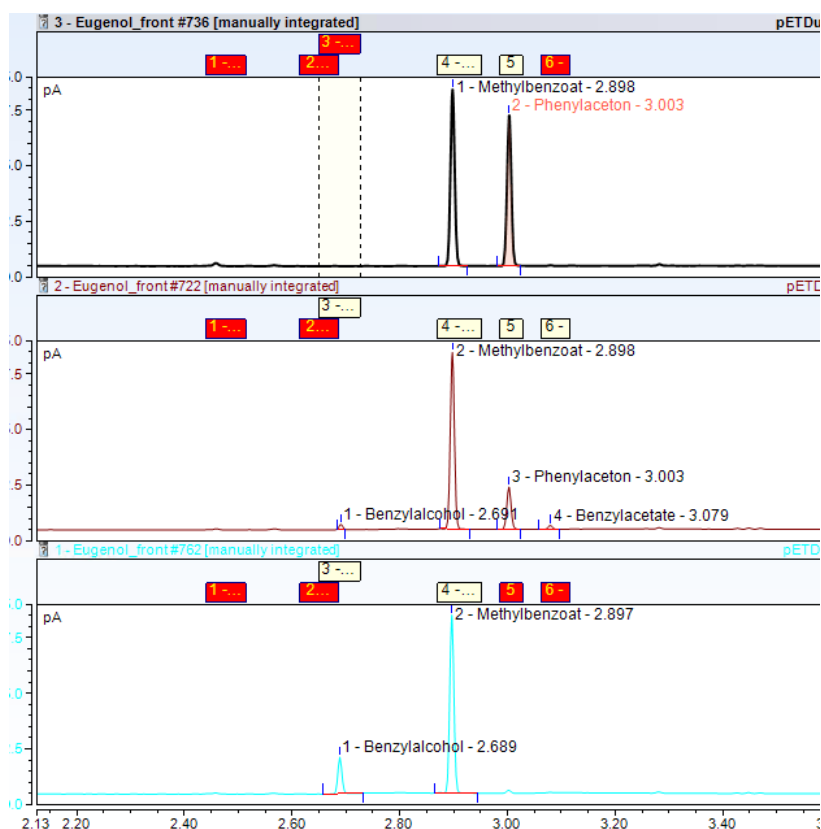


Figure 29: Chromatogram of the biotransformation.

Over the course of the reaction time, the amount of benzyl alcohol also gradually increases. Due to the previously mentioned issues of only partial extraction of the polar alcohol, full mass recovery was not achieved. Performing the biotransformation with a higher substrate concentration (5 mM) led to a decrease in conversion. This is a consequence of the poor TmCHMO production, as seen in figure 28. Nevertheless, these results successfully demonstrate that the construct affords functional enzymes for PflI as well as for TmCHMO, although in very low amounts.

B.9.2. Co-transformation with TmCHMO::PflI and AlkJ

After the successful validation of the pETDuet1_TmCHMO::PflI vector, co-transformation with pKA1-AlkJ in *E. coli* BL21(DE3) was performed. Twenty colonies were tested for protein production. Autoinduction was employed to induce protein production. SDS-PAGE analysis of the whole-cell biocatalyst only showed the protein bands for PflI and AlkJ but no or hardly any for TmCHMO (figure 30). Nevertheless, a biotransformation was conducted with phenylacetone as the model substrate. Unfortunately, only marginal conversion of the substrate was observed. Experiments were repeated with different expression conditions (induction with IPTG), but no difference in the outcome was observed.

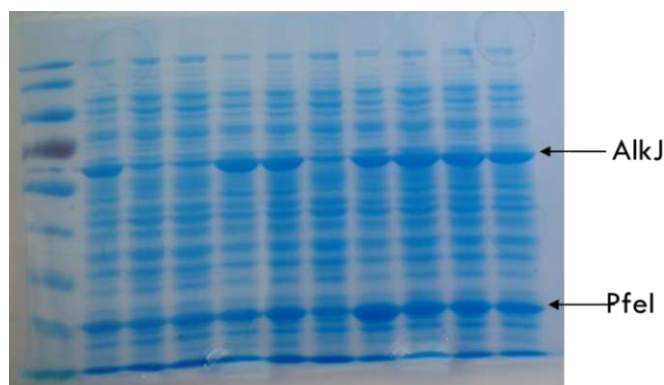
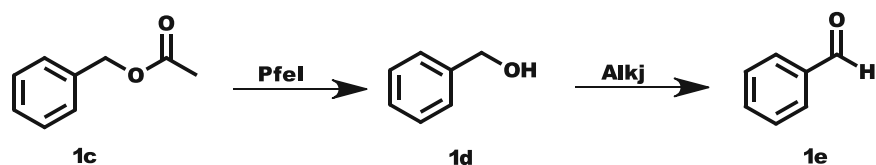


Figure 30: SDS-PAGE analysis of the co-expression of pETDuet1-TmCHMO::PfeI and pKA1-AlkJ.

To test for the activity of AlkJ and PfeI a biotransformation with benzyl acetate as the substrate was performed (scheme 43).



Scheme 43: Two-Step enzymatic cascade for the conversion of benzyl acetate to benzaldehyde performed by a whole-cell biocatalyst co-expressing AlkJ and PfeI.

Full consumption of the starting material was observed after one hour, indicating a strong overexpression of at least AlkJ and PfeI (figure 31). Since the acetate is hydrolyzed almost immediately, mainly alcohol was detected in the 0 h sample.

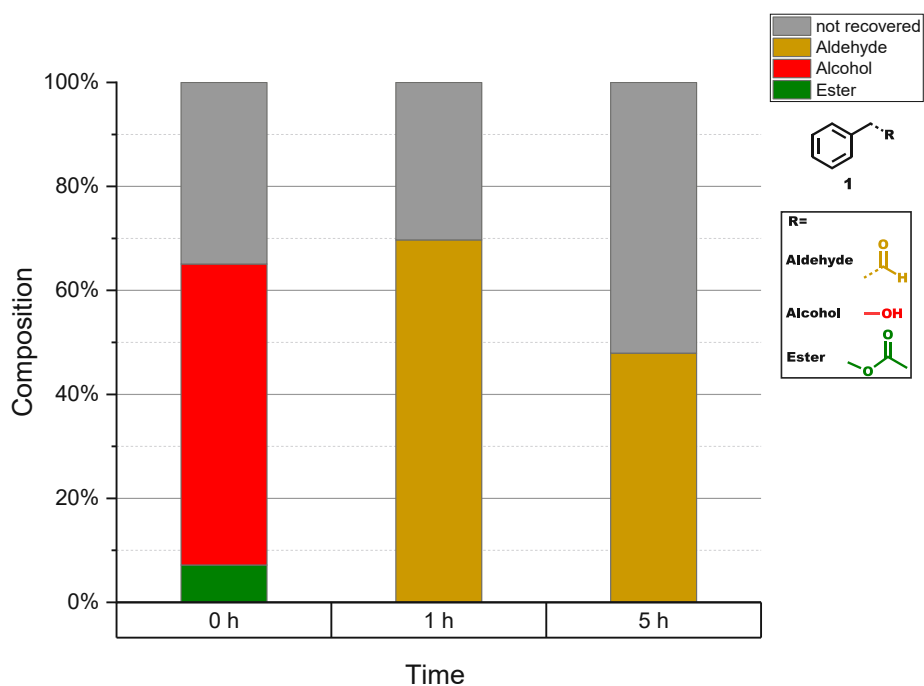


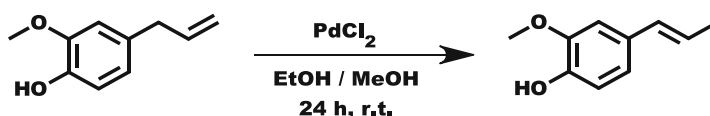
Figure 31: Results of the biotransformation with pETDuet1_TmCHMO::PfeI-pKA1_AlkJ and benzyl acetate **1c**.

Co-transformation of the two plasmids led to the complete stop of the expression of TmCHMO. Since PflI is produced in adequate amounts, as seen in the successful transformation of benzyl acetate, both plasmids are present in the host cells and are also functional. The expression of TmCHMO was already weak in the case of the single plasmid-containing system. The addition of a second vector led to a complete overshadowing of either the translation or transcription of the gene. Nevertheless, the construction of the plasmid and the attempted co-transformation is an essential first step in the development of a single cell expression system for this enzymatic cascade. For further improvements in either the transcription or the translation of the gene, the design of the plasmid needs to be modified.

B.10. ADO: Route B

B.10.1. Isomerization

As mentioned in the introduction, the typical methods for the isomerization of 2-propenylbenzenes include metal-mediated (e.g., palladium) and base-mediated procedures. Palladium-catalyzed isomerization is typically performed in a degassed alcoholic solvent like MeOH or EtOH at r.t.-40 °C for 24 to 48 hours. Base-mediated procedures rely on stoichiometric amounts of a base like KOH. Since we wanted to incorporate only catalytic procedures in route B, we decided on a palladium-catalyzed isomerization. For preliminary testing, the standard conditions (5 mol% PdCl₂, MeOH or EtOH, rt.) with eugenol as a model substrate were successfully employed to obtain isoeugenol (scheme 44).¹³¹



Scheme 44: PdCl₂ catalyzed isomerization of eugenol 7a to isoeugenol 7g in EtOH or MeOH.

To achieve bio-compatibility of the chemical transformation with the subsequent enzymatic transformation, the water content of the solvent (EtOH) used in the reaction was gradually increased. To determine the optimal solvent composition for this reaction, four different mixtures were tested (50 %, 80 %, 90 % and 95 % water content). After 24 hours, the reaction mixture was extracted, the solvent removed, and the residue analyzed by ¹H-NMR (figure 32).

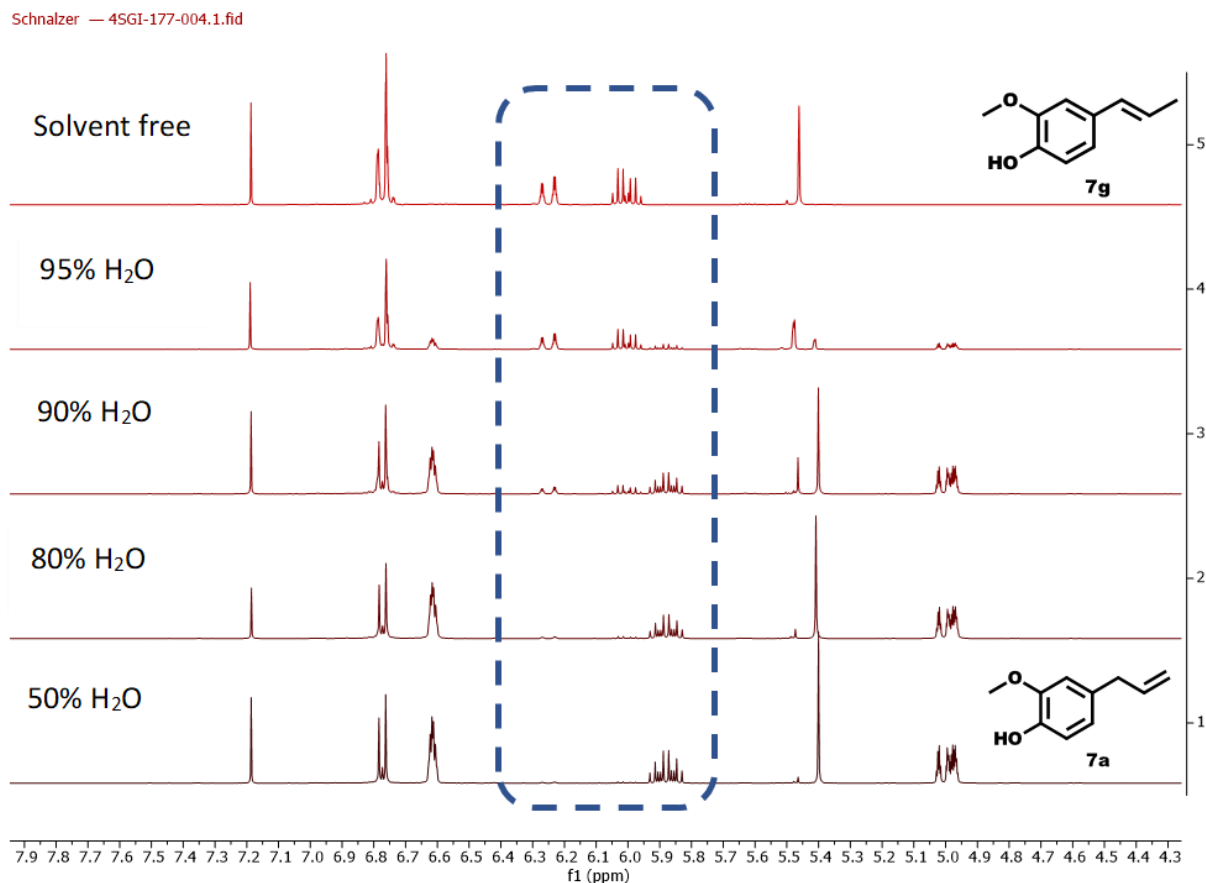
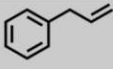
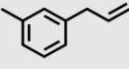
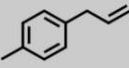
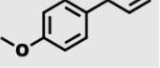
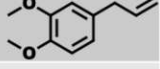
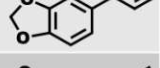

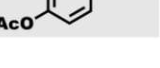


Figure 32: Comparison between different amounts of water in the reaction solvent. The signal at 5.9 ppm corresponds to one of the olefinic protons of eugenol **7a**.

Increasing the water content from 0 to 50 % resulted in an almost complete stop of the conversion of eugenol to isoeugenol. In this case, the substrate and PdCl₂ were fully dissolved in the solvent. Interestingly, a further increase in the water content of the solvent mixture (to 80-95 %) again afforded the isomerized product. This is shown in the ¹H-NMR by the appearance of the characteristic olefinic signals of isoeugenol after 24 hours (6.1 and 6.3 ppm). Neither the substrate nor the catalyst were fully dissolved at 90 to 95% water content, which resulted in a heterogeneous reaction mixture. Additionally, it was observed that the catalyst was primarily located around the organic substrate phase and not evenly distributed in the entire reaction flask. The more pronounced this effect was (less dissolved reaction components), the higher the conversion of eugenol after 24 hours.

These results made it evident that the isomerization could probably proceed without any solvent at all. Surprisingly, complete conversion was indeed achieved when just the substrate and catalyst were added together and stirred at room temperature for 24 hours. To determine the substrate scope of this isomerization procedure, 2-propenylbenzenes **1a-8a** were tested (table 9).

Table 9: Substrate scope of the solvent-free isomerization procedure.

Substrate	Number	Cat.	T	Conv.
	1	5 mol%	r.t.	Quant.
	2	5 mol%	r.t.	Quant.
	3	5 mol%	r.t.	99 %
	4	5 mol%	40 °C	Quant.
	5	5 mol%	40 °C	Quant.
	6	5 mol%	40 °C	Quant.
	7	5 mol% 2.5 mol%	r.t.	Quant.
	8	5 mol%	40 °C	94 %

It was possible to convert all tested 2-propenylbenzenes **1a-8a** into the desired isomers **1g-8g** with almost quantitative conversions (except for **8a**). For less reactive substrates, the reaction temperature had to be increased from r.t. to 40 °C to increase the conversion speed. For eugenol **7a**, it was also possible to decrease the amount of catalyst necessary for the isomerization from 5 mol% to 0.5 mol%. Additionally, it was also possible to recover the PdCl₂ catalyst by dissolving the product in Et₂O after the reaction, followed by centrifugation. To perform a subsequent biotransformation, the product was dissolved in EtOH and added directly to the cell suspension.

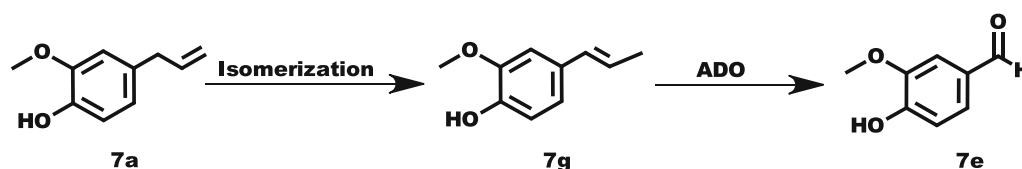
It should be noted that Sharma *et. al.* developed a similar solvent free catalytic system for the isomerization of estragole **4a** and eugenol **7a**. Their system uses 1.00 g of the respective substrate together with 0.01 g of “PdCl₂ · 3H₂O” at reflux temperatures (217 °C for **4a** and 239 °C for **7a**) to obtain the desired isomers **4g** and **8g** with a conversion of 65 % for estragole **4a** and 33 % for eugenol **7a** after five hours.¹³²

B.10.2. Assembly of the chemoenzymatic one-pot reaction with ADO

ADO or aromatic dioxygenase is an enzyme that allows the oxidative cleavage of double bonds conjugated to an aromatic system (see introduction). It is cofactor independent and contains an Iron histidine complex in its active site. ADO displays great activity towards various types of 1-

propenylbenzenes, including isoeugenol **7g**. This makes ADO an ideal candidate to be used for the second chemoenzymatic transformation route to transform propenylbenzenes into aromatic aldehydes. The construct, a pET1 vector, containing the gene for ADO was obtained from Twist. It consists of a T7/LacO promoter region which is inducible by IPTG. The gene was transformed into *E. coli* BL21(DE3) cells for protein production. The experimental procedure for the gene expression and the subsequent biotransformation can be found in the experimental part in chapter D.6.

For preliminary testing, the standard reaction conditions of Ni *et al.* were employed (10 mM PBS buffer pH 7.4, OD₅₉₀ 60, 10 mM substrate, 50 °C) using isoeugenol (obtained from the PdCl₂ catalyzed isomerization) as the model substrate (scheme 45).⁶¹



Scheme 45: Chemoenzymatic one-pot reaction for the production of vanillin **7e** from eugenol **7a**.

The biotransformation was conducted at 50 °C. After 24 h, almost complete consumption of the starting material was observed (figure 33).

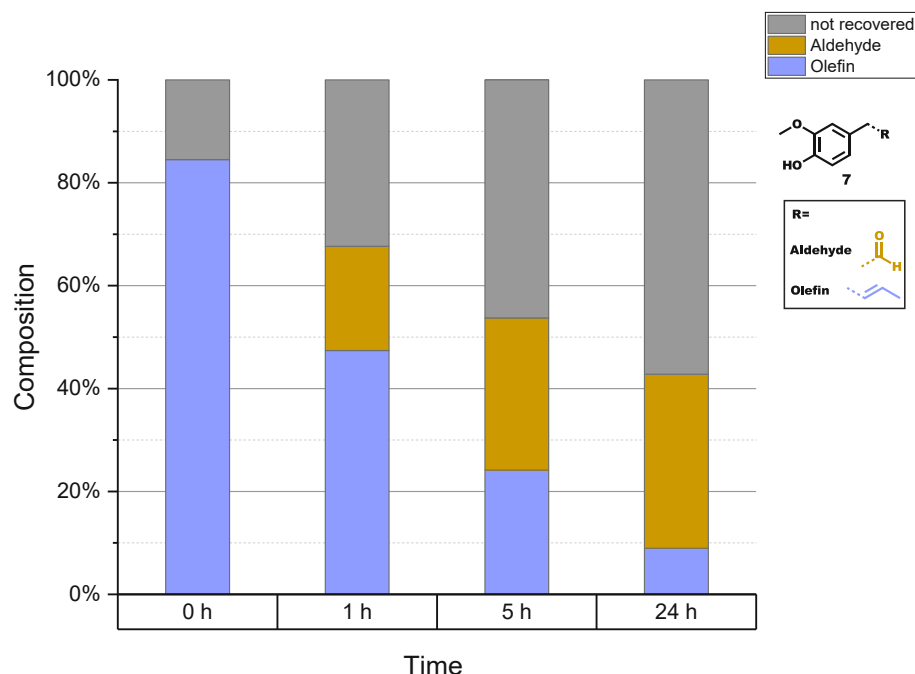


Figure 33: Results of the biotransformation with ADO at 50°C with isoeugenol **7g**.

Vanillin **7e** could be obtained with a yield of 40 % after 24 hours. Again, full mass recovery was not achieved due to incomplete extraction or further metabolization of the product.

In accordance with Ni *et al.*, it was also observed that at 30 °C, mainly vanillyl alcohol **7d** is obtained after 24 hours. This is a result of the subsequent reduction of vanillin **7e**, catalyzed by alcohol dehydrogenases which are naturally expressed by the respective *E. coli* strain, as can be seen in the GC trace for the biotransformation (figure 34).

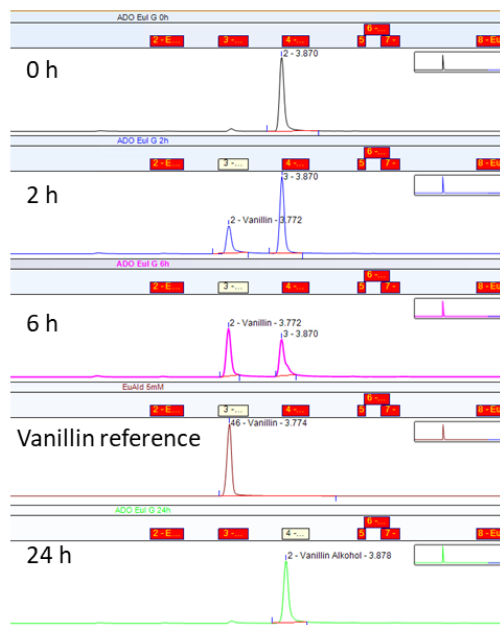


Figure 34: GC trace of the biotransformation with ADO at 30 °C using isoeugenol **7g** as the substrate. Vanillin formation is observed after 2 and 6 hours. After 24 hours, the formed vanillin has further reacted to vanillyl alcohol.

This was additionally validated through the isolation and ¹H-NMR analysis of the product of the transformation (figure 35). After 24 hours, most of the vanillin **7e** was converted into the corresponding alcohol **7d** (85 %).

SchloeglSGT-226-001.1.fid

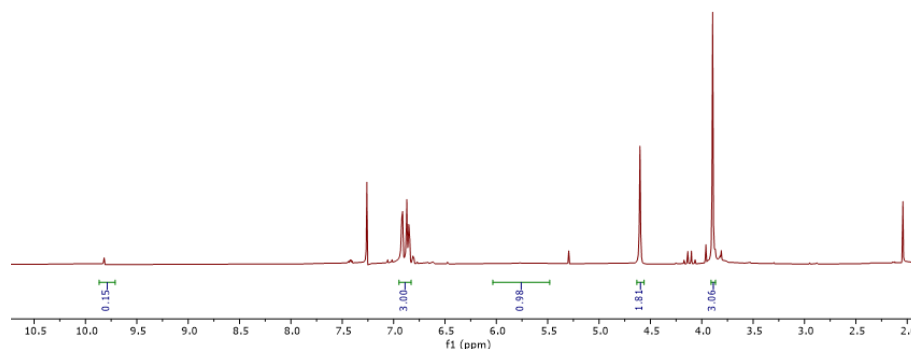
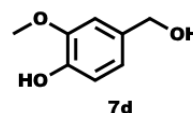
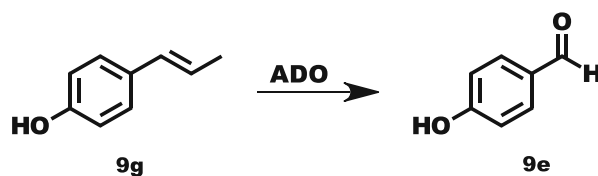


Figure 35: ¹H-NMR analysis of the product of the biotransformation with ADO at 30 °C using isoeugenol **7g** as the substrate.

In contrast, at 50 °C only vanillin **7e** formation was observed (figure 33). This is a result of the high temperature that deactivates most thermolabile ADHs.

To further determine the scope of this transformation, the other products of the isomerization (**1g-8g**) were also subjected to ADO. Unfortunately, little to no conversion of the respective 1-propenylbenzenes (except **8g**, which yielded vanillin **7e**) was observed. This was surprising since Ni demonstrated in his publication that at least anethole **4g** is an accepted substrate for this enzyme. To test for experimental deviations, the procedure was repeated under standard conditions with anethole **4g** and isoeugenol **7g** as control five times. No significant change in the outcome was detected.

Nevertheless, the enzyme proved to be a reliable catalyst for the successful conversion of isoeugenol to vanillin. Since the exact structure of ADO has not been elucidated yet, only little knowledge is available of the structure of its active site, as described in chapter. ⁶¹ This makes identifying the probable cause for the discrepancies in the reactivity between the substrates difficult. Nevertheless, a possible explanation for why only isoeugenol **7g** was successfully converted into the desired aldehyde **7e** could lie in its unique structural features on the aromatic moiety compared to the other substrates. Only isoeugenol **7g** has a hydroxyl group in the para position on the aromatic ring system. It is not improbable that the binding efficiency of the substrate in the active site of the enzyme is strongly dependent on hydrogen bonding in this position. To further test this hypothesis, 4-propenyl phenol **9g** was synthesized, as described in the experimental chapter, and subjected to the enzyme (scheme 46). This molecule also contains a hydroxyl group in the aromatic moiety similar to isoeugenol **7g**. The biotransformation was performed with an OD₅₉₀ of 30, 30 ml of whole-cell catalyst, and a substrate concentration of 5 mM at 50 °C.



Scheme 46: Whole-cell biotransformation of **9g** catalyzed by ADO.

After 24 hours, the suspension was extracted with EtOAc. After removal of the solvent, the residue was analyzed with ¹H-NMR (figure 36).

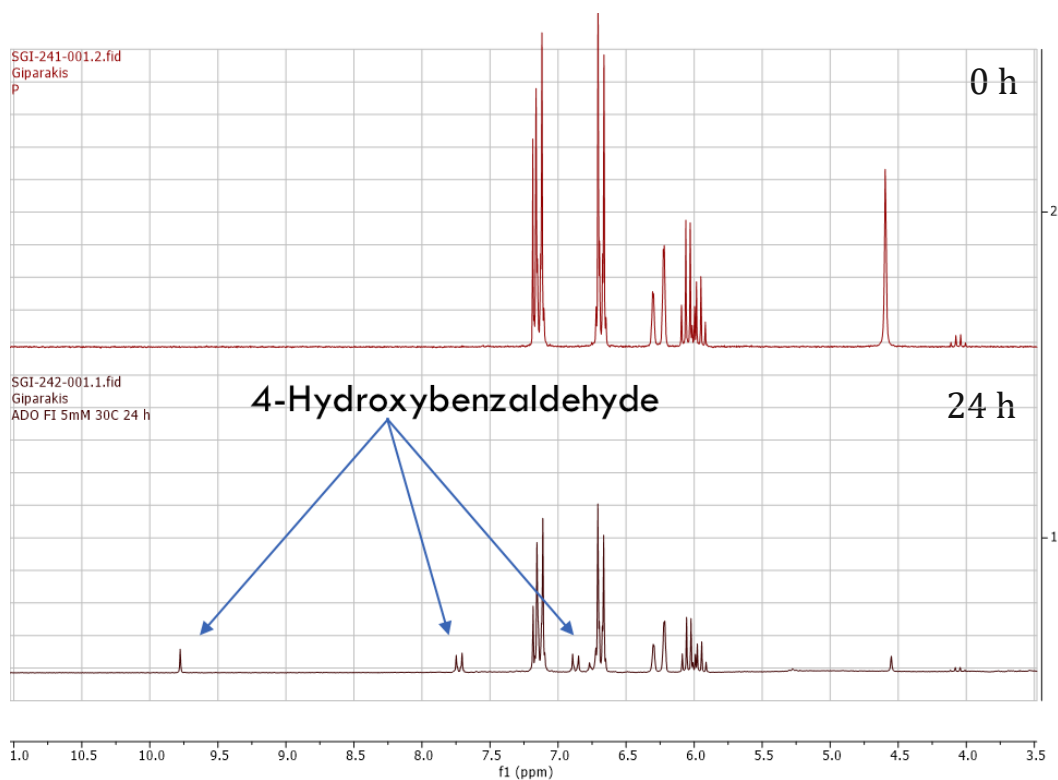


Figure 36: $^1\text{H-NMR}$ analysis of the product from the biocatalysis with ADO at 30 °C with 4-propenylphenol.

Interestingly, the desired aldehyde was indeed formed, although only with a yield of 12 %. This result reinforces the suspicion that ADO relies on hydrogen bonding from a hydroxyl group in the substrate. Nevertheless, to increase the substrate scope of ADO, further work needs to be conducted in the form of structure elucidation and mutagenesis studies.

B.11. Conclusion and outlook

In conclusion, it was possible to provide a proof of concept for both chemoenzymatic one-pot reaction sequences (Route **A** and **B**) for the production of aromatic aldehydes.

Route **A** allowed for the synthesis of seven different aromatic aldehydes **1e-7e** from the respective 2-propenylbenzenes **1a-8a** (eugenol **7a** and eugenol acetate **8a** formed the same product **7e**) in acceptable yields. A biocompatible procedure for the Wacker oxidation was found in the literature and optimized. The enzymatic cascade in the form of a mixed culture approach was tested, and lastly, the chemoenzymatic one-pot reaction was assembled. Initial results for increasing the scale of the transformation were also achieved. Lastly, a vector was constructed for the co-expression and protein production of all enzymes (TmCHMO, Pfl and AlkI), which are part of the enzymatic cascade in a single host cell. However, TmCHMO was not adequately expressed using this system.

Route **B**, on the other hand, allowed only for the synthesis of vanillin **7e**. A solvent-free and biocompatible palladium-catalyzed isomerization procedure was used for the production of 1-propenylbenzenes. The substrate scope of ADO was further elucidated. Due to the low substrate acceptance of ADO only the conversion of isoeugenol **7g** was achieved in a satisfying manner. However, the initial steps in the elucidation of the mechanistic pathway of ADO were also taken.

To further optimize both chemoenzymatic one-pot reaction sequences the analytical method (currently in the form of GC analysis) needs to be replaced by HPLC or UHPLC analysis. They would allow for the accurate and quantifiable detection of aromatic carboxylic acids, which is also supported by preliminary tests. Additionally, this change would make the extraction step, which is needed to prepare the analytic GC samples, unnecessary, further improving the mass recovery.

A few different strategies can be employed to reduce the amount of carboxylic acid formed in route **A** over the course of the biotransformation and increase the yield. Firstly, a carboxylic acid reductase in the form of CAR_{NI} (as mentioned in chapter A.4.) may be added to the enzymatic cascade to “recycle” the formed carboxylic acids back to the respective aldehydes. Secondly, the necessary cell density of the whole-cell biocatalyst may be lowered by creating a single host organism that can produce all enzymes of the enzymatic cascade. Decreasing the cell density should slow product degradation, thus improving the yield. Initial efforts to construct a vector that carries multiple genes were promising but suffered from low enzyme production. Therefore, an optimized plasmid design that improves transcription or translations of the genes needs to be devised. Lastly, switching from in-vivo to in-vitro catalysis would also prevent product metabolism by the host’s metabolism and thus increase the yield of the cascade (as mentioned in chapter A.1.4.).

For route **B**, the primary focus should lie on improving the substrate acceptance of ADO by genetic engineering. Accomplishing rational protein design would make the elucidation of the enzymatic structure necessary. Random mutagenesis studies in combination with a high throughput screening system would be more promising for faster results.

C. Materials and Methods

C.1. Stock Solutions

C.1.1. Antibiotics

Table 10: Stock solutions of the antibiotics used for the cultivation of bacteria.

Antibiotic	Stock concentration [mg/ml]	Working concentration [µg/ml]
Ampicillin in H ₂ O	100	100
Chloramphenicol in abs. EtOH	34	34

Stock solutions were sterilized by filtration (0.2 µm) and stored at - 20°C.

C.1.2. Inducer

Table 11: Stock solutions of the inducer used for protein production.

Inducer	Stock concentration
IPTG in H ₂ O	1 M
20 % L-Arabinose in H ₂ O	20 % (w/v)
20 % L-Ramnose in H ₂ O	20 % (w/v)

Stock solutions were sterilized by filtration (0.2 µm) and stored at - 20°C

C.1.3. Compounds used for biotransformation

The substrates used in the enzymatic cascade reactions (**1b-8b**, **1c**, **1d-8d**, and **1g-8g**) were dissolved in EtOH to obtain stock solutions with a concentration of 0.5 M. The stock solutions were stored at -20 °C.

C.2. Standard media and buffers

C.2.1. Buffers

Table 12: Compositions of the buffers used in biotransformation.

100 mM PBS-Buffer (1L)	50 mM PBS-Buffer (1L)
20.21 g Na ₂ HPO ₄ ·7H ₂ O	10.10 g Na ₂ HPO ₄ ·7H ₂ O
3.39 g NaH ₂ PO ₄ ·H ₂ O	1.69 g NaH ₂ PO ₄ ·H ₂ O
2M HCl for pH adjustment	2M HCl for pH adjustment

Buffers were sterilized by autoclavation and stored at room temperature.

C.2.2. Standard media

Table 13: Composition of the standard media used for the cultivation of bacteria.

LB Medium (400 ml)	TB Medium (400 ml)	LB Agar (400 ml)
4 g bacto-peptone	4.8 g bacto-tryptone	4 g bacto-peptone
2 g yeast extract	9.6 g yeast extract	2 g yeast extract
4 g NaCl	0.9 g KH ₂ PO ₄	4 g NaCl
	5 g K ₂ HPO ₄	6 g Agar No. 1

Standard media were sterilized by autoclavation and stored at room temperature.

C.2.3. Autoinduction media

Table 14: Composition of the autoinduction media used for the cultivation of bacteria.

LB-0.8G (400 ml)	LB-5052 (400 ml)	50 x 5052 (200 ml)	20 x NPS (200 ml)
4 g bacto-peptone	4 g bacto-peptone	23.2 g (NH ₄) ₂ SO ₄	50 g glycerol
2 g yeast extract	2 g yeast extract	27.2 g KH ₂ PO ₄	5 g glucose
4 g NaCl	4 g NaCl	28.4 Na ₂ HPO ₄	20 g α-lactose
0.4 ml 1M MgSO ₄	0.4 ml 1M MgSO ₄		
8 ml 40 % (w/v) glucose	8 ml 50 x 5052		
20 ml 20 x NPS	20 ml 20 x NPS		

Glucose and glucose-containing solutions were added last and sterilized by filtration. All other components were dissolved in water and sterilized by autoclavation.

C.2.4. SDS-PAGE

Table 15: Reagents for SDS-PAGE.

30 % (w/v) Acrylamide (100 ml)	10 % (w/v) APS (10 ml)
29.2 g acrylamide	1 g APS
0.8 g N',N'-bis-methylene acrylamide	

Reagents were sterilized by filtration. 30 % (w/v) Acrylamide was stored in a brown glass container. Reagents were stored at 4 °C.

Table 16: Buffers used for SDS-PAGE

10 x SDS running buffer (1000 l)	Resolving gel buffer (250 ml, pH 8.8)	Stacking gel buffer (50 ml, pH 6.8)	Sample buffer
30.3 g Trizma base	46.2 g Tris (1.5 M)	15.1 g Tris (0.5 M)	7.3 ml dH ₂ O
144 g glycine	10 ml 10 % (w/v) SDS	10 ml 10 % (w/v) SDS	2.3 ml stacking gel buffer
10 g SDS	2 M HCl for pH adjustment	2 M HCl for pH adjustment	5 ml glycerol
			4 ml 10 % (w/v) SDS
			0.2 ml 1% (w/v) bromphenol blue
			1 ml β-mercapto ethanol

Buffers were autoclaved/filtered for sterilization and stored at room temperature.

C.3. General procedures

C.3.1. Preparation of chemically competent cells

All media and buffers used to produce chemically competent cells were prepared fresh and sterilized before use. The components for the buffers can be found in table 17.

Table 17: Buffers used for the preparation of chemically competent cells.

RF1 buffer (30 ml, pH 5.8)	RF2 buffer (10 ml, pH 6.8)
3 ml 1 M RbCl (100 mM)	0.1 ml 1 M RbCl (10 mM)
0.3 ml 1M CaCl ₂ (10 mM)	0.75 ml 1 M CaCl ₂ (75 mM)
1.5 ml 1 M MnCl ₂ (50 mM)	1m 0.1 M MOPS (10 mM)
0.9 ml 1 M KOAc (30 mM)	8.15 ml H ₂ O
4.5 g glycerol (15 % w/v)	1.5 g Glycerol (15 % w/v)
24.3 ml H ₂ O	1 M NaOH for pH adjustment
0.2 M Acetic acid for pH adjustment	

A single colony of the respective bacterial strain was grown in 4 ml of LB-Miller medium for 17 hours (37 °C, 180 rpm). Afterwards, a 500 ml flask charged with LB-Miller medium (100 ml) was inoculated with 1% (v/v) of the overnight culture and grown until an OD₅₉₀ of 0.35 was reached.

The cells were then harvested by centrifugation (4000 rcf, 4° C, 10 min) and resuspended in RF1 buffer (20 ml) on ice. Cells were incubated on ice for 15 min. Cells were then centrifuged, and the pellet was resuspended in RF2 buffer (4 ml). Aliquots (50 µl) were filled in Eppendorf tubes, snap-frozen in liquid nitrogen, and stored at -80 °C for later use.

C.3.2. Transformation of chemically competent cells

Chemically competent cells stored at -80 °C were thawed for 5 minutes on ice. Subsequently, plasmid DNA (1µl, 50 - 100 ng/µl) was added to the cell suspension (50 µl) and incubated for 30 minutes on ice. The cells were heat-shocked at 42 °C for 1 minute and then immediately placed in ice for 2 minutes. SOC-Medium (400 µl) warmed to 37 °C was then added, and the cells were incubated at 37 °C, 1000 rpm for 1 hour. The cell suspension was then plated on an LB-Agar plate (warmed to 37 °C) supplemented with the necessary antibiotic and incubated upside down at 37 °C for 17 hours.

C.3.3. General procedure for the preparation of cryostocks

A single colony of the respective bacterial strain was grown in LB-Miller medium (4 ml) for 17 hours (37 °C, 180 rpm). To make a cryostock, the overnight culture (0.5 ml) was combined with 60 % glycerol (0.5 ml) in a cryogenic vial and stored at -80 °C.

C.3.4. Plasmid DNA isolation and quantification

Plasmid DNA isolation was performed with the GeneJET Plasmid Miniprep kit by Thermo Scientific. The cell suspension of an overnight culture (5ml) was filled into a 15 ml falcon tube and centrifuged (10 min, 6000 rfc.). The supernatant was discarded, and the pellet was then resuspended with 250 µl of the resuspension solution and transferred into a 1.5 ml Eppendorf tube. The cells were then lysed by the addition of lysis-solution (250 µl) and inverting the Eppendorfer tube five times. After the solution became viscous and slightly clear, neutralization solution (350 µl) was added to the tube, mixed immediately by inverting five times, and centrifuged (16000 rpm, 5 min). Subsequently, the supernatant was transferred into a GeneJet spin column by decanting, leaving the pellet cell debris behind. The column was then centrifuged (16000 rpm, 1 min), wash solution was added (500 µl), and the wash procedure was repeated again. The column was then transferred into a new 1.5 ml Eppendorf tube and incubated with the lid of the column open for 5 minutes at 50 °C. Lastly, nuclease-free water (50 µl) was placed directly on the column membrane, incubated for 2 minutes, and centrifuged (16000 rpm, 2 min). The DNA concentration was determined with NanoDrop measurements (NanoDrop, OneC

Microvolume UV-Vis spectrophotometer, Thermo Scientific). The DNA solution was then stored at -20 °C.

C.3.5. DNA-Sequencing

DNA sequencing was performed by Microsynth Switzerland. Samples were prepared according to their specifications: 480 - 1200 ng DNA in 12 µl and 3 µl primer (10 mM) to a total volume of 15 µl. Alternatively, a primer from their standard primer list was used instead.

C.3.6. Preparation of primers

Primers were obtained from Sigma Aldrich as a pellet. Nuclease-free water was added to obtain a stock concentration of 100 µM. The stock primer concentration was further diluted to 10 µM prior use and stored at -20 °C.

C.3.7. Polymerase Chain Reaction (PCR)

The Q5 high fidelity DNA polymerase (NEB, M0491) was used for the amplification of inserts and backbones. For a single PCR run, the following reaction mixture was prepared on ice:

Table 18: Reaction mixture for PCR.

<i>Components</i>	<i>Amount [µl]</i>
5 x Q5 Reactions Buffer	10
10 mM dNTPs	1
10 µM Forward primer	2.5
10 µM Reverse primer	2.5
Template DNA (~1ng/µl)	2
Q5 DNA Polymerase	0.5
Nuclease free water	31.5
Sum	50 µl

For fragments with a high GC content, Q5 high GC enhancer (10 µl) was used to improve amplification. The DNA polymerase was added last to the mixture. The samples were centrifuged for 2 minutes and placed into the thermocycler (Biometra TAdvanced, Twin 48 Thermal Cycler, Analytic Jena) for amplification utilizing the temperature program found in table 19.

Table 19 PCR temperature program.

Step	Temperature [°C]	Time
Initial denaturation – 1 cycle	98	30 seconds
Denaturation – 10 cycles	98	10 seconds
Annealing – 10 cycles	50- 72	30 seconds
Extension – 10 cycles	72	45 minute per kb
Denaturation – 20 cycles	98	10 seconds
Annealing – 20 cycles	50- 72	30 seconds
Extension – 20 cycles	72	45 minute per kb
Final extension – 1 cycle	68	2 minutes
Hold	4	

The annealing temperatures were calculated from the SnapGene® software. Two different PCR cycle conditions were used for backbone amplification in the case of a large overhang (30 bp.) between primers and fragments. The annealing temperatures for the first PCR cycles were generally chosen 5-9 °C under the annealing temperatures used in the second phase of the PCR.

C.3.8. Colony PCR

Colony PCR was performed with Taq DNA Polymerase (OneTaq Quick-Load DNA Polymerase). In table 20, the PCR reaction mixture for a single run can be found.

Table 20: Components of the colony PCR reaction mixture. (Taken from NEB.com)

Components	Amount [µl]
5x OneTaq Quick-Load Buffer	5
10 mM dNTPs	0.5
Forward primer	0.5
Reverse primer	0.5
OneTaq Quick-Load DNA Polymerase	0.125
Template DNA	Variable
Nuclease free water	18.375 µl
Sum	25 µl

The components were mixed on ice. The DNA polymerase was added last to the mixture. Subsequently, the PCR reaction mixture was aliquoted (25 μ l) and transferred into cooled PCR reaction tubes. Colonies were picked from an agar plate with a 10 μ l pipette tip by hand and transferred into the PCR reaction tube. The samples were centrifuged for 2 minutes and placed into the thermocycler (Biometra TAdvanced, Twin 48 Thermal Cycler, Analytic Jena) for amplification utilizing the temperature program found in table 21. Annealing temperatures were chosen 5 $^{\circ}$ C under the melting temperature of the average T_m of the primers.

Table 21: Colony PCR temperature program. (Taken from NEB.com)

Step	Temperature [$^{\circ}$ C]	Time
Initial denaturation – 1 cycle	94	30 seconds
Denaturation – 30 cycles	94	15- 30 seconds
Annealing – 30 cycles	45 – 68	15 – 60 seconds
Extension – 30 cycles	68	1 minute per kb
Final extension – 1 cycle	68	5 minutes
Hold	4	

C.3.9. Agarose gel electrophoresis

Agarose gel was prepared by dissolving Agarose (0.8 g) in 80 ml TAE buffer (1% w/v) under heat in the microwave for approximately 3 minutes. The solution was cooled to touching temperature in a water bath, and SYBR Safe DNA Gel Stain (8 μ l) was then added. The gel was then poured into a suitable agarose gel tray, and a comb was inserted. After the gel solidified, the tray was placed into the electrophoresis chamber and covered in TAE buffer. Samples were prepared by mixing 6 x purple DNA loading dye (NEB B7024S) and PCR product 1:5 and loaded into the wells. DNA ladder (10 μ l, Thermo Scientific SM01313) was used as a reference. Products from colony PCR were directly loaded onto the gel without DNA loading dye. Electrophoresis was performed at 100 V for 40-45 min. DNA visualization was performed under UV light (UVP UVsolo touch, Analytic Jena).

C.3.10. Gel purification of PCR products

Electrophoresis was performed as described in chapter C.3.9. The gel was loaded onto a UV-transilluminator (UV Transilluminator 2000, Bio-Rad), and the desired DNA bands were excised using a scalpel. The cutouts were weighed and placed into a 2ml Eppendorf tube. Gel purification was performed with the GeneJET gel extraction kit (Thermo Scientific K0691). For that, binding buffer (1:1 w%) was added to the tube and incubated for 10 minutes at 50 °C until the gel was dissolved. The solution was then transferred into a GeneJet purification column and centrifuged for 2 minutes (16000 rpm, Sigma Tabletop Centrifuge). The flow-through was discarded, and 700 µl of wash buffer was added to the column. The tube was centrifuged for 1 min (16000 rpm), the flow-through discarded, and the centrifugation repeated to remove the residual wash solution. The purification column was then transferred into a clean 1.5 ml Eppendorf tube. The tube was placed with an open lid into a heating block (50 °C) for 5 minutes to remove the residual wash solution entirely. Subsequently, 30 µl of nuclease-free water was placed directly on the column membrane, incubated for 2 minutes, and centrifuged for 1 minute (16000 rpm). The DNA concentration was determined with NanoDrop measurements (NanoDrop, OneC Microvolume UV-Vis spectrophotometer, Thermo Scientific). The DNA solution was then stored at -20 °C.

C.3.11. NEBuilder® Hifi DNA assembly

Linearized products obtained by PCR, as described in chapter C.3.7. were assembled by NEBuilder® Hifi DNA Assembly. Primers for the PCR were designed in such a way that approximately 20-30 bp long homologous overhangs were introduced into the backbone and insert. For this, the online assembly tool provided at [NEBuilder](#) was utilized. In general, the recommendations that were suggested by the platform, such as GC base pairs at the start and the end of the primers and reducing the stability of secondary structures, were followed. PCR products were purified *via* gel electrophoresis and gel extraction before use. For assembly, the ratio between insert and backbone was set to 3:1, and around 100 ng of backbone was used. The components of the reaction mixture for each assembly run can be found in table 22.

Table 22: Components of the NEBuilder HiFi DNA assembly.

Components	Amount
NEBuilder HiFi DNA assembly master mix	10 μ l
Backbone DNA	Variable (~100 ng)
Insert DNA	Variable (3:1 insert / backbone)
Water	Fill up to 20 μ l
Sum	20

The mixture was then placed into a thermocycler at 50 °C for 15 min – 3h. After completion, the mixture was directly used for the transformation of *E. coli* as described in chapter C.3.2.

C.3.12. Sodium Dodecyl Sulfate Polyacrylamide Gel Electrophoresis (SDS-PAGE)

For SDS-PAGE, usually, a 12 % (w/v), 0.75 mm thick gel was prepared with the following components:

Table 23: Components of the SDS-PAGE gel.

Resolving gel	Stacking gel
3.2 ml H ₂ O	2.2 ml H ₂ O
2.5 ml resolving gel buffer	1.3 ml stacking gel buffer
4.2 ml 30 % (w/v) acrylamide	0.5 ml 30 % (w/v) acrylamide
50 μ l 10 % (w/v) APS	25 μ l 10 % (w/v) APS
8 μ l TEMED	8 μ l TEMED
	30 μ l bromophenol blue

Components were mixed by inverting. The resolving gel was prepared first and poured after the addition of TEMED into the preassembled chamber. The gel was covered with iPrOH to obtain an even and bubble-free surface. The gel was allowed to harden for 20 minutes afterwards the iPrOH layer was removed, and the stacking gel was poured on top. Lastly, the comb was inserted, and the gel cured for 20 minutes. Samples were prepared by mixing with SDS-PAGE sample buffer (Whole-cell samples normalized to OD₅₉₀:20 were mixed 1:4, Protein samples were mixed 1:1) and denatured at 95 °C (whole-cell samples: 10 minutes, protein samples: 4 minutes). The samples (usually 5 μ l) were then loaded into the sample wells, together with 5 μ l of protein ladder standard reference (Thermo Scientific, 26616) in lane 1. Electrophoresis was performed at 80 V until the protein bands wandered from the stacking gel into the resolving gel, then 120 V. The gel

was then removed from the chamber, and the resolving gel separated from the stacking gel. Proteins bands were visualized by staining (Invitrogen™ Simplyblue™ Safestain, LC6065). Gels were then photographed and stored in H₂O for preservation.

D. Experimental Part

D.1. General considerations

If not mentioned otherwise, all glassware, media, and all other solutions in contact with *E. coli* during its cultivation, were sterilized *via* autoclavation (120 °C for 20 min, at a higher pressure in a WMF Chromargan Stainless Steel Pressure Cooker) before use. If necessary, sterile filtration (0.2 µm cellulose acetate sterile syringe filter) was used to sterilize instead.

D.2. Construction of pETDuet1_TmCHMO::PfeI

Step1 The assembly of the vector pETDuet1_TmCHMO::PfeI was split into two steps. In the first step, PfeI was inserted into the backbone in the form of a pETDuet1 vector system containing two placeholder genes (see chapter B.9.). The gene for PfeI was subcloned from a pGaston vector system obtained from Thomas Bayer. The fragments were linearized by PCR (described in chapter C.3.7.) with the following primers and annealing temperatures:

Table 24: PCR conditions for the first construction step of pETDuet1_TmCHMO::PfeI.

PfeI	pETDuet1_step1
Forward primer: SGI-001 GATATACATATGAGCACATTTGTTGCAAAAGAC G	Forward primer: SGI-003 GACCTGTTGGCGTTCTTGAAACGCTGACTCGAG TCTGGTAAAGAAACC
Reverse primer: SGI-002 GAGTCAGCGTTTCAAGAACGCCAACAG	Reverse primer: SGI-004 CTTTTGCAACAAATGTGCTCATATGTATATCTC CTTCTTATACTTAACTAATATACTAAGATGG
Annealing Temperature: 67 °C	Annealing Temperature: 63°C for the first 10 cycles, 72 °C for the last 20 cycles
Cycles: 20	Cycles 30
High GC Enhancer: No	High GC Enhancer: No
Fragment Size: 820 bp	Fragment Size: 5850 pb

Purification and assembly were then performed as described in chapter C.3.10. and chapter C.3.11. respectively. For that, the vector (3 µl, pETDuet1_step1) and the insert (7 µl, PfeI) were subjected to the NEBuilder HiFi Assembly mix (10 µl) for 15 minutes at 50 °C. *E. coli* BL21(DE3) cells were then transformed with the product of the assembly as described in chapter C.3.2. The obtained colonies were screened for the successful insertion of PfeI *via* colony PCR (chapter C.3.8.) which was additionally verified *via* sequencing. The results for the first construction step can be found in figure 37.

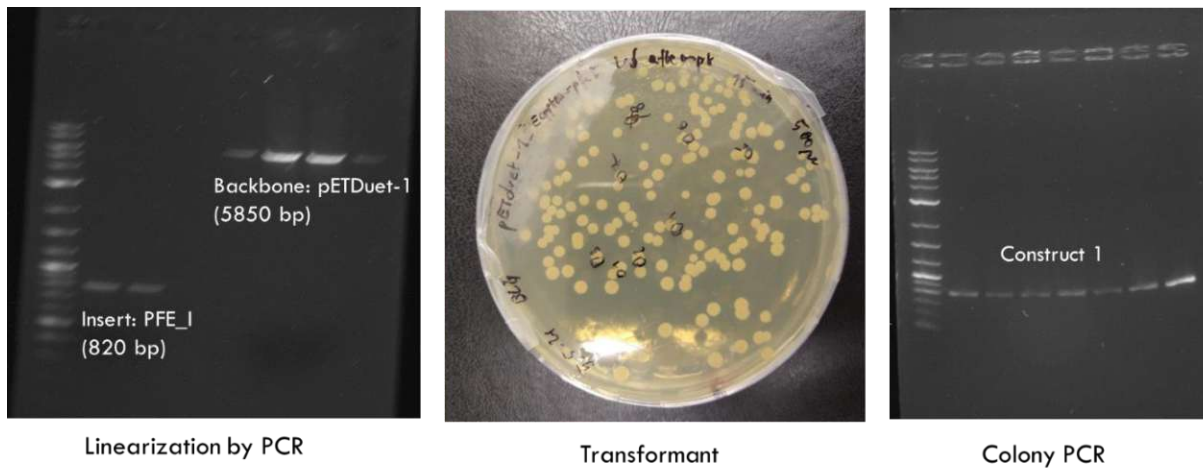


Figure 37: Pictures from left to right: 1) Successful linearization of the individual fragments. 2) Colonies obtained after the successful transformation. 3) Product of the colony PCR (PfeI)

D.2.1. Step 2

In the second step, TmCHMO was inserted into the backbone in the last remaining position (see chapter B.9. The gene for TmCHMO was subcloned from a pBAD vector system. The fragments were linearized by PCR (described in chapter C.3.7.) with the following primers and annealing temperatures:

Table 25: PCR conditions for the second construction step of pETDuet1_TmCHMO::PfeI.

TmCHMO	pETDuet1_step2
Forward primer: SGI-005: CTTTAAGAAGGAGATATACCATGAGCACCACCC AGACCCCGG	Forward primer: SGI-007: CGTGGTGAACGTGCGCAAGCGGTGGCGTAAGCT TGCGGCCGCATAATGCTTAAGTC
Reverse primer: SGI-006: TTACGCCACCGCTTGCGCAGG	Reverse primer: SGI-008: GTCTGGGTGGTGCTCATGGTATATCTCCTTCTT AAAGTTAAACAAAATTATTTCTAGAGG
Annealing Temperature: 72 °C	Annealing Temperature: 66°C for the first 10 cycles, 71 °C for the last 20 cycles.
Cycles: 20	Cycles 30
High GC Enhancer: No	High GC Enhancer: Yes
Fragment Size: 1600 bp	Fragment Size: 6150 pb

Purification and assembly were then performed as described in chapter C.3.10. and chapter C.3.11. respectively. For the assembly, the vector (3 µl, pETDuet1_step2) and the insert (7 µl, TmCHMO) were subjected to the NEBuilder HiFi Assembly mix (10 µl) for 60 minutes at 50 °C. *E. coli* BL21(DE3) cells were then transformed with the product of the assembly as described in chapter C.3.2. The obtained colonies were screened for the successful insertion of TmCHMO via

colony PCR (chapter C.3.8.) which was additionally verified *via* sequencing. The results for the second construction step can be found in figure 38.

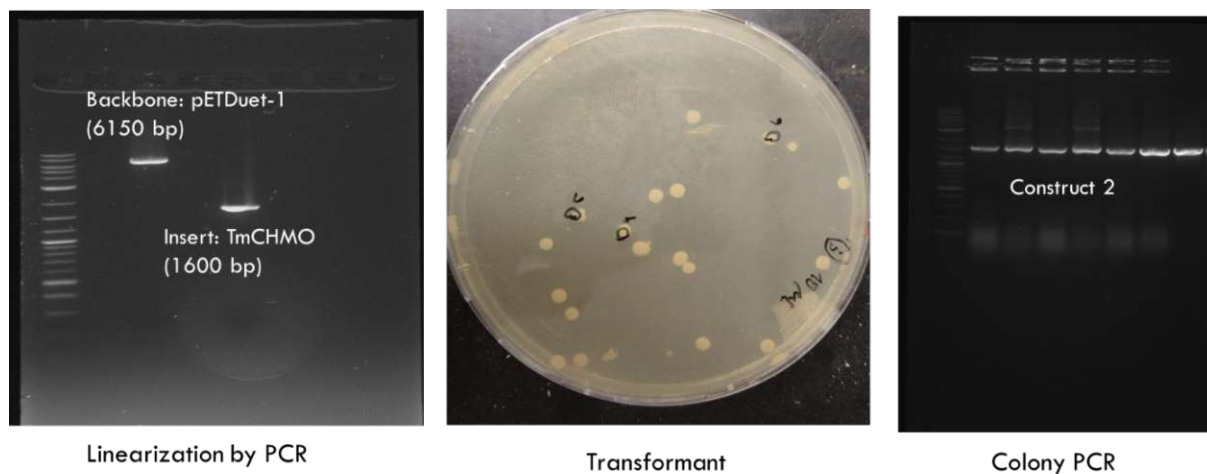


Figure 38: Pictures from left to right: 1) Successful linearization of the individual fragments. 2) Colonies obtained after the successful transformation. 3) Product of the colony PCR (TmCHMO).

D.3. Sample preparation for GC analysis and quantification

For GC analysis, samples (150 μ l) from the biotransformation were taken after usually 0, 1, 5, and 24 hours and filled into Eppendorf tubes loaded with EtOAc (300 μ l and 50 μ l 1N HCl if necessary) spiked with 1 mM of methylbenzoate as internal standard. The tubes were then sealed and mixed vigorously by vortexing for a few seconds. The samples were then centrifuged to separate the phases (14000 rpm, 2min). The organic phase was then decanted and placed into a second Eppendorf tube loaded with Na₂SO₄. The organic phases were dried by inverting the tube a few times. After a second centrifugation, the samples were filled into GC vials, sealed, and injected into the column.

D.4. General procedure for the cultivation of *E. coli* for enzyme expression by induction

A 15 ml falcon tube filled with LB-Miller medium (5 ml), supplemented with the appropriate antibiotic, was inoculated with the respective *E. coli* strain. The culture was then incubated for 19 hours at 37 °C and 220 rpm. The next day, a 20-500 ml baffled flask charged with TB medium (1/5 of the flask volume), and the antibiotic was inoculated with 1% (v/v) of the ON-culture and grown until an OD₅₉₀ of 0.6 was reached (37 °C, 150 rpm). Then the appropriate inducing agent was added to the cell suspension to induce protein production. To achieve sufficient expression levels protein productions was performed for 22 hours (20 - 25°C, 150 rpm).

D.5. General procedure for the cultivation of *E. coli* for enzyme expression by autoinduction

A 50 ml falcon tube filled with LB-0.8G medium (12 ml), supplemented with the appropriate antibiotic, was inoculated with the respective *E. coli* strain. The culture was then incubated for 19 hours at 37 °C and 250 rpm. The next day, a 100 ml baffled flask charged with LB-5052 medium (20 ml) and antibiotic was inoculated with 0.2 % (v/v) of the ON-culture and grown for 4 hours (37 °C, 150 rpm). To achieve sufficient expression levels, protein production was performed for 22 hours (20 °C, 150 rpm).

D.6. General procedure for whole-cell biotransformation

Cells were harvested by centrifugation (6000 rcf., 10 min). The pellet was resuspended in 1/10 of the volume of the main culture with 50 mM PBS buffer pH 7.4 (10 mM PBS buffer pH 7.4 for ADO) and centrifuged again. To obtain the resting cells, the pellet was resuspended in a sufficient volume of 50 mM PBS buffer pH 7.4 (10 mM PBS buffer pH 7.4 for ADO) to obtain a working cell density of OD₅₉₀ 20 (up to 60 for ADO). Biotransformation was then performed in glass vials with 1 ml of the prepared cell suspension at 30 °C (for AlkJ, TmCHMO, ADO), 37 ° (for PAMO) or 50 °C (for ADO) and 220 rpm . The substrate was added last. Typically, concentrations between 1 – 10 mM were obtained by the addition of an appropriate volume of the stock solution (usually 0.5 M in EtOH) or the reaction mixture after the PdCl₂ catalyzed isomerization dissolved in EtOH (route B). The conversion was monitored *via* GC analysis. GC sample preparation is described in chapter D.3.

D.7. Procedure for the mixed culture whole-cell biotransformation (route A)

Each component of the mixed culture biocatalyst (PAMO/TmCHMO and AlkJ) was prepared as described above, except for the final resuspension. For this, a variable volume of 50 mM PBS buffer (100 mM PBS buffer in the case of a chemoenzymatic one-pot reaction) was added to each cell pellet to obtain a working cell density of OD₅₉₀ 40 (80 in the case of a chemoenzymatic one-pot reaction). After resuspension, the two cell suspensions (one BVMO and AlkJ) were combined to obtain the mixed culture with an OD₅₉₀ of 20 (40 in the case of a chemoenzymatic one-pot reaction) for each component of the whole-cell biocatalyst, respectively (double the volume). Biotransformation was then performed in glass vials (loaded with 100 U of PflI in the form of lyophilized cells) with 1 ml of the prepared cell suspension. The substrate was added last. Typically, a concentration between 1 – 10 mM was obtained by the addition of an appropriate

volume of the stock solution (usually 0.5 M in EtOH). The conversion was monitored *via* GC analysis. GC sample preparation is described in chapter D.3.

D.8. General Procedure for the whole-cell chemoenzymatic one-pot reaction (route A)

Unless stated otherwise, the reaction mixture of the Wacker oxidation (25 mM substrate concentration) was diluted with 2.5 times the amount of water, and, if necessary, the pH of the solution was adjusted to 7.0 – 8.0 with 2 M NaOH. The formed precipitate was then removed by centrifugation. The mixed culture whole-cell biocatalyst was prepared as described above. For the sequential one-pot reaction, 0.5 ml of the mixed cell suspension (OD₅₉₀ 40) was filled into a glass vial. Then, 100 U of PflI was added, followed by the addition of 0.5 ml of the prepared reaction mixture to obtain a theoretical substrate concentration of 5 mM with an OD₅₉₀ of 20. The biotransformation was performed at 33 °C for PAMO or 30 °C for TmCHMO and 220 rpm. The conversion was monitored *via* GC analysis. GC sample preparation is described in chapter D.3.

D.9. Large scale biotransformation (route A and B)

The whole-cell biocatalyst in the form of a single enzyme or in the form of a mixed culture was prepared as described above. The cell suspension was then filled into a 250 ml Erlenmeyer flask (loaded with 100 U of PflI if necessary) equipped with a rubber septum. The substrate was added last. The working concentration (1-5 mM) was obtained by the addition of an appropriate volume of the stock solution (usually 0.5 M in EtOH) or the reaction mixture after the Wacker oxidation. The biotransformation was then performed at 33 °C for route A or 30-50 °C for route B and 220 rpm. Reaction progress was monitored *via* GC. After full consumption of the substrate was observed, the mixture was extracted with EtOAc. The combined organic phases were dried over Na₂SO₄, filtered and the solvent removed under reduced pressure. Analysis of the product was performed *via* ¹H-NMR. If necessary, the product was purified *via* column-chromatography.

D.10. Preparation of lyophilized cells containing PflI

The respective *E. coli* strain containing the pGaston-PflI vector was cultivated as described above. For the main culture, a 1000 ml baffled flask charged with TB medium (200 ml) and Ampicillin (200 µl, 100 mg/ml) was used. Protein production was induced after an OD₅₉₀ of 0.29 was reached by the addition of 20%-L-Rhamnose (0.2% v/v). The cells were incubated at 37 °C for 3 hours. Afterwards, the cells were harvested by centrifugation (6000 rcf., 10 min.) and resuspended in sterile water (10 ml) in a 15 ml falcon tube. The suspension was snap-frozen in

liquid nitrogen and the flask was placed into a 1000 ml round bottom flask. The cells were then lyophilized for 24 hours, leading to a dry off-white powder which was stored at -80 °C.

D.11. Activity assay of Pfel⁵⁴

The activity of the esterase was determined photometrically by the hydrolysis of p-nitrophenol acetate (pNPA). For this, the lyophilized enzyme (1.2 mg) was diluted with 50 mM PBS buffer (1 ml). From this stock solution, 10 µl were diluted with PBS buffer (990 µl). Lastly 10 µl of the second dilution was combined with 50 mM PBS-buffer (890 µl) and a 10 mM pNPA stock solution (100 µl). The sample was homogenized by pipetting and measured immediately. The absorption at a wavelength of 410 nm as a function of time was recorded by the photometer (figure 39).

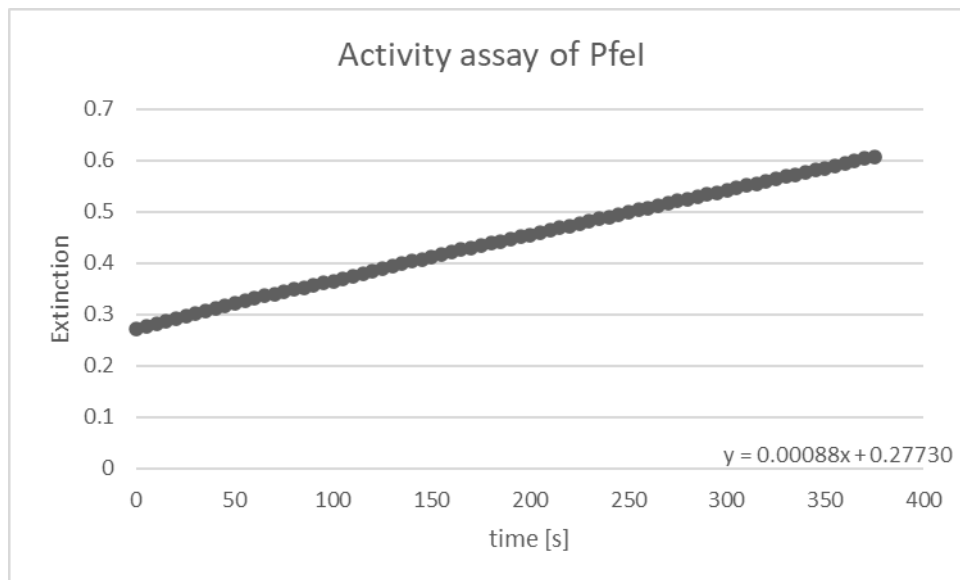


Figure 39: Absorption of the solution recorded as a function of time

By using the extinction coefficient ($\epsilon = 15 \times 10^3 \text{ M}^{-1} \text{ cm}^{-1}$) the length of the optical path (1cm), the volume of the cuvette (0.010 ml), the dilution of the sample (10000) and the slope of the absorption curve, the specific activity of the enzyme was calculated.

For the previously prepared Pfel the specific activity was determined as: $U_{\text{spet}} = 36.7 \text{ } \mu\text{mol}/\text{min}$ for 1 mg of enzyme.

D.12. Protein expression conditions by induction

Table 26: Expression conditions by induction for various proteins

Protein	T [°C]	Inducer	Antibiotic	Rpm/Time
TmCHMO	25	0.02 % (v/v) 20% L-Arabinose	Amp	150rpm, 22h
AlkJ	25	0.5 mM IPTG	Camp	150rpm, 22h
PAMO	25	0.02 % (v/v) 20% L-Arabinose	Amp	150rpm, 22h
ADO	20	0.5-1 mM IPTG	Amp	150rpm, 22h
TmCHMO::PFE	25	1 mM IPTG	Amp	150rpm, 22h

D.13. Synthetic procedures

D.13.1. General remarks

The following practices were carried out in all synthetic procedures, unless stated otherwise. All glassware was flame dried before use and to guarantee water and oxygen exclusion for sensitive reactions Schlenk techniques were employed. In general, reactions were carried out under slight argon pressure and stirred magnetically. Liquid reagents were added by syringe through a rubber septum and solid reagents were added in a slight argon countercurrent.

NMR-analysis (¹H-NMR) was performed on the Bruker Avance 400 at 400 Mhz. Depending on the substance, measurements were performed in chloroform-d or methanol-d₄.

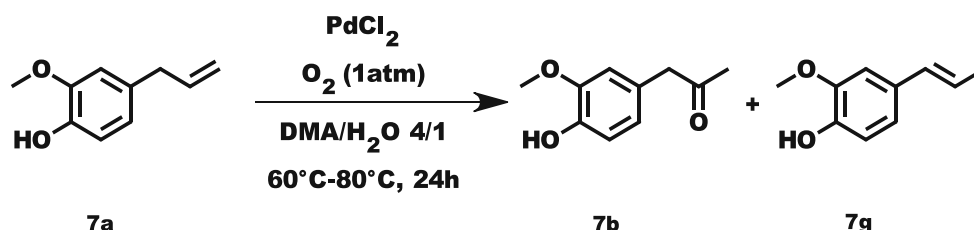
TLC-analysis was performed with silica-gel coated aluminum plates (Silica gel 60 F254, Merck). Anisaldehyde, basic KMNO₄ and phosphomolybdic acid/cerium sulphate solution were used as dip reagents for the visualization of the compounds.

The following solvents were used for synthesis:

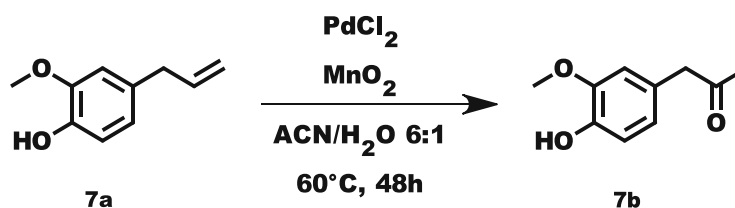
- MeOH, EtOH, ACN, DMA, EtOAc and DMSO were obtained in p.a. grade and used as received.
- H₂O was obtained from an ultrapure filtration system
- PE and EtOAC used for column chromatography were obtained in technical grade.

D.13.2. Screened Wacker oxidation procedures

The following chapter concerns the screened Wacker oxidation procedures as mentioned in chapter B.2.

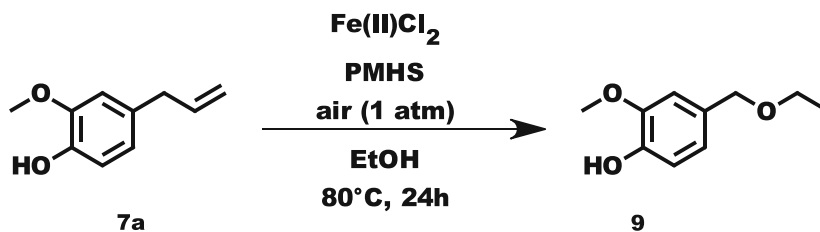
D.13.2.1. PdCl₂ catalyzed Wacker oxidation in DMA using molecular oxygen as terminal oxidant

A 25 ml screw-cap vial equipped with septum and magnetic stirring was charged with PdCl₂ (22 mg, 2.5 mol%). Subsequently, a mixture of DMA/H₂O (0.9 ml/0.1 ml) was added, and the flask flushed with oxygen using a balloon. The mixture was then heated to 80 °C and **7a** (0.82 g, 5.0 mmol, 1.0 equiv.) was added dropwise with a syringe. The reaction was stirred for 24 hours. Afterwards, the heating block was removed allowing the reaction to cool down to room temperature. H₂O (5 ml) was then added, and the mixture extracted with EtOAc (3x 5 ml). The combined organic phases were washed with H₂O (3 x 5 ml), brine (1 x 5ml) dried over Na₂SO₄ and filtered. Removal of the solvent left a yellow oil as residue behind which was purified *via* column chromatography (PE/EA 20:1). ¹H-NMR analysis revealed that a product mixture of **7b** (0.11g, 0.6 mmol, 12 %) and **7g** (0.18 g, 1.1 mmol, 22 %) was obtained.

D.13.2.2. PdCl₂ catalyzed Wacker oxidation in ACN using MnO₂ as terminal oxidant

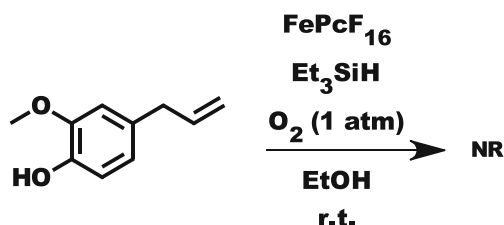
An 8 ml screw-cap vial equipped with septum and magnetic stirring was charged with **7a** (82 mg, 0.5 mmol, 1.0 equiv.) and dissolved in a mixture of ACN/H₂O (3.5 ml/0.5 ml). Subsequently, PdCl₂ (8.9 mg, 10 mol%) and MnO₂ (90%, 193 mg, 2.0 mmol, 4.0 equiv.) were added and the mixture heated to 60 °C under stirring. After 48 hours the heating block was removed allowing the reaction to cool down to room temperature. The mixture was then filtered over a pad of silica and the solvent was removed *via* rotary evaporation. GC-analysis of the residue revealed a product mixture between **7a** (2%) and **7b** (45 %).

D.13.2.3. Iron(II)chloride catalyzed Wacker oxidation using molecular oxygen



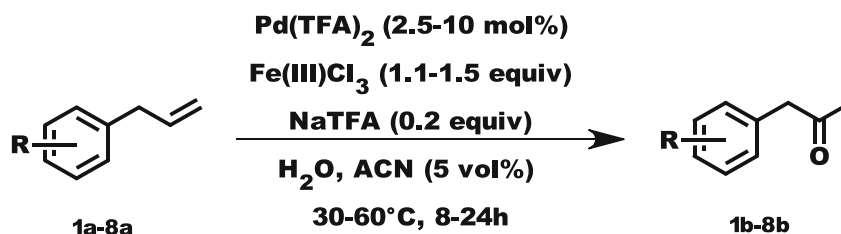
A 25 ml screw-cap vial equipped with septum and magnetic stirring was charged with 7a (164 mg, 1 mmol, 1.0 equiv.), Fe(II)Cl₂ (12.8 mg, 0.1 mmol, 0.1 equiv.), PMHS (680 μl, 3 mmol, 3.0 equiv.) and dissolved in EtOH (4 ml). The mixture was heated to 80 °C and stirred for 27 hours under air atmosphere until full consumption of the starting material was observed *via* TLC (PE/EtOAc 1:1). The mixture was removed from the heating block allowing it to cool down to room temperature. 1.5 mmol of aq. KF was then added to the flask and stirred for one hour. The mixture was then diluted with H₂O and extracted with EtOAc (3 x 15 ml). The combined organic phases were dried over Na₂SO₄, filtered and the solvent removed under reduced pressure. The crude was further purified *via* column chromatography (PE/EtOAc 2:1). ¹H-NMR analysis revealed the formation of **9** (60 mg, 0.33 mmol, 33 %).

D.13.2.4. Hexadecafluorinated-iron-phthalocyanine catalyzed Wacker oxidation using molecular oxygen



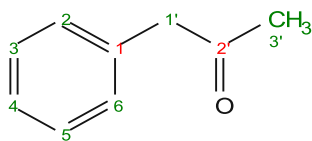
A 25 ml screw-cap vial equipped with septum and magnetic stirring was charged with 7a (104 mg, 0.65 mmol, 1.0 equiv.), FePCF₁₆ (27.3 mg, 5 mol%), and dissolved in 10 ml EtOH. The flask was then flushed with oxygen using a balloon. Subsequently, Et₃SiH (151 mg, 1.30 mmol, 2.0 equiv.) was added with a syringe. The reaction was stirred at room temperature for 24 hours. Afterwards, the solution was diluted with EtOAc (20 ml) and filtered through Celite®. The mixture was then washed with 0.2 N HCl, H₂O and brine. The organic phase was then dried over Na₂SO₄, filtered and the solvent removed under reduced pressure. The resulting residue was further purified by filtration through a pad of silica. ¹H-NMR analysis revealed that the starting material was not converted under these conditions.

D.13.3. Wacker oxidation of propenylbenzenes

D.13.3.1. General procedure **A** for the Wacker oxidation

A 25 ml screw-cap vial equipped with septum and magnetic stirring was charged with NaTFA (0.2 equiv.), FeCl₃ (or Fe₂(SO₄)₃) and Pd(TFA)₂ and the reaction vessel flushed with argon applying standard Schlenk-techniques. Afterwards degassed H₂O (9.5 ml) was added to the mixture followed by the slow addition of the solution of **1a-8a** (0.25 mmol) in ACN (0.5 ml) with a syringe. The reaction was vigorously stirred in the dark for 24 h. Reaction progress was monitored *via* TLC. After complete consumption of the starting material was observed the reaction vessel was either stored in the freezer for subsequent biotransformation or the reaction mixture extracted with EtOAc (3x 15 ml). The combined organics were washed with NaHCO₃ (1 x 10 ml) and Brine (1 x 10 ml), then dried over Na₂SO₄ and filtrated. Removal of the solvent with rotary evaporation led to the isolation of a brown oil, which was further purified *via* column chromatography.

D.13.3.2. Synthesis of phenylpropan-2-one **1b**



1b

C₉H₁₀O

M= 134.17 g/mol

1b was prepared according to the general procedure **A** for Wacker oxidation. The reaction was conducted at 45 °C with PdTFA₂ (4.1 mg, 5mol%), **1a** (29 mg, 0.25 mmol, 1.0 equiv.) and FeCl₃ (60 mg, 0.375 mmol, 1.5 equiv.).

Purification: column chromatography (PE/EtOAc 20:1)

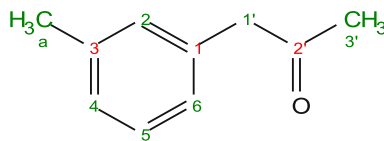
Yield: 77% (GC)

Appearance: pale yellow oil

¹H-NMR (400 MHz, CDCl₃) δ(ppm): 7.36 – 7.14 (m, 5H, H₂, H₃, H₄, H₅, H₆), 3.68 (s, 2H, H_{1'}), 2.13 (s, 3H, H_{3'}).

Spectrum in accordance with the literature⁹⁴.

D.13.3.3. Synthesis of 1-(3-methylphenyl)propan-2-one **2b**



2b

$C_{10}H_{12}O$

M=148.20 g/mol

2b was prepared according to the general procedure **A** for Wacker oxidation. The reaction was conducted at 30 °C with PdTFA₂ (4.1 mg, 5mol%), **2a** (33 mg, 0.25 mmol, 1.0 equiv.) and Fe₂(SO₄)₃ (150 mg, 0.375 mmol, 1.5 equiv.).

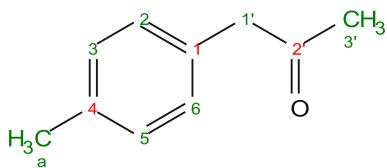
Purification: column chromatography (PE/EtOAc 20:1)

Yield: 73 % (GC)

Appearance: lightly green oil

¹H-NMR (400 MHz, CDCl₃) δ(ppm): 7.21 (t, J = 7.4 Hz, 1H, H5), 7.07 (d, J = 7.4 Hz, 1H, H4), 7.03 – 6.95 (m, 2H, H2, H6), 3.64 (s, 2H, H1'), 2.32 (s, 3H, Ha), 2.13 (s, 3H, H3').

Spectrum in accordance with the literature⁹⁴.

D.13.3.4. Synthesis of 1-(4-methylphenyl)propan-2-one **3b****3b****C₁₀H₁₂O**

M=148.20 g/mol

3b was prepared according to the general procedure **A** for Wacker oxidation. The reaction was conducted at 30 °C with PdTFA₂ (4.1 mg, 5mol%), **3a** (33 mg, 0.25 mmol, 1.0 equiv.) and Fe₂(SO₄)₃ (150 mg, 0.375 mmol, 1.5 equiv.).

Purification: column chromatography (PE/EtOAc 20:1)

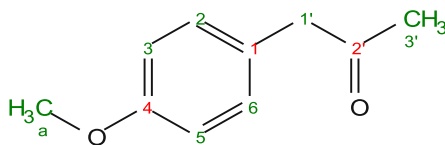
Yield: 71 % (GC)

Appearance: lightly green oil

¹H-NMR (400 MHz, CDCl₃) δ(ppm): 7.17 – 7.10 (m, 2H, H2, H6, or H3, H5), 7.10 – 7.04 (m, 2H, H3, H5, or H2, H6), 3.63 (s, 2H, H1'), 2.32 (s, 3H, H3'), 2.12 (s, 3H, Ha).

Spectrum in accordance with the literature⁹⁴.

D.13.3.5. Synthesis of 1-(4-methoxyphenyl)propan-2-one **4b**



4b

$C_{10}H_{12}O_2$

M=164.20 g/mol

4b was prepared according to the general procedure **A** for Wacker oxidation. The reaction was conducted at 45 °C with PdTFA₂ (4.1 mg, 5mol%), **4a** (37 mg, 0.25 mmol, 1.0 equiv.) and FeCl₃ (49 mg, 0.3 mmol, 1.2 equiv.).

Purification: column chromatography (PE/EtOAc 5:1)

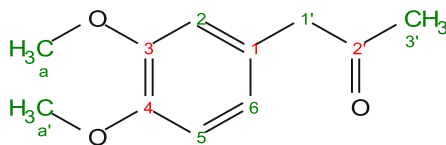
Yield: 75% (GC)

Appearance: colorless oil

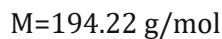
¹H-NMR (400 MHz, CDCl₃) δ(ppm): 7.14 – 7.06 (m, 2H, H2, H6 or H3, H5), 6.89 – 6.81 (m, 2H, H3, H5 or H2, H6), 3.78 (s, 3H, Ha), 3.61 (s, 2H, H1'), 2.12 (s, 3H, H3').

Spectrum in accordance with the literature⁹⁴.

D.13.3.6. Synthesis of 1-(3,4-dimethoxyphenyl)propan-2-one **5b**



5b



5b was prepared according to the general procedure **A** for Wacker oxidation. The reaction was conducted at 60 °C with PdTFA₂ (4.1 mg, 5 mol%), **5a** (44 mg, 0.25 mmol, 1.0 equiv.) and FeCl₃ (60 mg, 0.375 mmol, 1.5 equiv.).

Purification: column chromatography (PE/EtOAc 5:1)

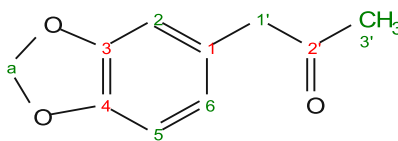
Yield: 65 % (GC)

Appearance: colorless oil

¹H-NMR (400 MHz, CDCl₃) δ(ppm): 6.81 (d, J = 8.1 Hz, 1H, H5 or H6), 6.77 – 6.66 (m, 2H, H2, H5 or H6), 3.85 (s, 6H, Ha, Ha'), 3.61 (s, 2H, H1'), 2.13 (s, 3H, H3').

Spectrum in accordance with the literature⁹⁴.

D.13.3.7. Synthesis of 1-(2H-1,3-benzodioxol-5-yl)propan-2-one **6b**



6b

$C_{10}H_{10}O_3$

M=178.18 g/mol

6b was prepared according to the general procedure **A** for Wacker oxidation. The reaction was conducted at 60 °C with PdTFA₂ (4.1 mg, 5 mol%), **6a** (40 mg, 0.25 mmol, 1.0 equiv.) and FeCl₃ (49 mg, 0.3 mmol, 1.2 equiv.).

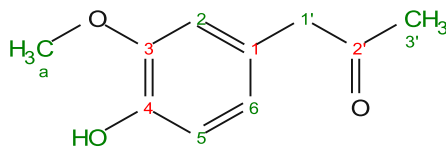
Purification: column chromatography (PE/EtOAc 5:1)

Yield: 73% (GC)

Appearance: lightly red oil

¹H-NMR (400 MHz, CDCl₃) δ(ppm): 6.78 – 6.71 (m, 1H, H₂), 6.69 – 6.59 (m, 2H, H₅, H₆), 5.93 (s, 2H, H_a), 3.58 (s, 2H, H_{1'}), 2.13 (s, 2H, H_{3'}).

Spectrum in accordance with the literature⁹⁴.

D.13.3.8. Synthesis of 1-(4-hydroxy-3-methoxyphenyl)propan-2-one **7b****7b****C₁₀H₁₂O₃**

M=180.20 g/mol

7b was prepared according to the general procedure **A** for Wacker oxidation. The reaction was conducted at 60 °C with PdTFA₂ (8.2 mg, 10 mol%), **7a** (41 mg, 0.25 mmol, 1.0 equiv.) and FeCl₃ (49 mg, 0.3 mmol, 1.2 equiv.). The pH of the aqueous solution was adjusted to 1 with conc. HCl before the reaction.

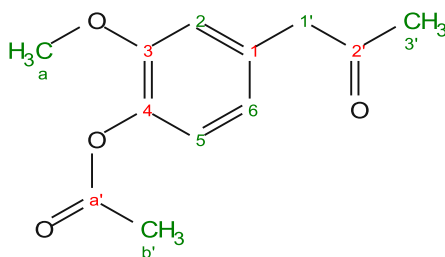
Purification: column chromatography (PE/EtOAc 5:1)

Yield: 54 % (GC)

Appearance: yellow oil

¹H-NMR (400 MHz, CDCl₃) δ(ppm): 6.86 (d, *J* = 7.8 Hz, 1H, H₆), 6.72 – 6.64 (m, 2H, H₂, H₅), 5.54 (s, 1H, OH), 3.86 (s, 3H, H_a), 3.59 (s, 2H, H_{1'}), 2.13 (s, 3H, H_{3'}).

Spectrum in accordance with the literature⁹⁴.

D.13.3.9. Synthesis of 1-(4-acetoxy-3-methoxyphenyl)propan-2-one **8b****8b** $C_{12}H_{14}O_4$

M=222.23 g/mol

8b was prepared according to the general procedure **A** for Wacker oxidation. The reaction was conducted at 45 °C with PdTFA₂ (8.2 mg, 10 mol%), **8a** (51 mg, 0.25 mmol, 1.0 equiv.) and FeCl₃ (60 mg, 0.375 mmol, 1.5 equiv.).

Purification: column chromatography (PE/EtOAc 3:1)

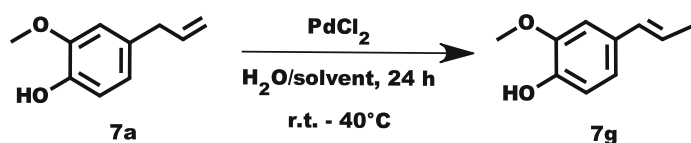
Yield: 57 % (GC)

Appearance: colorless oil

¹H-NMR (400 MHz, CDCl₃) δ(ppm): 6.97 (d, *J* = 7.7 Hz, 1H, H₆), 6.81 – 6.73 (m, 2H, H₂, H₅), 3.80 (s, 3H, H_a), 3.65 (s, 2H, H_{1'}), 2.29 (s, 3H, H_{b'}), 2.15 (s, 3H, H_{3'}).

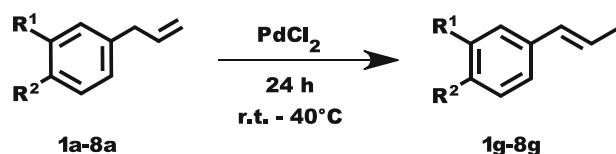
Spectrum in accordance with the literature¹³³.

D.13.4. Isomerization of 2-propenylbenzenes

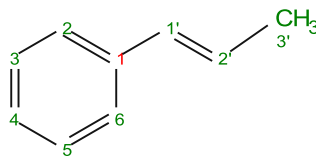
D.13.4.1. Isomerization of eugenol **7a**

Starting material **7a** (0.1 g, 0.61 mmol, 1.0 equiv.) was added into a 25 ml screw cap vial equipped with magnetic stirring and septum. A mixture of EtOH (0.2-4 ml) or MeOH (4 ml) and water (0-3.8 ml) was then added to the reaction flask (water content of the solvent: 0, 50, 80, 90 or 95%). The solution was degassed in an ultrasonic bath under argon counter flow, for ten minutes. Subsequently PdCl₂ (5.4 mg, 5 mol%) was added, and the mixture was stirred at room temperature for 24 hours. The solution was then concentrated in *vacuo* and extracted with EtOAc (3 x 5 ml) in the case that water was used in the reaction solvent. The combined organic phases were then dried over Na₂SO₄, filtrated and the solvent removed under reduced pressure. Conversion was determined *via* ¹H-NMR analysis. The results can be found in chapter B. 10.1.

D.13.4.2. General procedure A for the isomerization of 2-propenylbenzenes



Starting material **1a-8a** (1.5 mmol, 1.0 equiv.) was added into a 2.5 ml brown glassed screw cap vial equipped with magnetic stirring. To this PdCl₂ (0.5 – 5 mol%) was added and the mixture stirred at room temperature or 40 °C for 24 hours. After full conversion of the starting material was confirmed *via* ¹H-NMR analysis the mixture was diluted with Et₂O and centrifuged (5 min, 14000 rpm). The supernatant was then removed, and the residue washed with a fresh portion of Et₂O. After a second centrifugation the supernatants were combined and the solvent removed under reduced pressure, leaving a brown oil behind. If necessary, the oil was purified *via* flash chromatography. The residue (PdCl₂) collected during the centrifugation could be reused for this reaction. For the chemoenzymatic one-pot reaction sequence the mixture was used directly for the following step without the removal of the catalyst and if not used immediately it was stored at -30 °C.

D.13.4.3. Synthesis of (E/Z)-1-(prop-2-en-1-yl)benzene **1g****1g****C₉H₁₀**

M=118.17 g/mol

1g was prepared according to the general procedure **A** for the isomerization of 2-propenylbenzenes. The reaction was conducted at room temperature with PdCl₂ (7.5 mg, 5 mol%) and **1a** (100 mg, 0.8 mmol, 1.0 equiv.).

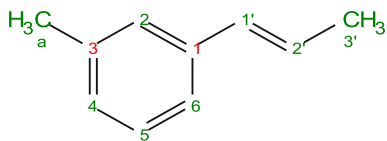
Yield: Quantitative (E/Z= 49:1, determined from the ¹H-NMR)

Appearance: reddish brown oil

¹H-NMR (400 MHz, CDCl₃): E-isomer, δ (ppm): 7.36 – 7.22 (m, 5H, H₂, H₃, H₄, H₅, H₆), 6.39 (dq, *J* = 15.8, 1.7 Hz, 1H, H_{1'}, E), 6.22 (dq, *J* = 15.8, 6.5 Hz, 1H, H_{2'}, E), 1.87 (dd, *J* = 6.6, 1.6 Hz, 3H, H_{3'}).

Spectrum in accordance with the literature¹³⁴.

D.13.4.4. Synthesis of (E/Z)-1-methyl-3-prop-1-enylbenzene **2g**



2g

C₁₀H₁₂

M=132.20 g/mol

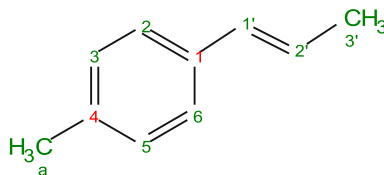
2g was prepared according to the general procedure **A** for the isomerization of 2-propenylbenzenes. The reaction was performed at room temperature with PdCl₂ (6.7 mg, 5 mol%) and **2a** (100 mg, 0.75 mmol, 1.0 equiv.).

Yield: Quantitative (E/Z= 49:1, determined from the ¹H-NMR)

Appearance: reddish brown oil

¹H-NMR (400 MHz, CDCl₃): E-isomer, δ (ppm): 7.22 – 7.11 (m, 2H, H2, H5), 7.14 – 7.07 (m, 1H, H6), 7.03 – 6.96 (m, 1H, H4), 6.36 (dq, *J* = 15.8, 1.7 Hz, 1H, H1'), 6.21 (dq, *J* = 15.7, 6.5 Hz, 1H, H2'), 2.32 (s, 3H, Ha), 1.86 (dd, *J* = 6.5, 1.6 Hz, 3H, H3').

Spectrum in accordance with the literature¹³⁵.

D.13.4.5. Synthesis of (E/Z)-1-methyl-4-prop-1-enylbenzene **3g****3g****C₁₀H₁₂**

M=132.20 g/mol

3g was prepared according to the general procedure **A** for the isomerization of 2-propenylbenzenes. The reaction was performed at room temperature with PdCl₂ (6.7 mg, 5 mol%) and **3a** (100 mg, 0.75 mmol, 1.0 equiv.).

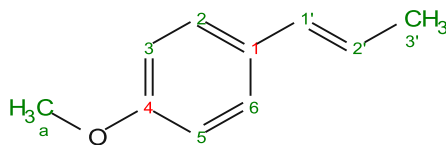
Yield: 99 % conversion (E/Z 24:1, determined from the ¹H-NMR)

Appearance: reddish brown oil

¹H-NMR (400 MHz, CDCl₃): E-isomer, δ (ppm): 7.23 – 7.18 (m, 2H, H2, H6), 7.08 (d, J = 7.9 Hz, 2H, H3, H5), 6.35 (dq, J = 15.7, 1.7 Hz, 1H, H1'), 6.16 (dq, J = 15.7, 6.6 Hz, 1H, H2'), 2.30 (s, 3H, Ha), 1.85 (dd, J = 6.6, 1.7 Hz, 3H, H3').

Spectrum in accordance with the literature¹³⁵.

D.13.4.6. Synthesis of (E/Z)-1-methoxy-4-(prop-1-en-1-yl)benzene **4g**



4g
C₁₀H₁₂O
 M=148.20 g/mol

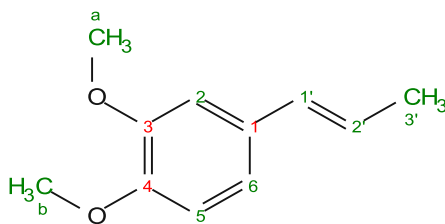
4g was prepared according to the general procedure **A** for the isomerization of 2-propenylbenzenes. The reaction was performed at 40 °C with PdCl₂ (6.0 mg, 5 mol%) and **4a** (100 mg, 0.67 mmol, 1.0 equiv.).

Yield: Quantitative (E/Z= 24:1, determined from the ¹H-NMR)

Appearance: lightly yellow oil

¹H-NMR (400 MHz, CDCl₃): E-isomer, δ (ppm): 7.27 – 7.21 (m, 2H, H₂, H₆), 6.85 – 6.78 (m, 2H, H₃, H₅), 6.33 (dq, *J* = 15.6, 1.7 Hz, 1H, H_{1'}), 6.07 (dq, *J* = 15.7, 6.6 Hz, 1H, H_{2'}), 3.78 (s, 3H, H_a), 1.84 (dd, *J* = 6.6, 1.7 Hz, 3H, H_{3'}).

Spectrum in accordance with the literature¹³⁵.

D.13.4.7. Synthesis of (E/Z)-1,2-dimethoxy-4-(prop-1-en-1-yl)benzene **5g****5g** $C_{11}H_{14}O_2$

M= 178.22 g/mol

5g was prepared according to the general procedure **A** for the isomerization of 2-propenylbenzenes. The reaction was performed at 40 °C with PdCl₂ (5.0 mg, 5 mol%) and **5a** (100 mg, 0.56 mmol, 1.0 equiv.).

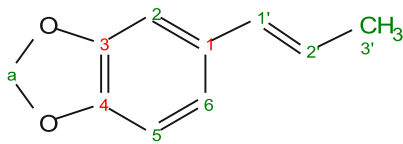
Yield: Quantitative (E/Z= 27:2, determined from the ¹H-NMR)

Appearance: reddish brown oil

¹H-NMR (400 MHz, CDCl₃): E-isomer, δ (ppm): 6.89 – 6.74 (m, 3H, H₂, H₅, H₆), 6.31 (dq, J = 15.7, 1.6 Hz, 1H, H_{1'}), 6.09 (dq, J = 15.7, 6.6 Hz, 1H, H_{2'}), 3.87 (s, 3H, a), 3.85 (s, 3H, Ha'), 1.85 (dd, J = 6.6, 1.7 Hz, 3H, H_{3'}).

Spectrum in accordance with the literature¹³⁵.

D.13.4.8. Synthesis of (E/Z)-5-(prop-1-en-1-yl)-2H-1,3-benzodioxole **6g**



6g

$C_{10}H_{10}O_2$

M=162.18 g/mol

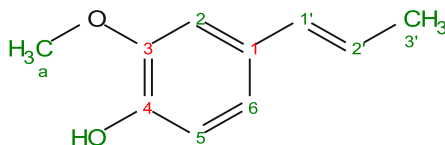
6g was prepared according to the general procedure **A** for the isomerization of 2-propenylbenzenes. The reaction was performed at 40 °C. The reaction was performed at 40 °C with PdCl₂ (5.5 mg, 5 mol%) and **6a** (100 mg, 0.61 mmol, 1.0 equiv.).

Yield: Quantitative (E/Z = 63: 2, determined from the ¹H-NMR)

Appearance: reddish brown oil

¹H-NMR (400 MHz, CDCl₃): E-isomer, δ (ppm): 6.88 – 6.83 (m, 1H, H2), 6.79 – 6.67 (m, 2H, H5, H6), 6.29 (dq, *J* = 15.7, 1.7 Hz, 1H, H1'), 6.04 (dq, *J* = 15.7, 6.6 Hz, 1H, H2'), 5.91 (s, 2H, Ha), 1.83 (dd, *J* = 6.6, 1.7 Hz, 3H, H3').

Spectrum in accordance with the literature¹³⁶.

D.13.4.9. Synthesis of (E/Z)-2-methoxy-4-(prop-1-en-1-yl)phenol **7g****7g**

M=164.20 g/mol

7g was prepared according to the general procedure **A** for the isomerization of 2-propenylbenzenes. The reaction was performed at room temperature with PdCl₂ (5.4 mg, 5 mol%) and **7a** (100 mg, 0.61 mmol, 1.0 equiv.).

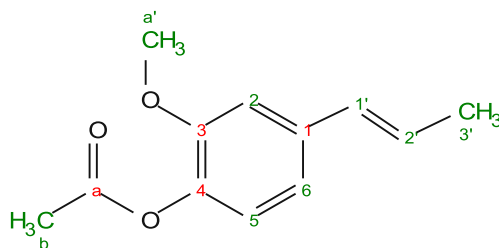
Yield: Quantitative (E/Z = 37:1, determined from the ¹H-NMR)

Appearance: reddish brown oil

¹H-NMR (400 MHz, CDCl₃): E-isomer, δ (ppm): 6.88 – 6.77 (m, 3H, H2, H5, H6), 6.30 (dq, J = 15.7, 1.7 Hz, 1H, H1'), 6.06 (dq, J = 15.7, 6.6 Hz, 1H, H2'), 5.52 (s, 1H, OH), 3.88 (s, 3H, Ha), 1.84 (dd, J = 6.6, 1.7 Hz, 3H, H3').

Spectrum in accordance with the literature¹³⁷.

D.13.4.10. Synthesis of (E/Z)-2-methoxy-4-(prop-1-en-1-yl)phenol acetate **8g**



8g

$C_{12}H_{14}O_3$

M=206.23 g/mol

8g was prepared according to the general procedure **A** for the isomerization of 2-propenylbenzenes. The reaction was performed at 40 °C temperature with PdCl₂ (4.5 mg, 5 mol%) and **8a** (100 mg, 0.48 mmol, 1.0 equiv.).

Yield: 94% conversion (E/Z = 23:1, determined from the ¹H-NMR)

Appearance: reddish brown oil

¹H-NMR (400 MHz, CDCl₃): E-isomer, δ (ppm): 6.95 – 6.88 (m, 3H, H₂, H₅, 6H), 6.39 (dq, J = 15.7, 1.7 Hz, 1H, H_{1'}), 6.21 (dq, J = 15.7, 6.6 Hz, 1H, H_{2'}), 3.86 (s, 3H, H_{b'}), 2.33 (s, 3H, H_a), 1.91 (dd, J = 6.6, 1.7 Hz, 3H, H_{3'}).

Spectrum in accordance with the literature¹³⁸.

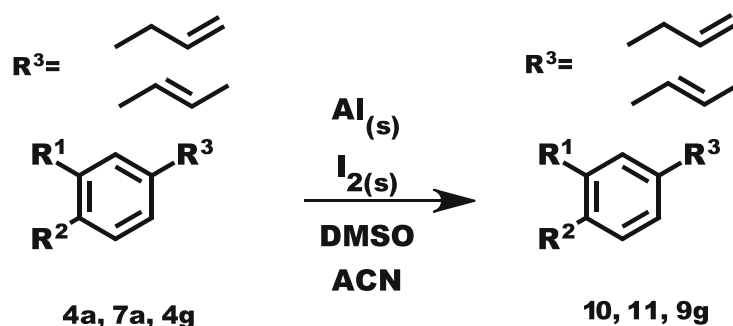
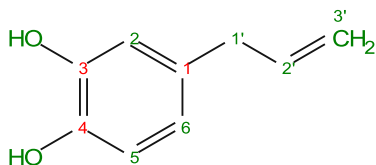
D.13.5. General procedure for the demethylation of aromatic mono methyl ethers¹³⁹

Table 27: Substrates for the demethylation of aromatic mono methyl ethers

Entry	Substrate	Product	Compound Number
Allylanisole 4a	R ¹ = H	R ¹ =H	10
	R ² =OMe	R ² =OH	
	R ³ = Allyl	R ³ = Allyl	
Eugenol 7a	R ¹ =OMe	R ¹ =OH	11
	R ² =OH	R ² =OH	
	R ³ = Allyl	R ³ = Allyl	
Anethol 4g	R ¹ =H	R ¹ =H	9g
	R ² =OMe	R ² =OH	
	R ³ = Vinyl	R ³ = Vinyl	

A flame dried three-necked round bottom flask equipped with, magnetic stirring, condenser and dropping funnel was loaded with Al_(s) and I_{2(s)}. The reaction flask was then purged with Argon three times using standard Schlenk techniques. ACN and DMSO were then added, and the mixture heated to 80 °C under vigorous stirring for 30 minutes. Subsequently, a solution of **7a/4g** was filled into the dropping funnel and added dropwise to the reaction mixture over the course of 30 minutes. The mixture was then stirred for 18 h at 80 °C. Reaction progress was monitored *via* TLC. After full consumption of the starting material was observed the heating bath was removed and the mixture was allowed to cool down to room temperature. The reaction was then quenched by the slow addition of 2 M HCl. The mixture was then extracted with EtOAc. The combined organics were washed with aq. Na₂S₂SO₃ and brine. The solvent was then dried over Na₂SO₄, and then removed under reduced pressure. The resulting residue was purified *via* flash chromatography to yield a colorless oil.

D.13.5.1. Synthesis of 4-(prop-2-en-1-yl)-1,2-benzodiol **11**:



11

C₉H₁₀O₂

M=150.17 g/mol

For the synthesis of **11** the general procedure for the demethylation of aromatic mono methyl ethers was followed. The reaction was conducted at 80 °C with Al (0.71 g, 26 mmol, 2.8 equiv.), I₂ (3.82 g, 30 mmol, 3.3 equiv.), DMSO (1.78 g, 23 mmol, 2.5 equiv.) and **7a** (1.50 g, 9.0 mmol, 1.0 equiv. in 5 ml ACN) in ACN (65 ml).

Work-up: Extraction with EtOAc: 4 x 25 ml. Washing with aq. Na₂S₂SO₃: until solution became clear. Washing with Brine: 2 x 25 ml.

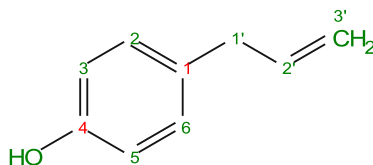
Purification: flash chromatography PE/EtOAc 3:1

Yield: 91% (1.12 g)

Appearance: colorless oil (solidified at -20 °C)

¹H-NMR (400 MHz, CDCl₃) δ(ppm): 6.77 (d, J = 8.0 Hz, 1H, H5), 6.69 (d, J = 2.0 Hz, 1H, H2), 6.61 (dd, J = 8.1, 2.0 Hz, 1H, H6), 5.91 (dt, J = 16.9, 10.1, 6.7 Hz, 1H, H2'), 5.09 – 4.94 (m, 4H, H, H3', -OH, -OH), 3.26 (d, J = 6.7 Hz, 2H, H1').

Spectrum in accordance with the literature¹³⁹.

D.13.5.2. Synthesis of 4-(prop-2-en-1-yl)phenol **10**.**10****C₉H₁₀O**

M=134.17 g/mol

For the synthesis of **10** the general procedure for the demethylation of aromatic mono methyl ethers was followed. The reaction was conducted at 80 °C with Al (0.26 g, 9.2 mmol, 2.8 equiv.), I₂ (1.41 g, 10.8 mmol, 3.3 equiv.), DMSO (0.65 g, 8.2 mmol, 2.5 equiv.) and **4a** (0.50 g, 3.3 mmol, 1.0 equiv. in 2 ml ACN) in ACN (25 ml).

Work-up: Extraction with EtOAc: 4 x 10 ml. Washing with aq. Na₂S₂O₃: until solution became clear. Washing with Brine: 2 x 10 ml.

Purification: flash chromatography PE/EtOAc 5:1

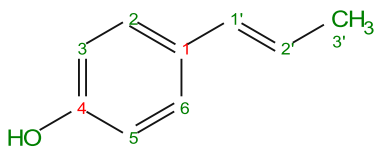
Yield: 77 % (0.35 g)

Appearance: colorless oil

¹H-NMR (200 MHz, DMSO) δ(ppm): 9.24 (s, 1H, -OH), 7.07 – 6.96 (m, 2H, H₂, H₆), 6.79 – 6.70 (m, 2H, H₃, H₅), 5.97 (dt, J = 16.8, 6.7 Hz, 1H, H_{2'}), 5.15 – 4.98 (m, 2H, H_{3'}), 3.29 (d, J = 6.8 Hz, 2H, H_{1'}).

Spectrum in accordance with the literature¹⁴⁰.

D.13.5.3. Synthesis of (E)-4-(prop-1-en-1-yl)phenol **9g**



9g
C₉H₁₀O
 M=134.17 g/mol

For the synthesis of **9g** the general procedure for the demethylation of aromatic mono methyl ethers was followed. The reaction was conducted at 80 °C with Al (0.26 g, 9.2 mmol, 2.8 equiv.), I₂ (1.41 g, 10.8 mmol, 3.3 equiv.), DMSO (0.65 g, 8.2 mmol, 2.5 equiv.) and **4g** (0.50 g, 3.3 mmol, 1.0 equiv. in 2 ml ACN) in ACN (25 ml).

Work-up: Extraction with EtOAc: 4 x 10 ml. Washing with aq. Na₂S₂SO₃: until solution became clear. Washing with brine: 2 x 10 ml.

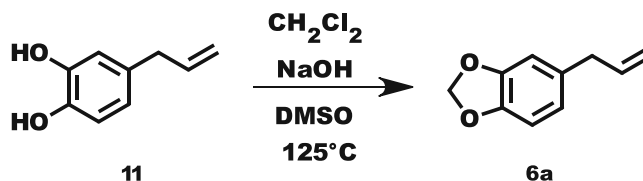
Purification: MPLC, 40 g silica, 25 ml/min, 5 % EtOAc for 10 minutes, 8-50% EtOAc in 20 minutes, 50-100% EtOAc in 10 minutes

Yield: 90% (0.41 g)

Appearance: white solid

¹H-NMR (200 MHz, CDCl₃) δ(ppm): δ 7.28 – 7.11 (m, 2H, H₂, H₆), 6.82 – 6.66 (m, 2H, H₃, H₅), 6.32 (dd, J = 15.7, 1.6 Hz, 1H, H_{1'}), 6.06 (dq, J = 15.7, 6.4 Hz, 1H, H_{2'}), 4.65 (d, J = 1.5 Hz, 1H, -OH), 1.83 (dd, J = 6.4, 1.5 Hz, 3H, H_{3'}).

Spectrum in accordance with the literature¹³⁵.

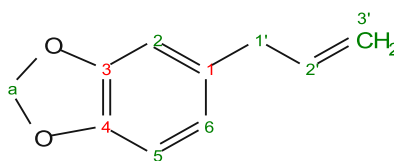
D.13.6. Synthesis of 5-(prop-2-en-1-yl)-2H-1,3-benzodioxole 6a ¹⁴¹

A flame dried three-necked round bottom flask equipped with magnetic stirring and condenser was loaded with NaOH (0.25 g, 6.2 mmol, 3.0 equiv.) and DMSO (5 ml). The reaction flask was then purged with Argon three times using standard Schlenk techniques. The mixture was heated to 120 -125 °C in an oil bath. Subsequently, a solution of **12** (0.4 g, 2.6 mmol, 1.0 equiv. in 1 ml DMSO) was added dropwise to the solution over a period of 10 min through a syringe. The mixture was then stirred for 45 minutes at that temperature. Reaction progress was monitored *via* TLC (PE/EtOAc 3:1). After full conversion was achieved the mixture was taken out of the oil bath allowing it to slowly cool down to room temperature. The reaction was quenched by the addition of 10 ml of water. The mixture was extracted with Et₂O (3 x 5 ml), the combined organic phase was washed with water (3 x 5ml) and dried of Na₂SO₄. After filtration the solvent was removed under reduces pressure, leaving a brown oil behind. The crude was further purified *via* column chromatography.

Purification: Column chromatography PE/EtOAc 20:1

Yield: 70% (0.325 g)

Appearance: colorless oil



6a

C₁₀H₁₀O₂

M=162.18 g/mol

¹H-NMR (400 MHz, CDCl₃) δ(ppm): δ 6.74 – 6.58 (m, 3H, H2, H5, H6), 5.98 – 5.84 (m, 3H, Ha, H2'), 5.10 – 4.99 (m, 2H, H3'), 3.28 (dd, J = 6.7, 0.6 Hz, 2H, H1').

Spectrum in accordance with the literature¹⁴¹.

D.13.7. Synthesis of benzyl acetates

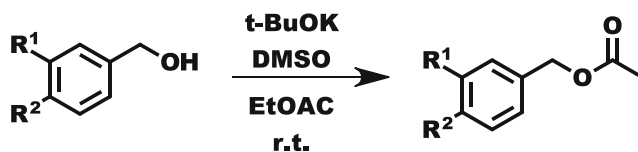
D.13.7.1. General procedure A for the synthesis of benzyl acetates¹⁴²

Table 28: Substrates for the acetylation of benzyl acetates with the general procedure A

Entry	Substrate	Compound Number
4d	R ¹ = H R ² =OMe	4c
5d	R ¹ =Ome R ² =Ome	5c
3d	R ¹ =H R ² =Me	3c

A flame dried Schlenk-flask equipped with magnetic stirring, was loaded with t-BuOK and the respective benzyl alcohol. The flask was then flushed with argon using standard Schlenk techniques. DMSO was then added, and the resulting mixture stirred at room temperature for 10 minutes. Subsequently, abs. EtOAc was added dropwise to the reaction through a syringe. The reaction progress was monitored *via* TLC (PE/EtOAc 2:1). After 30 mins of stirring reaction progress came to a halt. The reaction was then quenched with 30 ml H₂O and the mixture extracted with EtOAc (3 x 10 ml). The combined organic phases were washed with brine, dried over Na₂SO₄, and filtered. The solvent was then removed under reduced pressure, leaving the crude product as an oil behind. Further purification was performed *via* column chromatography.

D.13.7.2. General procedure B for the synthesis of benzyl acetates

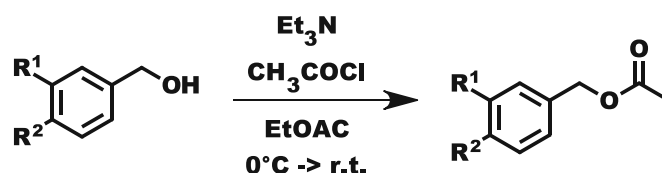
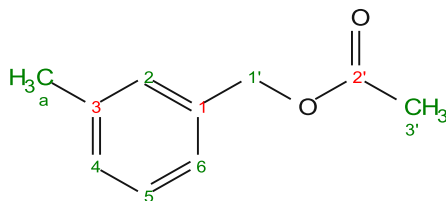
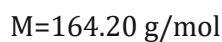


Table 29: Substrates for the acetylation of benzyl acetates with the general procedure B

Entry	Substrate	Compound Number
2d	R ¹ = Me R ² =H	2c
6d	R ¹ , R ² = OCH ₂ O	6c
7d	R ¹ =Ome R ² =OH	8c, 8d

A flame dried Schenk flask was loaded with the respective benzyl alcohol (**2d**, **6d**, **7d**) and dissolved in abs. EtOAc. The reaction mixture was then cooled to 0 °C in ice bath and stirred for 10 minutes. Et₃N was then added to the mixture and the solution stirred for 5 minutes. Subsequently, a solution of CH₃COCl in abs. EtOAc was added dropwise through a syringe over a period of 20- 30 minutes. After one hour of stirring at 0 °C the cooling bath was removed allowing the mixture to slowly warm up to room temperature. Reaction progress was monitored *via* TLC. After full conversion of the starting material was confirmed, the reaction was quenched by the addition of abs. MeOH. The mixture was then filtered, and the residue washed with EtOAc. The filtrates were pooled, and the solvent removed under reduced pressure. The resulting residue in the form of an almost colorless oil, was further purified *via* column chromatography.

D.13.7.3. Synthesis of 3-methylbenzyl acetate **2c**

2c


For the preparation of **2c** the general procedure **B** for the synthesis of benzyl acetates was followed. The reaction was conducted at 0 °C with CH₃COCl (77 mg, 0.98 mmol, 1.2 equiv. in 1 ml EtOAc), Et₃N (99 mg, 0.98 mmol, 1.2 equiv.) and **2d** (100 mg, 0.81 mmol, 1.0 equiv.) in dry EtOAc (2 ml).

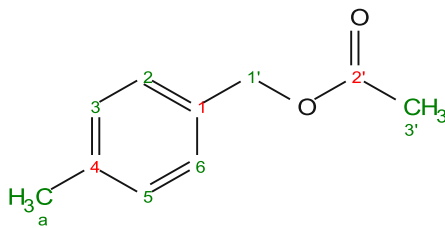
Purification: flash chromatography PE/EtOAc 10:1

Yield: 85% (112 mg)

Appearance: colorless oil

¹H-NMR (400 MHz, CDCl₃) δ(ppm): 7.27 – 7.20 (m, 2H, H₂, H₆), 7.19 – 7.12 (m, 2H, H₃, H₅), 5.05 (s, 2H, H_{1'}), 2.33 (s, 3H, H_a), 2.07 (s, 3H, H_{3'}).

Spectrum in accordance with the literature¹⁴³.

D.13.7.4. Synthesis of 4-methylbenzyl acetate **3c****3c****C₁₀H₁₂O₂****M=164.20**

For the preparation of **3c** the general procedure **A** for the synthesis of benzyl acetates was followed. The reaction was conducted at room temperature with tBuOK (112 mg, 1 mmol, 2.0 equiv.), EtOAc (1ml) and **3d** (61 mg, 0.5 mmol, 1.0 equiv.) in DMSO (2 ml).

Purification: column chromatography PE/EtOAc 10:1

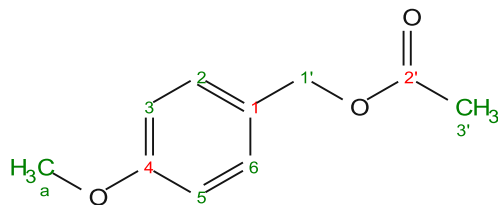
Yield: 50 % (41.0 mg)

Appearance: colorless oil

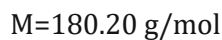
¹H-NMR (400 MHz, CDCl₃) δ(ppm): 7.25 (d, J = 8.0 Hz, 2H, H₂, H₆ or H₃, H₅), 7.21 – 7.14 (m, 2H, H₃, H₅ or H₂, H₆), 5.07 (s, 2H, H_{1'}), 2.35 (s, 3H, H_a), 2.09 (s, 3H, H_{3'}).

Spectrum in accordance with the literature¹⁴³.

D.13.7.5. Synthesis of 4-methoxybenzyl acetate **4c**



4c



For the preparation of **4c** the general procedure **A** for the synthesis of benzyl acetates was followed. The reaction was conducted at room temperature with tBuOK (112 mg, 1 mmol, 2.0 equiv.), EtOAc (1ml) and **4d** (69 mg, 0.5 mmol, 1.0 equiv.) in DMSO (2 ml).

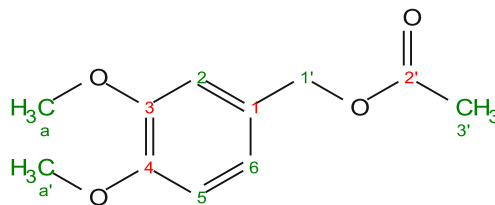
Purification: column chromatography PE/EtOAc 2:1

Yield: 44 % (39.3 mg)

Appearance: colorless oil

1H -NMR (400 MHz, $CDCl_3$) δ (ppm): 7.32 – 7.24 (m, 2H, H2, H6, or 2H, H3), 6.91 – 6.83 (m, 2H, H3, H5, or H2, H6), 5.02 (s, 2H, H1'), 3.79 (s, 3H, Ha), 2.06 (s, 3H, H3').

Spectrum in accordance with the literature¹⁴⁴.

D.13.7.6. Synthesis of 3,4-dimethoxybenzyl acetate **5c****5c**

M=210.22 g/mol

For the preparation of **5c** the general procedure **A** for the synthesis of benzyl acetates was followed. The reaction was conducted at room temperature with tBuOK (112 mg, 1 mmol, 2.0 equiv.), EtOAc (1ml) and **5d** (84 mg, 0.5 mmol, 1.0 equiv.) in DMSO (2 ml).

Purification: column chromatography PE/EtOAc 2:1

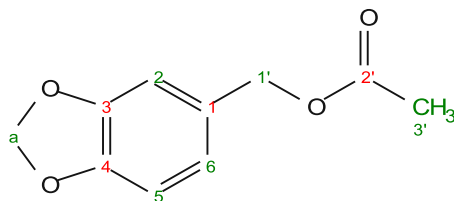
Yield: 60% (58 mg)

Appearance: colorless oil

$^1\text{H-NMR}$ (400 MHz, CDCl_3) δ (ppm): 6.95 – 6.85 (m, 3H, 2, 5, 6), 5.02 (s, 2H, 1'), 3.88 (s, 3H, a'), 3.86 (s, 3H, a), 2.07 (s, 3H, 3').

Spectrum in accordance with the literature¹⁴⁵.

D.13.7.7. Synthesis of (2*H*-1,3-Benzodioxol-5-yl)methyl acetate **6c**



6c

C₁₀H₁₀O₄

M=194.18 g/mol

For the preparation of **6c** the general procedure **B** for the synthesis of benzyl acetates was followed. The reaction was conducted at 0 °C with CH₃COCl (92 mg, 1.18 mmol, 1.2 equiv. in 1 ml EtOAc), Et₃N (120 mg, 1.18 mmol, 1.2 equiv.) and **2d** (150 mg, 0.98 mmol, 1.0 equiv.) in dry EtOAc (2 ml).

Purification: flash chromatography PE/EtOAc 2:1

Yield: 99% (191 mg)

Appearance: colorless oil

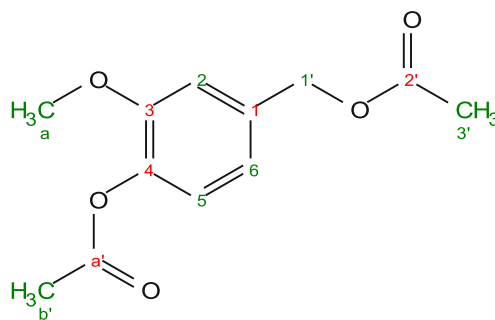
¹H-NMR (400 MHz, CDCl₃) δ(ppm): 6.86 – 6.73 (m, 3H, H₂, H₅, H₆), 5.94 (s, 2H, H_a), 4.98 (s, 2H, H_{1'}), 2.06 (s, 3H, H_{3'}).

Spectrum in accordance with the literature¹⁴⁵.

D.13.7.8. Synthesis of 4-(acetoxymethyl)-2-methoxyphenol acetate **8c** and 4-(hydroxymethyl)-2-methoxyphenol acetate **8d**

For the preparation of **8c** and **8d** the general procedure **B** for the synthesis of benzyl acetates was followed. The reaction was conducted at 0 °C with CH₃COCl (70 mg, 0.9 mmol, 1.2 equiv. in 1 ml EtOAc), Et₃N (91 mg, 0.9 mmol, 1.2 equiv.) and **2d** (115 mg, 0.75 mmol, 1.0 equiv.) in dry EtOAc (2 ml). Both species were separated after the reaction *via* column chromatography.

Purification: column chromatography PE/EtOAc 1:2



8c

C₁₂H₁₄O₅

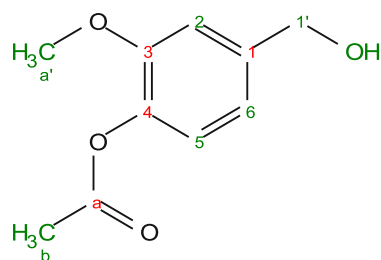
M=238.23 g/mol

Yield: 15 % (22 mg)

Appearance: colorless oil

¹H-NMR (400 MHz, CDCl₃) δ(ppm): 7.03 – 6.89 (m, 3H, H₂, H₅, H₆), 5.06 (s, 2H, H_{1'}), 3.82 (s, 3H, H_a), 2.29 (s, 3H, H_{b'}), 2.09 (s, 3H, H_{3'}).

Spectrum in accordance with the literature¹⁴⁶.



8d

C₁₀H₁₂O₄

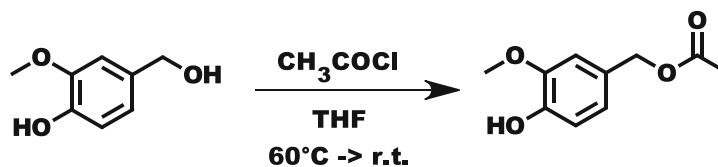
M=196.20 g/mol

Yield: 49% (87 mg)

Appearance: colorless oil

¹H-NMR (400 MHz, CDCl₃) δ(ppm): 7.03 – 6.96 (m, 2H, H₂, H₅), 6.90 (s, 1H, H₆), 4.66 (d, J = 5.3 Hz, 2H, H_{1'}), 3.83 (s, 3H, H_{a'}), 2.29 (s, 3H, H_b), 1.67 (t, J = 5.9 Hz, 1H, -OH).

Spectrum in accordance with the literature¹⁴⁷.

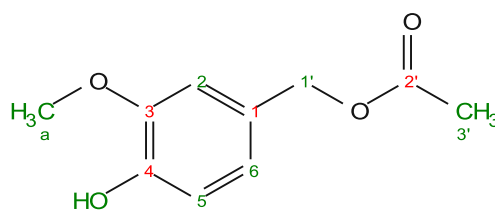
D.13.7.9. Synthesis of 4-acetoxymethyl-2-methoxyphenol **7c**¹⁴⁸

A flame dried Schenk flask equipped with magnetic stirring and septum was loaded with **7d** (77 mg, 0.5 mmol, 1.0 equiv.) and dissolved in abs. THF (7 ml). The flask flushed with argon utilizing standard Schlenk techniques. The reaction mixture was then heated to 60 °C in a heating bath and stirred for 5 minutes. Subsequently, CH₃COCl (2 mmol, 80 μl, 2.0 equiv.) was added dropwise to the mixture with a syringe. After five hours of stirring at 60 °C the heating bath was removed allowing the mixture to slowly cool up to room temperature. The reaction was then stirred at that temperature for 15 hours. Reaction progress was monitored *via* TLC (PE/EtOAc 3:1). After full conversion of the starting material was confirmed, the reaction was quenched by the addition of abs. MeOH (0.5 ml). The solvent was then removed in *vacuo*. The residue in the form of a yellow oil was purified *via* column chromatography.

Purification: column chromatography PE/EtOAc 5:1

Yield: 31% (30 mg)

Appearance: colorless oil



7c

C₁₀H₁₂O₄

M=196.20 g/mol

¹H-NMR (400 MHz, CDCl₃) δ(ppm): 6.88 – 6.84 (m, 3H, H₂, H₅, H₆), 5.63 (s, 1H, -OH), 5.00 (s, 2H, H_{1'}), 3.89 (s, 3H, H_a), 2.06 (s, 3H, H_{3'}).

Spectrum in accordance with the literature¹⁴⁹.

E. References

Cited Literature

- Bornscheuer, U. T.; Huisman, G. W.; Kazlauskas, R. J.; Lutz, S.; Moore, J. C.; Robins, K., Engineering the third wave of biocatalysis. *Nature* **2012**, *485* (7397), 185-94.
- Chojnacka, K., Fermentation products. In *Chemical engineering and chemical process technology - volume v: Chemical engineering education and main products*, Pohorecki, R.; Bridgwater, J.; Molzahn, M.; Gani, R.; Gallegos, C., Eds. EOLSS Publications: Isle of Man, 2010; Vol. 5, pp 189-218.
- Farag, M. A.; Elmassry, M. M.; Baba, M.; Friedman, R., Revealing the constituents of Egypt's oldest beer using infrared and mass spectrometry. *Sci. Rep.* **2019**, *9* (1), 16199.
- Bornscheuer, U. T.; Buchholz, K., Highlights in biocatalysis – historical landmarks and current trends. *Eng. Life Sci.* **2005**, *5* (4), 309-323.
- Rosenthaler, L., Enzyme effected asymmetrical synthesis. *Bio. Z.* **1908**, *14*, 238-253.
- Kolmar, H., Protein engineering comes of age. *Biol. Chem.* **2019**, *400* (3), 255-256.
- Jumper, J.; Evans, R.; Pritzel, A.; Green, T.; Figurnov, M.; Ronneberger, O.; Tunyasuvunakool, K.; Bates, R.; Žídek, A.; Potapenko, A.; Bridgland, A.; Meyer, C.; Kohli, S. A. A.; Ballard, A. J.; Cowie, A.; Romera-Paredes, B.; Nikolov, S.; Jain, R.; Adler, J.; Back, T.; Petersen, S.; Reiman, D.; Clancy, E.; Zielinski, M.; Steinegger, M.; Pacholska, M.; Berghammer, T.; Bodenstein, S.; Silver, D.; Vinyals, O.; Senior, A. W.; Kavukcuoglu, K.; Kohli, P.; Hassabis, D., Highly accurate protein structure prediction with AlphaFold. *Nature* **2021**, *596* (7873), 583-589.
- Wood, C. W.; Heal, J. W.; Thomson, A. R.; Bartlett, G. J.; Ibarra, A. Á.; Brady, R. L.; Sessions, R. B.; Woolfson, D. N., Isambard: An open-source computational environment for biomolecular analysis, modelling and design. *Bioinformatics* **2017**, *33* (19), 3043-3050.
- Weng, J.-K.; Philippe, R. N.; Noel, J. P., The rise of chemodiversity in plants. *Science* **2012**, *336* (6089), 1667-1670.
- Fani, R.; Fondi, M., Origin and evolution of metabolic pathways. *Phys Life Rev* **2009**, *6* (1), 23-52.
- Hedstrom, L., Enzyme specificity and selectivity. In *eLS*, 2010.
- Adams, J. P.; Brown, M. J. B.; Diaz-Rodriguez, A.; Lloyd, R. C.; Roiban, G.-D., Biocatalysis: A pharma perspective. *Adv. Synth. Catal.* **2019**, *361* (11), 2421-2432.
- Zaparucha, A.; de Berardinis, V.; Vaxelaire-Vergne, C., Chapter 1 genome mining for enzyme discovery. In *Modern biocatalysis: Advances towards synthetic biological systems*, The Royal Society of Chemistry: 2018; pp 1-27.
- Servi, S.; Tessaro, D.; Pedrocchi-Fantoni, G., Chemo-enzymatic deracemization methods for the preparation of enantiopure non-natural α -amino acids. *Coord. Chem. Rev.* **2008**, *252* (5), 715-726.
- Hall, M., Enzymatic strategies for asymmetric synthesis. *RSC Chem. Biol.* **2021**, *2* (4), 958-989.
- Raveendran, S.; Parameswaran, B.; Ummalyma, S. B.; Abraham, A.; Mathew, A. K.; Madhavan, A.; Rebello, S.; Pandey, A., Applications of microbial enzymes in food industry. *Food Technol. Biotechnol.* **2018**, *56* (1), 16-30.
- Sun, S.; Ding, Y.; Liu, M.; Xian, M.; Zhao, G., Comparison of glucose, acetate and ethanol as carbon resource for production of poly(3-hydroxybutyrate) and other acetyl-coa derivatives. *Front. Bioeng. Biotechnol.* **2020**, *8*.
- Nikolau, B. J.; Perera, M. A. D. N.; Brachova, L.; Shanks, B., Platform biochemicals for a biorenewable chemical industry. *Plant J.* **2008**, *54* (4), 536-545.
- Intasian, P.; Prakinee, K.; Phintha, A.; Trisrivirat, D.; Weeranoppanant, N.; Wongnate, T.; Chaiyen, P., Enzymes, in vivo biocatalysis, and metabolic engineering for enabling a circular economy and sustainability. *Chem. Rev.* **2021**, *121* (17), 10367-10451.
- Hanefeld, U.; Hollmann, F.; Paul, C. E., Biocatalysis making waves in organic chemistry. *Chem. Soc. Rev.* **2022**, *51* (2), 594-627.
- Turner, N. J.; O'Reilly, E., Biocatalytic retrosynthesis. *Nat. Chem. Biol.* **2013**, *9* (5), 285-288.
- Studier, F. W.; Moffatt, B. A., Use of bacteriophage τ 7 rna polymerase to direct selective high-level expression of cloned genes. *J. Mol. Biol.* **1986**, *189* (1), 113-30.
- Cohen, S. N.; Chang, A. C.; Boyer, H. W.; Helling, R. B., Construction of biologically functional bacterial plasmids in vitro. *Proc Natl Acad Sci USA* **1973**, *70* (11), 3240-4.
- Gibson, D. G.; Young, L.; Chuang, R. Y.; Venter, J. C.; Hutchison, C. A., 3rd; Smith, H. O., Enzymatic assembly of DNA molecules up to several hundred kilobases. *Nat. Methods* **2009**, *6* (5), 343-5.
- Engler, C.; Kandzia, R.; Marillonnet, S., A one pot, one step, precision cloning method with high throughput capability. *PLoS One* **2008**, *3* (11), e3647.
- Bayer, T.; Milker, S.; Wiesinger, T.; Rudroff, F.; Mihovilovic, M. D., Designer microorganisms for optimized redox cascade reactions – challenges and future perspectives. *Adv. Synth. Catal.* **2015**, *357* (8), 1587-1618.
- Sørensen, H. P.; Mortensen, K. K., Soluble expression of recombinant proteins in the cytoplasm of *escherichia coli*. *Microb. Cell Factories* **2005**, *4* (1), 1.
- Demain, A. L.; Vaishnav, P., Production of recombinant proteins by microbes and higher organisms. *Biotechnol. Adv.* **2009**, *27* (3), 297-306.
- Bayer, T. Design, application, and optimization of synthetic enzyme cascades in *escherichia coli*. Technical University of Vienna, 2017.
- Lin, B.; Tao, Y., Whole-cell biocatalysts by design. *Microb. Cell Factories* **2017**, *16* (1), 106.
- France, S. P.; Hepworth, L. J.; Turner, N. J.; Flitsch, S. L., Constructing biocatalytic cascades: In vitro and in vivo approaches to de novo multi-enzyme pathways. *ACS Catal.* **2017**, *7* (1), 710-724.
- Datta, S.; Christena, L. R.; Rajaram, Y. R. S., Enzyme immobilization: An overview on techniques and support materials. *3 Biotech* **2013**, *3* (1), 1-9.
- Lopez-Gallego, F.; Schmidt-Dannert, C., Multi-enzymatic synthesis. *Curr. Opin. Chem. Biol.* **2010**, *14* (2), 174-83.
- Mordhorst, S.; Andexer, J. N., Round, round we go – strategies for enzymatic cofactor regeneration. *Nat. Prod. Rep.* **2020**, *37* (10), 1316-1333.
- de Carvalho, C. C., Enzymatic and whole cell catalysis: Finding new strategies for old processes. *Biotechnol. Adv.* **2011**, *29* (1), 75-83.
- Carrea, G., Biocatalysis in water-organic solvent two-phase systems. *Trends Biotechnol.* **1984**, *2* (4), 102-106.
- Bell, E. L.; Finnigan, W.; France, S. P.; Green, A. P.; Hayes, M. A.; Hepworth, L. J.; Lovelock, S. L.; Niikura, H.; Osuna, S.; Romero, E.; Ryan, K. S.; Turner, N. J.; Flitsch, S.

- L., Biocatalysis. *Nat. Rev. Methods Primers* **2021**, *1* (1), 46.
38. An, J.; Nie, Y.; Xu, Y., Structural insights into alcohol dehydrogenases catalyzing asymmetric reductions. *Crit. Rev. Biotechnol.* **2019**, *39* (3), 366-379.
39. Reid, M. F.; Fewson, C. A., Molecular characterization of microbial alcohol dehydrogenases. *Crit. Rev. Microbiol.* **1994**, *20* (1), 13-56.
40. Goswami, P.; Chinnadayala, S. S.; Chakraborty, M.; Kumar, A. K.; Kakoti, A., An overview on alcohol oxidases and their potential applications. *Appl. Microbiol. Biotechnol.* **2013**, *97* (10), 4259-75.
41. Gvozdev, A. R.; Tukhvatullin, I. A.; Gvozdev, R. I., Quinone-dependent alcohol dehydrogenases and fad-dependent alcohol oxidases. *Biochem. (Mosc.)* **2012**, *77* (8), 843-56.
42. Sützl, L.; Foley, G.; Gillam, E. M. J.; Bodén, M.; Haltrich, D., The gmc superfamily of oxidoreductases revisited: Analysis and evolution of fungal GMC oxidoreductases. *Biotechnol. Biofuels* **2019**, *12* (1), 118.
43. Wongnate, T.; Chaiyen, P., The substrate oxidation mechanism of pyranose 2-oxidase and other related enzymes in the glucose-methanol-choline superfamily. *FEBS J.* **2013**, *280* (13), 3009-3027.
44. Zhu, D.; Hua, L., How carbonyl reductases control stereoselectivity: Approaching the goal of rational design. *Pure Appl. Chem.* **2010**, *82* (1), 117-128.
45. Parkin, G., Synthetic analogues relevant to the structure and function of zinc enzymes. *Chem. Rev.* **2004**, *104* (2), 699-768.
46. Kirmair, L.; Skerra, A., Biochemical analysis of recombinant alkj from *pseudomonas putida* reveals a membrane-associated, flavin adenine dinucleotide-dependent dehydrogenase suitable for the biosynthetic production of aliphatic aldehydes. *Appl. Environ. Microbiol.* **2014**, *80* (8), 2468-2477.
47. Raj, S. B.; Ramaswamy, S.; Plapp, B. V., Yeast alcohol dehydrogenase structure and catalysis. *Biochemistry* **2014**, *53* (36), 5791-803.
48. Bornscheuer, U. T., Microbial carboxyl esterases: Classification, properties and application in biocatalysis. *FEMS Microbiol. Rev.* **2002**, *26* (1), 73-81.
49. Lam, L. K. P.; Hui, R. A. H. F.; Jones, J. B., Enzymes in organic synthesis. 35. Stereoselective pig liver esterase catalyzed hydrolyses of 3-substituted glutarate diesters. Optimization of enantiomeric excess via reaction conditions control. *J. Org. Chem.* **1986**, *51* (11), 2047-2050.
50. Domínguez de María, P.; García-Burgos, C. A.; Bargeman, G.; van Gemert, R. W., Pig liver esterase (ple) as biocatalyst in organic synthesis: From nature to cloning and to practical applications. *Synthesis* **2007**, *2007* (10), 1439-1452.
51. Kazlauskas, R. J.; Weissfloch, A. N. E.; Rappaport, A. T.; Cuccia, L. A., A rule to predict which enantiomer of a secondary alcohol reacts faster in reactions catalyzed by cholesterol esterase, lipase from *pseudomonas cepacia*, and lipase from *candida rugosa*. *J. Org. Chem.* **1991**, *56* (8), 2656-2665.
52. Rauwerdink, A.; Kazlauskas, R. J., How the same core catalytic machinery catalyzes 17 different reactions: The serine-histidine-aspartate catalytic triad of α/β -hydrolase fold enzymes. *ACS Catal.* **2015**, *5* (10), 6153-6176.
53. Voet, D. V., Judith G., *Lehrbuch der biochemie*. Wiley-VCH: Deutschland, 2010.
54. Krebsfänger, N.; Zocher, F.; Altenbuchner, J.; Bornscheuer, U. T., Characterization and enantioselectivity of a recombinant esterase from *pseudomonas fluorescens*. *Enzyme Microb. Technol.* **1998**, *22* (7), 641-646.
55. Fürst, M. J. L. J.; Gran-Scheuch, A.; Aalbers, F. S.; Fraaije, M. W., Baeyer-Villiger monooxygenases: Tunable oxidative biocatalysts. *ACS Catal.* **2019**, *9* (12), 11207-11241.
56. Bučko, M.; Gemeiner, P.; Schenk Mayerová, A.; Krajčovič, T.; Rudroff, F.; Mihovilovič, M. D., Baeyer-villiger oxidations: Biotechnological approach. *Appl. Microbiol. Biotechnol.* **2016**, *100* (15), 6585-6599.
57. Clark, D. E., Peroxides and peroxide-forming compounds. *Chem. Health Saf.* **2001**, *8* (5), 12-22.
58. Goodman, R. M.; Kishi, Y., Experimental support for the primary stereoelectronic effect governing Baeyer-Villiger oxidation and criegee rearrangement. *J. Am. Chem. Soc.* **1998**, *120* (36), 9392-9393.
59. Snowden, M.; Bermudez, A.; Kelly, D. R.; Radkiewicz-Poutsma, J. L., The preference for anti over gauche migration in the Baeyer-Billiger reaction. *J. Org. Chem.* **2004**, *69* (21), 7148-7156.
60. Li, G.; Garcia-Borras, M.; Furst, M.; Ilie, A.; Fraaije, M. W.; Houk, K. N.; Reetz, M. T., Overriding traditional electronic effects in biocatalytic Baeyer-Billiger reactions by directed evolution. *J. Am. Chem. Soc.* **2018**, *140* (33), 10464-10472.
61. Ni, J.; Wu, Y.-T.; Tao, F.; Peng, Y.; Xu, P., A coenzyme-free biocatalyst for the value-added utilization of lignin-derived aromatics. *J. Am. Chem. Soc.* **2018**, *140* (47), 16001-16005.
62. Liang, Y.; Wei, J.; Qiu, X.; Jiao, N., Homogeneous oxygenase catalysis. *Chem. Rev.* **2018**, *118* (10), 4912-4945.
63. Leuenberger, M. G.; Engeloeh-Jarret, C.; Woggon, W.-D., The reaction mechanism of the enzyme-catalyzed central cleavage of β -carotene to retinal. *Angew. Chem. Int. Ed.* **2001**, *40* (14), 2613-2617.
64. Geng, J.; Liu, A., Heme-dependent dioxygenases in tryptophan oxidation. *Arch. Biochem. Biophys.* **2014**, *544*, 18-26.
65. McAndrew, R. P.; Sathitsuksanoh, N.; Mbughuni, M. M.; Heins, R. A.; Pereira, J. H.; George, A.; Sale, K. L.; Fox, B. G.; Simmons, B. A.; Adams, P. D., Structure and mechanism of NOV1, a resveratrol-cleaving dioxygenase. *Proc. Natl. Acad. Sci. USA* **2016**, *113* (50), 14324-14329.
66. Rajagopalan, A.; Lara, M.; Kroutil, W., Oxidative alkene cleavage by chemical and enzymatic methods. *Adv. Synth. Catal.* **2013**, *355* (17), 3321-3335.
67. van Beilen, J. B.; Duetz, W. A.; Schmid, A.; Witholt, B., Practical issues in the application of oxygenases. *Trends Biotechnol.* **2003**, *21* (4), 170-177.
68. Tietze, L. F.; Beifuss, U., Sequential transformations in organic chemistry: A synthetic strategy with a future. *Angew. Chem. Int. Ed.* **1993**, *32* (2), 131-163.
69. Ricca, E.; Brucher, B.; Schrittwieser, J. H., Multi-enzymatic cascade reactions: Overview and perspectives. *Adv. Synth. Catal.* **2011**, *353* (13), 2239-2262.
70. Rudroff, F.; Mihovilovic, M. D.; Gröger, H.; Snajdrova, R.; Iding, H.; Bornscheuer, U. T., Opportunities and challenges for combining chemo- and biocatalysis. *Nat. Catal.* **2018**, *1* (1), 12-22.
71. Bruggink, A.; Schoevaart, R.; Kieboom, T., Concepts of nature in organic synthesis: Cascade catalysis and multistep conversions in concert. *Org. Process Res. Dev.* **2003**, *7* (5), 622-640.

72. Sheldon, R. A., Metrics of green chemistry and sustainability: Past, present, and future. *ACS Sustainable Chem. Eng.* **2018**, *6* (1), 32-48.
73. Gröger, H.; Hummel, W., Combining the 'two worlds' of chemocatalysis and biocatalysis towards multi-step one-pot processes in aqueous media. *Curr. Opin. Chem. Biol.* **2014**, *19*, 171-179.
74. Wu, S.; Li, Z., Whole-cell cascade biotransformations for one-pot multistep organic synthesis. *ChemCatChem* **2018**, *10* (10), 2164-2178.
75. Oberleitner, N.; Ressmann, A. K.; Bica, K.; Gärtner, P.; Fraaije, M. W.; Bornscheuer, U. T.; Rudroff, F.; Mihovilovic, M. D., From waste to value – direct utilization of limonene from orange peel in a biocatalytic cascade reaction towards chiral carvulactone. *Green Chem.* **2017**, *19* (2), 367-371.
76. Abdelaal, A. S.; Yazdani, S. S., A genetic toolkit for co-expression of multiple proteins of diverse physiological implication. *Biotechnology Reports* **2021**, *32*, e00692.
77. Schmid, A.; Dordick, J. S.; Hauer, B.; Kiener, A.; Wubbolts, M.; Witholt, B., Industrial biocatalysis today and tomorrow. *Nature* **2001**, *409* (6817), 258-68.
78. Baer, K.; Kraußner, M.; Burda, E.; Hummel, W.; Berkessel, A.; Gröger, H., Sequential and modular synthesis of chiral 1,3-diols with two stereogenic centers: Access to all four stereoisomers by combination of organo- and biocatalysis. *Angew. Chem. Int. Ed.* **2009**, *48* (49), 9355-9358.
79. Pauly, J.; Gröger, H.; Patel, A. V., Developing multicompartment biopolymer hydrogel beads for tandem chemoenzymatic one-pot process. *Catalysts* **2019**, *9* (6), 547.
80. Sato, H.; Hummel, W.; Gröger, H., Cooperative catalysis of noncompatible catalysts through compartmentalization: Wacker oxidation and enzymatic reduction in a one-pot process in aqueous media. *Angew. Chem. Int. Ed. Engl.* **2015**, *54* (15), 4488-92.
81. Baiju, T. V.; Gravel, E.; Doris, E.; Namboothiri, I. N. N., Recent developments in Tsuji-Wacker oxidation. *Tetrahedron Lett.* **2016**, *57* (36), 3993-4000.
82. Fernandes, R. A.; Jha, A. K.; Kumar, P., Recent advances in Wacker oxidation: From conventional to modern variants and applications. *Catal. Sci. Technol.* **2020**, *10* (22), 7448-7470.
83. Tsuji, J.; Shimizu, I.; Yamamoto, K., Convenient general synthetic method for 1,4- and 1,5-diketones by palladium catalyzed oxidation of α -allyl and α -3-butenyl ketones. *Tetrahedron Lett.* **1976**, *17* (34), 2975-2976.
84. Keith, J. A.; Henry, P. M., The mechanism of the Wacker reaction: A tale of two hydroxypalladations. *Angew. Chem. Int. Ed. Engl.* **2009**, *48* (48), 9038-49.
85. Hu, K.-F.; Ning, X.-S.; Qu, J.-P.; Kang, Y.-B., Tuning regioselectivity of Wacker oxidation in one catalytic system: Small change makes big step. *J. Org. Chem.* **2018**, *83* (18), 11327-11332.
86. Fahey, D. R.; Zeuch, E. A., Aqueous sulfolane as solvent for rapid oxidation of higher α -olefins to ketones using palladium chloride. *J. Org. Chem.* **1974**, *39* (22), 3276-3277.
87. Zahalka, H. A.; Januszkiwicz, K.; Alper, H., Olefin oxidation catalyzed by palladium chloride using cyclodextrins as phase transfer agents. *J. Mol. Catal.* **1986**, *35* (2), 249-253.
88. Tsuji, J., Synthetic applications of the palladium-catalyzed oxidation of olefins to ketones. *Synthesis* **1984**, *1984* (05), 369-384.
89. Wang, J.-L.; He, L.-N.; Miao, C.-X.; Li, Y.-N., Ethylene carbonate as a unique solvent for palladium-catalyzed wacker oxidation using oxygen as the sole oxidant. *Green Chem.* **2009**, *11* (9).
90. Mitsudome, T.; Umetani, T.; Nosaka, N.; Mori, K.; Mizugaki, T.; Ebitani, K.; Kaneda, K., Convenient and efficient Pd-catalyzed regioselective oxyfunctionalization of terminal olefins by using molecular oxygen as sole reoxidant. *Angew. Chem. Int. Ed. Engl.* **2006**, *45* (3), 481-5.
91. Cornell, C. N.; Sigman, M. S., Discovery of a practical direct O₂-coupled Wacker oxidation with Pd[(-)-sparteine]Cl₂. *Org. Lett.* **2006**, *8* (18), 4117-4120.
92. Chaudhari, D. A.; Fernandes, R. A., Hypervalent iodine as a terminal oxidant in Wacker-type oxidation of terminal olefins to methyl ketones. *J. Org. Chem.* **2016**, *81* (5), 2113-21.
93. Fernandes, R. A.; Ramakrishna, G. V.; Bethi, V., MnO₂ as a terminal oxidant in Wacker oxidation of homoallyl alcohols and terminal olefins. *Org. Biomol. Chem.* **2020**, *18* (31), 6115-6125.
94. González-Martínez, D.; Gotor, V.; Gotor-Fernández, V., Stereoselective synthesis of 1-arylpropan-2-amines from allylbenzenes through a Wacker-Tsuji oxidation-biotransamination sequential process. *Adv. Synth. Catal.* **2019**.
95. Fernandes, R. A.; Chaudhari, D. A., Iron(iii) sulfate as terminal oxidant in the synthesis of methyl ketones via wacker oxidation. *J. Org. Chem.* **2014**, *79* (12), 5787-93.
96. Piera, J.; Backvall, J. E., Catalytic oxidation of organic substrates by molecular oxygen and hydrogen peroxide by multistep electron transfer-A biomimetic approach. *Angew. Chem. Int. Ed. Engl.* **2008**, *47* (19), 3506-23.
97. Ho, Y. A.; Paffenholz, E.; Kim, H. J.; Orgis, B.; Rueping, M.; Fabry, D. C., Catalytic Wacker-type oxidations using visible light photoredox catalysis. *ChemCatChem* **2019**, *11* (7), 1889-1892.
98. Baeckvall, J.-E.; Hopkins, R. B.; Grennberg, H.; Mader, M.; Awasthi, A. K., Multistep electron transfer in palladium-catalyzed aerobic oxidations via a metal macrocycle quinone system. *J. Am. Chem. Soc.* **1990**, *112* (13), 5160-5166.
99. Puls, F.; Knolker, H. J., Conversion of olefins into ketones by an iron-catalyzed Wacker-type oxidation using oxygen as the sole oxidant. *Angew. Chem. Int. Ed. Engl.* **2018**, *57* (5), 1222-1226.
100. Liu, B.; Han, W., Iron-catalyzed Wacker-type oxidation. *Synlett* **2018**, *29* (04), 383-387.
101. Liu, B.; Jin, F.; Wang, T.; Yuan, X.; Han, W., Wacker-type oxidation using an iron catalyst and ambient air: Application to late-stage oxidation of complex molecules. *Angew. Chem. Int. Ed.* **2017**, *56* (41), 12712-12717.
102. Hassam, M.; Taher, A.; Arnott, G. E.; Green, I. R.; van Otterlo, W. A., Isomerization of allylbenzenes. *Chem. Rev.* **2015**, *115* (11), 5462-569.
103. Fahlbusch, K.-G.; Hammerschmidt, F.-J.; Panten, J.; Pickenhagen, W.; Schatkowski, D.; Bauer, K.; Garbe, D.; Surburg, H., *Flavors and fragrances*. 2003.
104. Sharma, A.; Sharma, N.; Shard, A.; Kumar, R.; Mohanakrishnan, D.; Saima; Sinha, A. K.; Sahal, D., Tandem allylic oxidation-condensation/esterification catalyzed by silica gel: An expeditious approach towards antimalarial diaryldienones and enones from natural methoxylated phenylpropenes. *Org. Biomol. Chem.* **2011**, *9* (14), 5211-5219.
105. Crabtree, R. H., The organometallic chemistry of the transition metals. *Appl. Organomet. Chem.* **2014**, *6* (6),

- 563-563.
- 106.Silveira, C. C.; Larghi, E. L.; Mendes, S. R.; Bracca, A. B. J.; Rinaldi, F.; Kaufman, T. S., Electrocyclization-mediated approach to 2-methyltrichlisine, an unnatural analog of the azafluoranthene alkaloid trichlisine. *Eur. J. Org. Chem.* **2009**, *2009* (27), 4637-4645.
- 107.Linder, T.; Geyrhofer, S.; Papaplioura, E.; Wang, L.; Atanasov, A. G.; Stuppner, H.; Dirsch, V. M.; Schnürch, M.; Mihovilovic, M. D., Design and synthesis of a compound library exploiting 5-methoxyleolin as potential cholesterol efflux promoter. *Molecules* **2020**, *25* (3), 662.
- 108.Shukla, V. B.; Kulkarni, P. R., L-phenylacetylcarbinol (l-pac): Biosynthesis and industrial applications. *World J. Microbiol. Biotechnol.* **2000**, *16* (6), 499-506.
- 109.Bruice, P. Y., *Organische chemie*. Pearson Studium: Germany, 2011.
- 110.Ferguson, L. N., The synthesis of aromatic aldehydes. *Chem. Rev.* **1946**, *38* (2), 227-254.
- 111.Kazimírová, V.; Rebroš, M., Production of aldehydes by biocatalysis. *Int. J. Mol. Sci.* **2021**, *22* (9), 4949.
- 112.Kunjapur, A. M.; Prather, K. L. J., Microbial engineering for aldehyde synthesis. *Appl. Environ. Microbiol.* **2015**, *81* (6), 1892-1901.
- 113.Kunjapur, A. M.; Tarasova, Y.; Prather, K. L. J., Synthesis and accumulation of aromatic aldehydes in an engineered strain of *escherichia coli*. *J. Am. Chem. Soc.* **2014**, *136* (33), 11644-11654.
- 114.Noordermeer, M. A.; van der Goot, W.; van Kooij, A. J.; Veldsink, J. W.; Veldink, G. A.; Vliegthart, J. F. G., Development of a biocatalytic process for the production of C6-aldehydes from vegetable oils by soybean lipoxygenase and recombinant hydroperoxide lyase. *J. Agric. Food. Chem.* **2002**, *50* (15), 4270-4274.
- 115.Schwendenwein, D.; Ressmann, A. K.; Entner, M.; Savic, V.; Winkler, M.; Rudroff, F., Chemo-enzymatic cascade for the generation of fragrance aldehydes. *Catalysts* **2021**, *11* (8).
- 116.Prasse, A.; Zeller, K.-P.; Siehl, H.-U.; Berger, S.; Sicker, D., Estragol aus estragon. *Chem. unserer Zeit* **2018**, *52* (1), 56-64.
- 117.Gupta, M. P.; Arias, T. D.; Williams, N. H.; Bos, R.; Tattje, D. H. E., Safrole, the main component of the essential oil from piper auritum of panama. *J. Nat. Prod.* **1985**, *48* (2), 330-330.
- 118.Nazrul, M.; Bhuiyan, M.; Begum, J.; Nandi, N.; Akter, F., Constituents of the essential oil from leaves and buds of clove (*syzigium caryophyllatum* (L.) alston). *Afr. J. Plant Sci.* **2010**, *4*, 451-454.
- 119.Gallage, N. J.; Hansen, E. H.; Kannangara, R.; Olsen, C. E.; Motawia, M. S.; Jørgensen, K.; Holme, I.; Hebelstrup, K.; Grisoni, M.; Møller, B. L., Vanillin formation from ferulic acid in *vanilla planifolia* is catalysed by a single enzyme. *Nat. Commun.* **2014**, *5* (1), 4037.
- 120.Vogt, T., Phenylpropanoid biosynthesis. *Mol. Plant* **2010**, *3* (1), 2-20.
- 121.Peter, K. V., *Handbook of herbs and spices*. Woodhead Publishing: England, 2012; Vol. 1.
- 122.Fraaije, M. W.; Wu, J.; Heuts, D. P.; van Hellemond, E. W.; Spelberg, J. H.; Janssen, D. B., Discovery of a thermostable Baeyer-Villiger monooxygenase by genome mining. *Appl. Microbiol. Biotechnol.* **2005**, *66* (4), 393-400.
- 123.Mansouri, H. R.; Mihovilovic, M. D.; Rudroff, F., Investigation of a new type I Baeyer-Villiger monooxygenase from *amycolatopsis thermoflava* revealed high thermodynamic but limited kinetic stability. *ChemBioChem* **2020**, *21* (7), 971-977.
- 124.Kamerbeek, N. M.; Olsthoorn, A. J. J.; Fraaije, M. W.; Janssen, D. B., Substrate specificity and enantioselectivity of 4-hydroxyacetophenone monooxygenase. *Appl. Environ. Microbiol.* **2003**, *69* (1), 419-426.
- 125.Mitsudo, K.; Fukunaga, S.; Fujita, T.; Mandai, H.; Suga, S.; Tanaka, H., Recyclable palladium catalyst in PEG/CH₃CN biphasic system for electro-oxidative wacker-type reaction. *Electrochemistry* **2013**, *81* (5), 347-349.
- 126.Mitsudome, T.; Mizumoto, K.; Mizugaki, T.; Jitsukawa, K.; Kaneda, K., Wacker-type oxidation of internal olefins using a PdCl₂/N,N-dimethylacetamide catalyst system under copper-free reaction conditions. *Angew. Chem. Int. Ed. Engl.* **2010**, *49* (7), 1238-40.
- 127.Parreira, L. A.; Menini, L.; da Cruz Santos, J. C.; Gusevskaya, E. V., Palladium-catalyzed aerobic oxidation of naturally occurring allylbenzenes as a route to valuable fragrance and pharmaceutical compounds. *Adv. Synth. Catal.* **2010**, *352* (9), 1533-1538.
- 128.Rodríguez, C.; de Gonzalo, G.; Gotor, V., Optimization of oxidative bioconversions catalyzed by phenylacetone monooxygenase from *thermobifida fusca*. *J. Mol. Catal. B: Enzym.* **2012**, *74* (1), 138-143.
- 129.Stumm, W. M. J. J., *Aquatic chemistry : Chemical equilibria and rates in natural waters*. Wiley: New York, 1996.
- 130.Iyer, M.; Rele, D. N.; Trivedi, G. K., Anomalous behaviour of substituted allyl benzenes in palladium(II) catalysed reaction. *Tetrahedron Lett.* **1989**, *30* (6), 759-762.
- 131.Curti, C.; Zanardi, F.; Battistini, L.; Sartori, A.; Rassa, G.; Pinna, L.; Casiraghi, G., Streamlined, asymmetric synthesis of 8,4'-oxyneolignans. *J. Org. Chem.* **2006**, *71* (22), 8552-8558.
- 132.Sharma, S. K.; Srivastava, V. K.; Pandya, P. H.; Jasra, R. V., Solvent-free isomerization of methyl chavicol to trans-anethole using transition metal complexes as catalysts. *Catal. Commun.* **2005**, *6* (3), 205-209.
- 133.Gierer, J. P., Ingegerd; Smedman, Leif-Åke, The reactions of lignin during sulphate pulping. Part xii. Reactions of intermediary o,p'-dihydroxy-stilbene structures. *Acta Chem. Scand.* **1972**, *26*, 3366-3376.
- 134.Yao, C.-Z.; Li, Q.-Q.; Wang, M.-M.; Ning, X.-S.; Kang, Y.-B., (E)-specific direct Julia-olefination of aryl alcohols without extra reducing agents promoted by bases. *Chem. Commun.* **2015**, *51* (36), 7729-7732.
- 135.Nakayama, K.; Maeta, N.; Horiguchi, G.; Kamiya, H.; Okada, Y., Radical cation Diels-Alder reactions by TiO₂ photocatalysis. *Org. Lett.* **2019**, *21* (7), 2246-2250.
- 136.Silva MGR, V. M., Chagas TAB, Cordeiro MM, Alves LB, Monti PAG, et al., Molecular modeling and chemical synthesis of new safrol oxime ether derivatives. *J. Braz. Chem. Soc.* **2021**, *32* (8), 1476-1490.
- 137.Gauthier, D.; Lindhardt, A. T.; Olsen, E. P. K.; Overgaard, J.; Skrydstrup, T., In situ generated bulky palladium hydride complexes as catalysts for the efficient isomerization of olefins. Selective transformation of terminal alkenes to 2-alkenes. *J. Am. Chem. Soc.* **2010**, *132* (23), 7998-8009.
- 138.Luu, T. X. T.; Lam, T. T.; Le, T. N.; Duus, F., Fast and green microwave-assisted conversion of essential oil allylbenzenes into the corresponding aldehydes via alkene isomerization and subsequent potassium permanganate promoted oxidative alkene group cleavage. *Molecules* **2009**, *14* (9), 3411-3424.
- 139.Sang, D.; Tian, J.; Tu, X.; He, Z.; Yao, M., Cleavage of

catechol monoalkyl ethers by aluminum triiodide-dimethyl sulfoxide. *Synthesis* **2019**, *51* (03), 704-712.

140.Jo, H.; Choi, M.; Viji, M.; Lee, Y. H.; Kwak, Y.-S.; Lee, K.; Choi, N. S.; Lee, Y.-J.; Lee, H.; Hong, J. T.; Lee, M. K.; Jung, J.-K., Concise synthesis of broussonone a. *Molecules* **2015**, *20* (9), 15966-15975.

141.Heather, E.; Shimmom, R.; McDonagh, A., Organic impurity profiling of 3,4-methylenedioxyethylamphetamine (MDMA) synthesised from catechol and eugenol via 4-allylcatechol. *Forensic Sci. Int.* **2020**, *309*, 110176.

142.Singha, R.; Ray, J. K., Selective acetylation of primary alcohols by ethyl acetate. *Tetrahedron Lett.* **2016**, *57* (48), 5395-5398.

143.Chen, Y.; Li, C.; Cui, Y.; Sun, M.; Jia, X.; Li, J., Bu₄Ni-catalyzed C-C bond cleavage and oxidative esterification of allyl alcohols with toluene derivatives. *Synthesis* **2019**, *51* (19), 3667-3674.

144.Chaubey, S. A.; Mishra, R., Synthesis of task-specific imidazolium ionic liquid as an efficient catalyst in acetylation of alcohols, phenols, and amines. *Chem. Pap.* **2020**, *74* (10), 3259-3268.

145.Zeng, T.; Song, G.; Li, C.-J., Separation, recovery and reuse of N-heterocyclic carbene catalysts in transesterification reactions. *Chem. Commun.* **2009**, (41), 6249-6251.

146.Mohammadpoor-Baltork, I.; Moghadam, M.; Tangestaninejad, S.; Mirkhani, V.; Khosropour, A. R.; Mirjafari, A., [C₄mim][InCl₄]: An efficient catalyst-medium for alkoxymethylation of alcohols and their interconversion to acetates and tms-ethers. *C. R. Chim.* **2011**, *14* (6), 568-579.

147.Mastihubová, M. P., M., A selective and mild glycosylation method of natural phenolic alcohols. *Beilstein J. Org. Chem.* **2016**, *12*, 524-530.

148.Miyazawa, T.; Yamamoto, M.; Maeda, Y., Microwave-accelerated selective acylation of (hydroxyalkyl)phenols using acid chlorides. *Synth. Commun.* **2009**, *39* (6), 1092-1099.

149.Allevi, P.; Ciuffreda, P.; Longo, A.; Anastasia, M., Lipase-catalysed chemoselective monoacetylation of hydroxyalkylphenols and chemoselective removal of a single acetyl group from their diacetates. *Tetrahedron: Asymmetry* **1998**, *9* (16), 2915-2924.



Die approbierte gedruckte Originalversion dieser Diplomarbeit ist an der TU Wien Bibliothek verfügbar
The approved original version of this thesis is available in print at TU Wien Bibliothek.



Die approbierte gedruckte Originalversion dieser Diplomarbeit ist an der TU Wien Bibliothek verfügbar
The approved original version of this thesis is available in print at TU Wien Bibliothek.